

SPFC BUS DESIGN STUDIES

ETSU F/02/00134/REP

Contractor

Johnson Matthey

Prepared by

L Potter
J Reinkingh

The work described in this report was carried out under contract as part of the New and Renewable Energy Programme, managed by ETSU on behalf of the Department of Trade and Industry. The views and judgements expressed in this report are those of the contractor and do not necessarily reflect those of ETSU or the Department of Trade and Industry.

First published 1999

© Crown copyright 1999

Table of Contents

Executive Summary	iii
Glossary	vii
1. Introduction.....	1
2. Commercial and Operational Requirements	3
2.1 Bus Performance and Specification	3
2.2 Fuelling	4
2.3 Costs.....	7
2.3.1 Capital Costs	7
2.3.2 Operator Costs	8
2.3.3 Maintenance Costs	8
2.3.3 Fuel Costs	9
2.3.4 Lifecycle costs	10
2.4 Constraints	12
3. Environmental and Market Drivers	13
4. Fuel Processor Modelling	16
4.1 Assumptions.....	16
4.1.1 Sensitivity of Assumptions	17
4.2 Definitions	19
4.3 FC System Simulation Results	21
4.3.1 System simulation: Wellman CJB Results	21
4.3.2 System simulation: Johnson Matthey Results	22
4.3.3 System simulation: BG Technology Results	23
4.4 Discussion on Fuel Processor Modelling Results.....	23
4.4.1 Fuel Processing Efficiencies	23
4.4.2 Comparison of System Efficiencies.....	26
4.4.3 Other system considerations	28
5. Conclusions of Phase 1	34
6. Power Train Specifications and Detailed System Design.....	37
6.1 Fuel Cell System Dynamic Response.....	37
6.1.1 Drive cycle power measurements	37
6.1.2 FCS requirements in FC hybrid bus: simulation input variables and output parameters	39
6.1.3 Simulation Results	40
6.2 Hybrid System Size	45
6.2.1 Scania/ Thoreb Hybrid Bus Power Train.....	45
6.2.2 FCS Hybrid Bus	46
6.2.3 Choice of FCS and Battery capacity.....	49
6.3 Fuel Cell System Start-up Time.....	49
6.3.1 FCS Start-up Using Heat from Methanol Combustion.....	50
6.3.2 FCS Start-up Using Electrical Heating.....	51
6.4 Fuel Cell System Specifications	52
6.4.1 Fuel cell stack	52
6.4.2 Fuel Processor Requirements.....	53
6.4.3 Parasitic Power Requirements	54
6.5 Hybrid Bus Component Dimensions and Costs	54
7. Conclusions of Phase 2	57
8. References.....	59

Appendix A: Fuel Issues.....	60
Appendix B: Palladium membrane.....	69
Appendix C: System Simulations.....	72
C1 - Wellman CJB methanol reformer and CO clean-up.....	72
C2 - Johnson Matthey HotSpot reformer and CO clean-up.....	74
C3 - BG Technology Natural Gas reformer.....	76
Appendix D: Aspen Models.....	78
D1 - Wellman CJB methanol steam reformer system.....	78
D2 - Johnson Matthey HotSpot reformer system.....	86
D3 - British Gas NG reformer system.....	96
Appendix E: Thoreb/Scania Bus and Basis for Simulations.....	104
Appendix References.....	107

EXECUTIVE SUMMARY

Buses will be the first transport application of fuel cells to be commercialised. Already, hydrogen fuelled buses are undergoing trials in Chicago and Vancouver. However, there are considerable uncertainties over the hydrogen infrastructure and cost. Hydrogen can be produced by reforming fuels such as methanol, ethanol, gasoline and natural gas. Use of these fuels could offer a nearer term solution for commercial transport applications.

Reforming of fuels such as methanol and natural gas is not new, as conventional systems have been designed for large-scale hydrogen generation. However, on-board reforming for vehicles is a concept which has to satisfy different requirements - the reformer must be compact and flexible enough to respond to the power requirements of the vehicle, and have rapid start-up.

This Bus Design Study was commissioned to assess system design options for Solid Polymer fuel cell buses. To do this, the suitability of various reformers for buses was determined, and more detailed examination of one system resulted in an outline design covering the performance, size, weight and projected costs of a fuel cell bus. This process raised awareness of issues to be addressed in a full design, build and demonstration of a bus in the next 1-2 years. To reduce uncertainties and risk, the analysis is based on data from an existing ICE/battery hybrid bus. The models also investigate the feasibility of a reformat fed fuel cell only bus.

The commercial and operational needs of the bus industry, the choice of fuel, fuel availability, fuel processor performance and the fuel cell system power requirements have been addressed.

Of all the commercial factors considered, cost was the most important to bus operators. This is not just the initial capital investment, but the bus lifecycle costs. When commercialising a fuel cell bus, consideration will need to be given to the cost of capital, fuel, maintenance and operator costs, and expected bus lifetime. Although this looks like a straightforward list, complications become immediately apparent on closer inspection. For example, the choice and cost of fuel is not certain. At present, many organisations are opting for methanol fuel – it is liquid and easy to handle, and is generally considered one of the “easiest” fuels to reform. However, methanol is not a transport fuel, and is therefore not yet subject to road fuel duty. Based on efficiency predictions from the modelling, the cost of methanol to the bus operator would need to be £0.17 per litre (compared to current diesel cost of £0.26 per litre) to give similar fuel cost per km of bus use. The average price of methanol (as a chemical not a fuel) was about £0.13 per litre (pre-tax) in 1998. If subjected to the same duty as diesel for bus operators, then methanol would cost in the region of £0.18 per litre. All reformer choices can potentially reduce the fuel cost, compared to diesel or natural gas ICE’s, and hydrogen fuelled fuel cell buses.

Maintenance schedules are also unknown. Only estimates can be made at present. As there are fewer moving parts, causing less vibration, fuel cell buses will most likely need less engine-based maintenance than conventional buses. As a result, fuel cell bus is

projected to have a life of about 15 years (compared to 12 for a diesel bus). For this lifetime, it is anticipated that the fuel cell will need replacing twice. Commercial urban buses travel about 250km per day and are expected to have about 95% availability. On average, a bus will be used for approaching 70,000 hours during its lifetime.

A FCS power train, based on 60kW (gross), with a power turn-up rate of 5kW/sec, would be of similar weight and volume to a diesel ICE power train. Using cost projections, based on several hundred units per year, the purchase cost of a fuel cell hybrid bus would be about £170,000, compared to £115,000 for a conventional diesel bus, and £155,000 for a CNG combustion engine bus. The three most expensive components are the stack, the inverter and the powertrain management system. It is widely believed that the bus market will benefit in the longer term from the entry of fuel cells into the car mass market, which should bring down the overall purchase cost of a bus FCS.

Based on capital cost alone, the fuel cell bus is 48% more than a diesel bus. However, however, taking the NPV of the *complete lifecycle* costs, - over a 15 year life - it has been estimated that a methanol fuel cell hybrid bus would cost about £0.31/km, the same as diesel. This of course is based on many assumptions and variables, and it will be some time before the economics of fuel cell buses can be made more definitive.

So, lifecycle costs seem comparable, but fuel cell buses also offer environmental benefits – both with regard to tailpipe emissions such as NO_x and particulates, and the expected overall reduction in CO₂.

As well as the commercial and operator criteria, the study looked in some detail at the technical feasibility of reformer-fuel cell systems.

The performance of various reformers were modelled including:

- Wellman CJB (methanol)
- Johnson Matthey HotSpot (methanol)
- BG Technology Compact reformer (natural gas)

Fuel cell system simulations to compare performance and specifications for these reformers were based on real operating data obtained in prototypes or laboratory scale reactors. Microscale tests and experience with the methanol HotSpot reformer were used to make projections of the HotSpot reformer operating on ethanol and natural gas. Comparisons were made to published data for the ADL ethanol and gasoline reformer.

The FC system analysis comprises various elements, namely technical feasibility, system complexity, size and weight, efficiency, expected costs, etc.

To assess the technical feasibility and efficiency, heat and mass balances of a series of FC systems were simulated in Aspen. The simulations represent steady state systems, where the systems were optimised to produce 50 kW_e net.

The reformers were comparable in performance, with net system efficiencies ranging from 23.5% to 34.8%, under different operating conditions (Table 1). The best system efficiency was achieved with the Wellman CJB methanol reformer using a palladium membrane to separate hydrogen from the other reformat components. However, the

currently available Pd membrane technology is calculated to be too expensive, and therefore this option is not suitable for transport applications. The Johnson Matthey and Wellman CJB methanol reformers, using a catalytic CO clean-up, were the next best. Net system efficiencies based on these reformers were predicted to be 29-32%.

Table 1: Estimated Net Fuel Cell System Efficiencies Based on Various Reformers

	Base case	Anode utilisation 0.9	Pd membrane
Wellman CJB	31.3%	31.3%	34.8%
JM Methanol	29.1%	32.4%	32.1%
BG Technology	28.1%	32.1%	23.5%

On evaluating the system size, and weights, the Johnson Matthey methanol reformer was found to be similar in size to Wellman CJB's reformer. The issue of weight differentiates the reformers more widely. Based on current design, the Wellman CJB reformer, for a 50kW system would weigh 460kg more than the Johnson Matthey methanol reformer.

The final criterion was technical status of the fuel processor technology. It became apparent during the course of the study that neither the Wellman CJB methanol reformer nor the BG Natural Gas reformer was sufficiently developed to provide full data sets for the study. In many cases performance, size, weight and cost data have been inferred or projected from laboratory or model calculations. The consequence was that, while the JM Hotspot data was also less than definitive in some respects, it was the only reformer available as a prototype at the end of phase 1. Hence, on this basis, it was chosen for the second phase of the design study.

This second phase involved more detailed system modelling and evaluation. First, the power flow in a real ICE hybrid bus was evaluated over two separate urban drivecycles in Stockholm, distinguishing between total power demand and the power supply by the ICE and batteries.

Next, a method was developed to simulate the FCS power supply as a function of various input variables, allowing the gap between the FCS and the ICE power supply to be assessed. This gap analysis forms the basis of the FC hybrid bus power requirements for the various FCS power flow, evaluating power demands on the batteries for the various FCS power supply scenarios.

Extreme cases were explored, ranging from a FCS with a very slow response rate backed up by batteries, to one where the FCS alone provided all the bus power requirements. The model simulations lay the groundwork for the design of a hybrid FCS bus, optimising the battery and FCS size within the constraints of the fuel cell system performance.

For a FC-battery hybrid system, it was demonstrated that with a slow FCS acceleration of 1 or 2 kW/s it is more sensible to operate the FCS at a semi-constant load, rather than load following. In this operation mode the FCS power output varies between a maximum and a minimum (e.g. 35 and 20 kW), dictated by the batteries rather than the total power demand. Such a strategy can only be implemented if the relevant battery

parameters can be measured and translated reliably into a value for the battery state of charge (SOC).

For a FC only bus, in the drive cycles considered, the dynamic response of the FCS needs to be at least 55 kW/s, while the maximum FCS power needs to be 110 kW.

The hybrid FCS power train is estimated to be slightly larger than the current hybrid ICE power train, for FCS dynamics of 1 or 2 kW/s (< 5%/s). For a more responsive FCS (5 kW/s or (10%/s) or more), the overall size and weight of the power train is expected to decrease as less battery capacity is required (see table 2).

Table 2: Estimated hybrid system weight [kg] and volume [litre]

FCS/ICE acceleration (kW/s)	<i>ICE</i>	1	2	5	10	20	55
Number of batteries	<i>10</i>	10	10	8	6	5	0
Maximum power (kW)	<i>~50</i>	35	37	45	55	60	110
Battery volume	<i>1000</i>	1000	1000	800	600	500	0
FCS/ICE volume	<i>200</i>	700	740	900	1100	1200	2200
Total Volume	<i>1200</i>	1700	1740	1700	1700	1700	2200
Battery weight	<i>1000</i>	1000	1000	800	600	500	0
FCS/ICE weight	<i>400</i>	140	148	180	220	240	440
Total weight	<i>1400</i>	1350	1370	1250	1150	1100	1100
FCS Specific Power:	0.1 kW/kg, 0.05 kW/litre						

For a FCS with a dynamic response of 5-10 kW/s (10-20%/s), the simulations showed that the battery capacity can probably be reduced by 2 to 4 units. The maximum power of such a system should be about 45-55 kWe. So, assuming FCS dynamic response can be met, it is anticipated that a 50kWe (net) FCS will be sufficient.

In terms of the start-up, fuel cell suitable reformat can be generated in less than 3 minutes. In reality, this time can probably even be improved to 2 minutes or less.

During these the 3 minutes no additional power is drawn from the batteries, if the fuel is vaporised using heat generated from the combustion of methanol. The 3 minutes start-up time imposes no problems for the batteries, where the bus starts driving after 50 seconds. If electrical heating is used during start-up, it is probably better to idle the bus for 2 minutes, while the FCS is started, before driving away.

This study has shown that a methanol FCS could directly replace the internal combustion engine in a hybrid bus. A methanol hybrid FC bus, is projected to cost marginally less than diesel, over the bus lifecycle. These cost projections, combined with the prospect of substantial reduction in harmful emissions, should motivate bus operators and government bodies to start the development and financial support of fuel cell buses.

GLOSSARY

A	Power turn-up rate (acceleration)
AHU	Anode hydrogen utilisation
CAPRI	Car Autothermal Process Reactor Initiative
CO	Carbon monoxide
CNG	Compressed natural gas
D	Power turn-down rate (deceleration)
DOD	Depth of discharge
FCS	Fuel cell system (fuel cell plus reformer)
HHV	Higher heating value
HTS	High temperature shift
ICE	Internal combustion engine
LHV	Lower heating value
LTS	Low temperature shift
NG	Natural gas
NPV	Net present value
NSE	Net system efficiency
PAFC	Phosphoric acid fuel cell
PEMFC	Proton exchange membrane fuel cell
PPR	Parasitic power ratio
S	Minimum power step size
SOC	State of charge
SR	Steam reformer

1. INTRODUCTION

The bus market is recognised as a key entry point for solid polymer fuel cells for transportation. Already, hydrogen powered demonstration vehicles are undergoing commercial trials in Chicago and Vancouver.

However, the fuel for these buses is pure hydrogen, stored on board the bus in high pressure cylinders. These buses perform well, but complications with refuelling and lack of hydrogen infrastructure makes a pure hydrogen fuel difficult to implement in the near term. Other fuelling options, such as methanol, ethanol or natural gas could offer a nearer term solution for commercial transport applications.

Reforming of fuels such as methanol and natural gas is not new, as conventional systems have been designed for large-scale hydrogen generation. However, on-board reforming for vehicles is a concept which has to satisfy different requirements - the reformer must be compact and flexible enough to respond to the power requirements of the vehicle, and have rapid start-up.

Several UK companies are developing innovative fuel reformers. Johnson Matthey has developed a methanol (HotSpot) reformer, CJB has a methanol steam reformer and BG Technology has a compact reformer for natural gas.

This Bus Design Study was commissioned to assess system design options for Solid Polymer fuel cell bus system.

The project is split into two phases. In Phase 1, we address the needs of the bus industry, the choice of fuel, fuel availability, fuel processor performance and the fuel cell system power requirements. The reformers modelled include JM's methanol HotSpot, WCJB's methanol steam reformer, and BG Technology's compact natural gas steam reformer. These reformers were simulated based on real operating data, achieved with laboratory scale reactors or prototypes. The analysis also includes HotSpot operating on ethanol and natural gas, although performance in these cases was based on microscale tests and experience with methanol. Comparisons were made to published information on ADL's ethanol and gasoline reformers. The choice of reformer is based on our estimates for system costs, system efficiency, feasibility of implementing the fuel cell power train into space and weight constraints of the bus, operational costs of the bus, technology risk and development issues to be addressed.

In Phase 2, we undertake a more detailed modelling and system evaluation, resulting in an outline design for bus, which could be built and used in a demonstration within the next 1-2 years. In the first step we analyse the bus power requirements during a drive cycle, using data measured on an ICE hybrid bus built by Thoreb and Scania, which distinguishes between the power supplied by the batteries and the ICE. Secondly, we simulate the FCS power supply as a function of various input variables, allowing us to assess the gap between the FCS and the ICE power supply. This gap analysis forms the

basis of the FC hybrid bus power requirements for the various FCS power supply scenarios. The model simulations lay the groundwork for the design of a hybrid FCS bus, optimising the battery and FCS size within the constraints of the FCS performance.

2. COMMERCIAL AND OPERATIONAL REQUIREMENTS

2.1 Bus Performance and Specification

Any bus in commercial operation will be required to have the comfort, driveability, range and passenger payload the same as, or better than conventional buses. Buses are generally used about 16 hours a day without refuelling, and carry about 70 passengers. In Europe a 12m bus weighs about 11,500 kg, and the gross vehicle weight is 16,000kg.

The assumptions used in the sections below are:

Daily route - 250km

Availability - 345 days (approx 95%)

Annual mileage - 86,250km

Diesel bus life - 12 years

Fuel cell bus life - 15 years⁽¹⁾

The bus specification will also include minimum top speed, on the flat and different gradients. In the US, this is:

Minimum top speed 88km/h

On a 2.5% gradient 70km/h

On a 16% gradient 11km/h

A 12m bus requires a peak power of about 200kW. The average power requirement may reach 50kW – more if air conditioning is added. However, on a flat route, the *average* power may be as low as 20-25kW with *minimum accessory power*. On an urban route, a bus will have an average speed of about 15km/hr. All these are of course very much route specific. Data from the Scania/Thoreb petrol hybrid bus showed a maximum power demand of 107kW, an average power demand of 26.2kW, a maximum speed of 40.8km/h and an average speed of 16.6km/h. [Julen, K, Thoreb]

The Braunschweig cycle is used as a standard urban bus test cycle. A normal city bus on the Braunschweig cycle has an average power demand of 30kW, and an average speed of 23km/h.

For comparison, the specifications of some fuel cell and ICE hybrid buses are given in Table 2.1. The Georgetown PEMFC power train (including radiator and transmission) weighs about twice that of a diesel engine (approx. 1200kg). With the batteries included, this increases to 3 times a diesel bus. The PAFC is about 30% bigger than the PEMFC system – mainly because it was packaged for easy access. However, because the fuel cell system can be packaged throughout the vehicle, this has not made an impact on passenger space. The PAFC fuel cell and reformer system weighs about 1800kg. Another 500kg must be added for the radiator/cooling subsystem [Wimmer, B, Georgetown University].

¹ expected life longer than conventional due to fewer moving parts, and hence less vibration

Table 2.1 Bus specifications for methanol fuel cell hybrid and petrol/electric hybrid buses

	DAB Citybus Series 15 Hybrid (petrol/battery)	Georgetown 100kW PAFC fuel cell bus	Georgetown 100kW PEMFC Bus
Length	12m	12m	12m
Weight unladen	12,460kg	15,880kg ¹	less than PAFC
Weight fully laden	17,800kg	20,300 ² (est)	
Top speed	65kph	106kph (66mph)	106kph (66mph)
Acceleration (0-50kph)	35secs?	14.5 sec (48kph)	14.5 sec (48kph)
Range	300km (hybrid mode)	560 km	560km
Passenger Capacity	66 passengers	40 seated 23 standing	40 seated, 23 standing
Motors	2 AC asynchronous motors, max traction power 150kW	190kW (250hp) induction motor	190kW (250hp) induction motor
Batteries	SAFT STH800 350V 80Ah (28kWh) 270 batteries in series, weight 1000kg, volume 1-1.3m ³	Pb-acid gel type (85Ah / 100kW)	Pb-acid gel type (50Ah / 100kW)
Fuel tank	250 litres	605.6 litre (160 US gallons)	605.6 litre (160 US gallons)
Engine	Saab 2.3 l; 16 valve; 50kW max output	110kW IFC PAFC	100kW dbb PEMFC
Fuel processor	N/A	High temperature steam reformer	Low temperature steam reformer

¹ Georgetown University believes this weight must be reduced to 13,600 to be commercially viable

²In USA, the maximum allowable gross vehicle weight for 12 m bus is 18,144kg

2.2 Fuelling

Fuel economy, and therefore running costs is very important to bus operators. An urban bus will travel about 250-300km in one day. The average fuel consumption is 4-5 litres per 10km. So a 300km range uses 150 litres of diesel. Fuel tanks on a diesel bus usually hold about 250 litres. This gives a range of 500-600km, allowing a generous margin. Based on the models of reformer system efficiencies (see Section 3), figure 2.1 shows the fuel economy of fuel cell buses compared to diesel and other ICE alternative fuel

buses. The km per litre equivalent is based on km travelled for the energy consumption of 35.7MJ (i.e. equivalent to 1 litre of diesel). This figure is also based on the assumption that the fuel cell buses weigh the same as a diesel bus, which consumes 16MJ of fuel per km.

When considering fleet operation, the refuelling time becomes critical. Liquid fuels are therefore marginally more attractive to operators.

Methanol, ethanol, compressed natural gas and compressed hydrogen fuels have been considered within the context of the report. Methanol is emerging as the preferred fuel for fuel cell transport applications. It is liquid at room

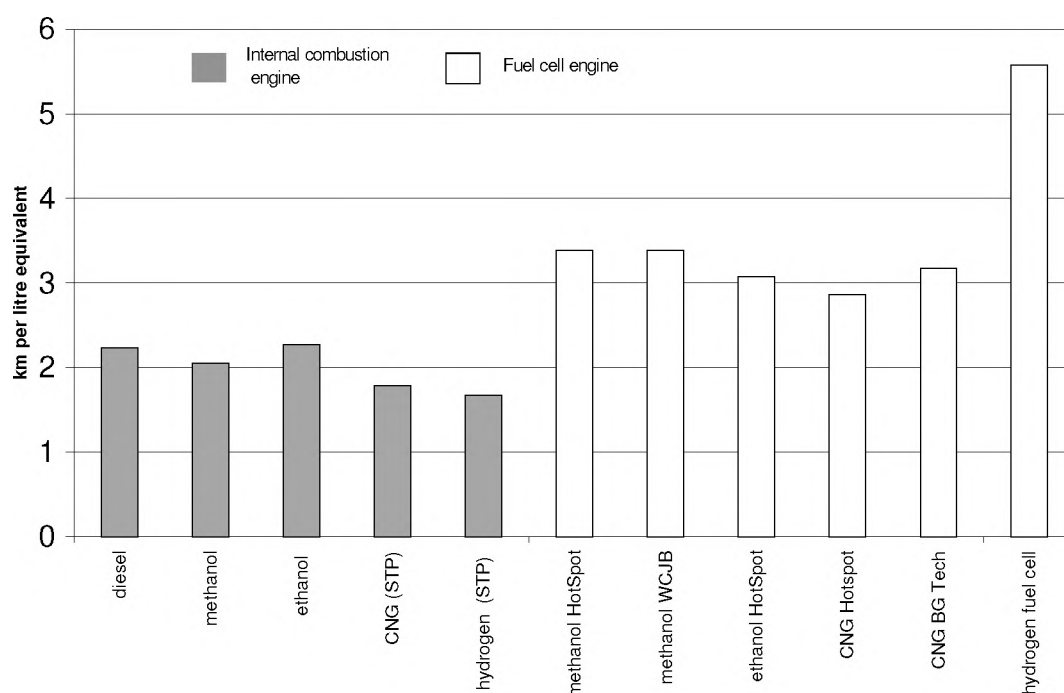


Figure 2.1: Fuel economy for various fuels (km per litre diesel equivalent)

temperature, and can be easily reformed into hydrogen. Although toxic, it is actually considered to be safer than gasoline as it is less likely to ignite, and if it does, it burns at a lower temperature. However, it does burn with a colourless flame, so it is likely that additives will be required for its widespread use [Bechtold, R.L., 1997]. Table 2.2 summarises the key properties and issues for alternative fuels. Further information can be found in Appendix A.

Table: 2.2 Comparison of alternative fuels

	Methanol	Ethanol	CNG	Compressed H ₂
Availability and infrastructure	Being introduced in the USA (M85 and M100) No infrastructure at present, but methanol industry poised to invest. Estimated cost of converting tank plus dispenser - \$50,000 per station	Most widely used in USA, Brazil and Sweden with feedstock agriculture (corn, sugar cane, wood). 300 ethanol buses are being trialed in Sweden, 4500 vehicles in USA use ethanol	Over 1 million vehicles being used worldwide. Needs special refuelling infrastructure. Fast flow dispensers available but more expensive. Widely available fuel	Not readily available in uncombined form in nature. Hydrogen pipelines do exist to supply factories that use it as a feedstock.
Storage and handling	Liquid fuel therefore similar to gasoline. Corrosive in the presence of water. Stainless steel is best material for storage tanks, but mild steel can be used if fully wetted with methanol. Elastomers with a high fluorine content should be used.	Liquid fuel, similar to gasoline to handle. Less corrosive than methanol. Materials such as aluminium are compatible. High fluorine content elastomers are preferred. Storage must be secure and use of fuel accounted for.	Stored in steel, aluminium or composite tanks, usually at 300 bar. (3.7 times the volume of gasoline at 300 bar) Heavy pressurised tanks must be used on vehicle (about 5x volume of diesel). Off vehicle storage area must be isolated from neighbouring buildings.	Needs to be pressurised. Large, heavy bulky storage tanks (20 times the volume of gasoline at 300bar)
Economics	Price in recent years ranges from \$0.09 to \$0.37 per litre. Price and taxation in future uncertain	Ethanol is expensive to produce. In Sweden, fuel cost for ethanol buses is twice that of diesel.	Cheap and abundant fuel. Need for compression, and requirement for pressurised storage tanks adds to cost.	Expensive to produce in useable form. Has potential to be produced from renewable sources.
Safety	Invisible flame. Additives required. Poisonous, toxic. Generally considered safer than gasoline because less likely to ignite, and emits less heat when burning	Luminous flame – no additives needed. Not harmful (in moderate quantities). Care must be taken to avoid vapour inhalation at filling stations as this might register if driver was breathalysed	Lighter than air, escapes into atmosphere. Burns with a visible flame	Burns with an invisible flame in air. Lighter than air, escapes into atmosphere.
Reforming issues	Easiest fuel to reform to hydrogen	More difficult than methanol, and can generate undesirable products	Higher temperatures required for reforming	Not required

2.3 Costs

Cost is the single most important factor to the bus operator. Cost includes not just purchasing cost, but also operator, maintenance, and fuel costs. Taken over the service life of the vehicle, these make up lifecycle costs. To evaluate costs over the lifecycle of the vehicle, some assumptions have to be made regarding the future value of monies involved. For the purposes of this evaluation, it has been assumed that the cost of capital is 8% per annum - based on average company overdraft rate of 8%. Also, it is assumed that income will be the same for diesel and fuel cell buses, so income has not been accounted for.

2.3.1 Capital Costs

Capital costs are assumed to include purchase cost of the bus, plus major engine refurbishment.

In the UK, a diesel bus costs about £115,000. Of this, the full diesel drivetrain accounts for about £20,000.

For a diesel engine, refurbishment occurs once during the bus's 12 year life. It has been assumed that the engine would be refurbished at 6years, at a present value cost of £8,000.

In section 6, models have estimated that a 50kW (net) or 60kW (gross) fuel cell system with a dynamic response rate of 5kW/s would be adequate, based on a moderate drivecycle. At a production rate of several hundred, a fuel cell hybrid bus, with a 60kW(gross) fuel cell engine, would cost in the region of £170,000. This is based on a lot of assumptions with regard to volume of production, cost reductions etc., but the breakdown of the main components would be as follows:

Chassis	£95,000
FC stack	£18,000
Fuel Processor	£6,000
Battery	£10,000
Traction motor	£12,000
PTMS	£12,000
Inverter	£15,000
Others	£2,000
TOTAL ²	£170,000

Again, an additional cost would be the cost of engine refurbishment. For a fuel cell engine, the stack may need to be replaced twice, and the battery once Provision has also been made for replacing the fuel processor catalyst. It is assumed that the stack and fuel processor would be refurbished at half the original cost.

Refurbishment:	Present value
Replace stack at 5 years	£ 7,500
Replace battery at 7 years	£10,000
Replace fuel processor cat	£ 3,000
Replace stack at 10 years	£ 7,500

² Table 6.15 in Section 6 provides details

2.3.2 Operator Costs

It is assumed that the operator overhead costs for a fuel cell bus will be the same as a diesel bus. At £0.1 per km, this amounts to £8,625 per year.

2.3.3 Maintenance Costs

Maintenance costs are broken down into those related to the engine (or power train), and non-engine costs, which includes general inspections, air conditioning, transmission, body, doors, air systems, brakes, lifts). Engine refurbishment costs have been accounted for in the capital cost.

Fuel cell buses have not yet been used long enough to generate information on maintenance costs. However, it is considered that engine related costs will be lower for fuel cell buses as there are few moving parts and therefore less stress from vibration. Non engine related costs will probably remain the same. – See Table 2.3.

Georgetown University has evaluated the potential costs of fuel cell bus maintenance - A fuel cell bus will have a longer life than a diesel bus – say 15 years. However, the stack may need replacing every five years (i.e. twice), and the battery once [Larkins, J.T. Dec1998]. This has been included in the capital costs.

	Diesel	Fuel Cell
Engine related	£0.03/km	£0.01/km
Non engine related	£0.07/km	£0.07/km
Total	£0.10/km	£0.08/km

¹ based on 86,250km per year

Stack lifetime for buses is an important factor. The fuel cells being designed for cars have a target life of 5,000 hours. This is not enough for buses. If the bus is on the road for 16 hours per day, 345 days per year, this amounts to 5,520 hours each year. An acceptable refurbishment period for a bus would be five years. A stack that is replaced every five years will therefore need a life of about 27,600 hours. Although PEMFC stacks have not been run for this length of time, phosphoric acid fuel cell systems for stationary applications have been operated for over 20,000 hours.

2.3.3 Fuel Costs

Currently in the UK, the bus operator pays about 26 pence per litre for diesel. This is made up of a basic price of about 10.35 pence per litre plus duty at about 15.05 pence per litre [European Energy Report, Jan 1999]. Assuming the buses have a fuel economy of 0.5l/km, and travel 250km per day the cost of diesel adds up to £32.5 per day.

However, the fuel costs are uncertain. Figure 2.2 shows an analysis of the cost of alternative fuels, comparing the cost per day (250km) of diesel for a combustion engine, and a fuel cell bus running on methanol, ethanol, natural gas, and hydrogen. The point at which the fuel costs for the fuel cell buses cross the horizontal line (current daily diesel cost) represents a target fuel cost to the operator, tax and duty inclusive. The *pre-tax* cost of methanol averaged £0.13 per litre from 1988 to 1998 [Clean Fuels Report, June 1998]. Natural gas is currently £0.5/kg, [BG Technology, 1998] and hydrogen ranges from £4-15/kg [Hart, D., 1998]. If fuel excise duty for alternative fuels is on an energy equivalent basis, this would work out at 4.5 pence per litre of methanol - assuming duty is equivalent to 0.29 pence per MJ⁽³⁾

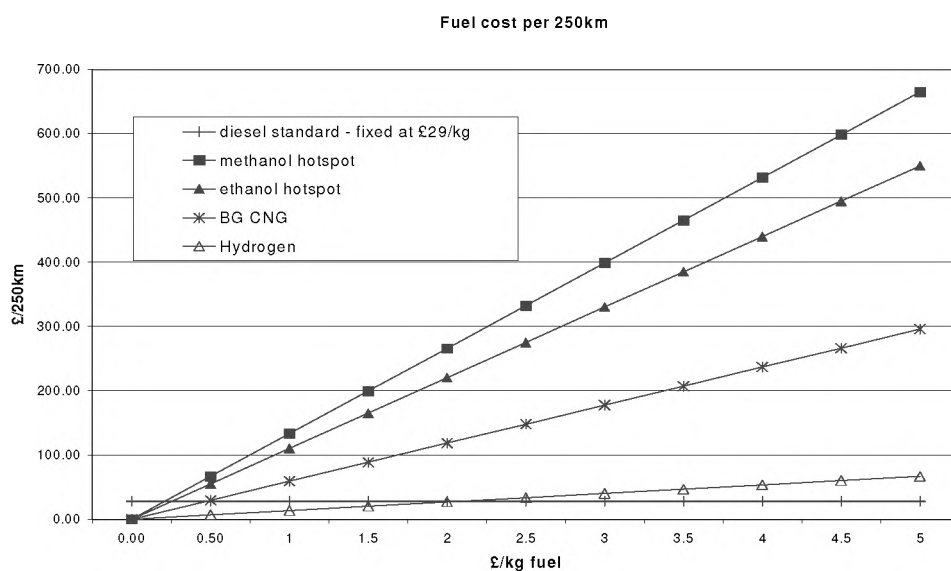


Figure 2.2: Analysis of fuel cost for ICE vs fuel cell bus (liquid and gaseous fuels)

For methanol to be comparable to diesel at current prices, the operator will need to pay in the region of £0.21/kg (£0.17/l), natural gas would need to cost in the region of £0.5/kg and hydrogen £2.25/kg. Based on the current prices for these fuels, the daily running cost of a bus travelling 250km per day is shown in table 2.4.

From this, it can be seen that methanol and natural gas look comparable in daily fuel costs to diesel.

³ based on a litre of diesel containing 35.7 MJ and duty on diesel of 15.05 pence per litre.

Table 2.4 Daily fuel cost for diesel ICE and fuel cell bus (250km)

Bus	Price	Daily cost	Price incl. duty ¹	Daily cost incl. duty
Diesel	£0.10/l	£15.13	£0.26/l	£29.13
Methanol fuel cell	£0.13/l	£21.93	£0.175/l	£29.52
Ethanol fuel cell	£0.30/l	£41.09	£0.36/l	£49.31
Natural gas fuel cell	£0.4/kg	£23.67	£0.51/kg	£30.81
Hydrogen fuel cell	£4.0/kg	£53.38	£4.35/kg	£58.04

¹ based on duty of 0.29p per MJ of fuel

At today's prices, fuel costs for diesel would total £121,000 over 12 years and for a methanol hybrid bus, fuel costs would be £153,000 over 15 years. This is of course assuming that methanol fuel duty is at the same rate as diesel, and does not take into account any changes in duties applied.

2.3.4 Lifecycle costs

The bus lifecycle costs combine all the above costs over the life of the bus. It has been assumed that a fuel cell bus will have a slightly longer life than a diesel bus. To take account of this, the lifecycle costs for a diesel and a methanol fuel cell bus have been normalised to a per km cost. Table 2.5 shows the assumptions and data used to calculate the NPV of lifecycle costs, and the normalised NPV/km lifecycle costs for these two types of buses. Although the fuel cell bus has a higher capital cost, the normalised running costs are marginally lower than the diesel bus. This is attributed to lower maintenance costs and longer bus life. As it is assumed that income will be the same for both buses, only the costs have been evaluated.

Table 2.5: Net present value of bus running costs

ASSUMPTIONS

	Fuel Cell	Diesel
vehicle life, years	15	12
km per year	86250	86250
km travelled	1293750	1035000
fuel cost per 250km £	29.52	29.13
capital cost £	170,000	115,000
operator overhead £/km	0.1	0.1
maintenance £/km	0.07	0.1
fuel £/km	0.12	0.12

NPV Diesel	0	1	2	3	4	5	6	7	8	9	10	11	12
outgoing (capital)	115,000						8,000						
operator overhead		8,625	8,625	8,625	8,625	8,625	8,625	8,625	8,625	8,625	8,625	8,625	8,625
maintenance		8,625	8,625	8,625	8,625	8,625	8,625	8,625	8,625	8,625	8,625	8,625	8,625
fuel		10,050	10,050	10,050	10,050	10,050	10,050	10,050	10,050	10,050	10,050	10,050	10,050
TOTAL		27,300	27,300	27,300	27,300	27,300	35,300	27,300	27,300	27,300	27,300	27,300	27,300
IRR	8.00%												
	NPV= £325,775												
	NPV/km= £0.31												

NPV Fuel Cell	0	1	2	3	4	5	6	7	8	9	10	11	12	13	14	15
outgoing (capital)	170,000					7,500		10,000	3,000		7,500					
operator overhead		8,625	8,625	8,625	8,625	8,625	8,625	8,625	8,625	8,625	8,625	8,625	8,625	8,625	8,625	8,625
maintenance		6,038	6,038	6,038	6,038	6,038	6,038	6,038	6,038	6,038	6,038	6,038	6,038	6,038	6,038	6,038
fuel		10,184	10,184	10,184	10,184	10,184	10,184	10,184	10,184	10,184	10,184	10,184	10,184	10,184	10,184	10,184
TOTAL		24,847	24,847	24,847	24,847	32,347	24,847	34,847	27,847	24,847	32,347	24,847	24,847	24,847	24,847	24,847
IRR	8.00%															
	NPV= £398,711															
	NPV/km= £0.31															

2.4 Constraints

Bus operators considering fuel cell power trains suggest that the reformer plus stack should take up no more than about 1m³ in volume. Added to this would be about 1-1.3m³ of battery power, and a fuel tank of up to 500l (0.5m³). A target weight for a fuel cell powered bus would be not more than 300-500kg heavier than a conventional vehicle (i.e. 12,000kg for a 12m bus) [Pedersen, P-L., 1998].

Table 2.7 compares the weight and powertrain constraints for a 12m conventional diesel bus with these outline targets for a hybrid methanol fuel cell bus with 50kW fuel cell stack.

Bus Type	12m conventional diesel - Europe	12m 50kW Fuel Cell Target
Gross vehicle weight	16,000kg	16,000kg
Curb weight	11,500kg	12,000kg
Driveline weight	1,500kg ⁽¹⁾	2000kg
Driveline volume	2.5m ³	2.8m ³ ⁽²⁾

¹ includes engine, gearbox, and fuel tank
² includes fuel processor, stack, batteries, and fuel tank (1m³ – f/c and reformer, batteries: 1-1.5m³. fuel tank. motor)

In Chapter 3, fuel processor projections and targets are given for methanol and natural gas fuel processors. And in Chapter 6, the projections for a methanol fuel cell hybrid bus power train weight, volume and costs are determined, including the fuel cell, fuel processor and other components, based on projections derived from a 20kW methanol FCS built under the CAPRI project.

3. ENVIRONMENTAL AND MARKET DRIVERS

Bus operators are subject to the policy of local authorities as well as national and European Union governments. An important driver for the introduction of fuel cell buses will be political decisions based on environmental considerations.

Present environmental standards, focus on the recognised emissions regulations (e.g. Euro 2 and Euro 3) for new buses or other measures, such as catalytic regenerative traps (CRT) and ultra low sulphur diesel (ULSD) fuel for older buses.

Although buses are only a small part of the total vehicle fleet and make a small contribution to ambient levels of air pollution, the visible nature of soot emissions makes them an easy target. If transport authorities wish to remove car traffic from city centres because of pollution, then the bus services they are contracting must be exemplary.

Through tendering regimes, a transit authority can specify that a service be met with ultra-clean vehicles. However, the additional cost of providing such a service would have to be met by the transit authority. London Transport for example has supported the introduction of ULSD and CRTs, whereas Swedish transit authorities have supported the introduction of ethanol buses.

Pollution in towns and cities can reach very high levels. The pollutants of most concern are NO_x, HC and CO. However, attention is increasingly turning to particulate matter (PM), noise, and globally, CO₂. Public transport is a particularly visible contributor to this pollution. To-date, bus operators have responded with conventional diesel buses meeting the tightest standards, or through alternative fuels. One driver for alternative fuels is concern over the ability of engine manufacturers to meet Euro 2 regulations, and more stringent Euro 3 and Euro 4 regulations. In the near term, diesel buses can be fitted with emission control systems, and cleaner fuels used. However, the fuel cell offers a more complete answer. Not only will the fuel cell bus⁴ lead to reduced emissions of regulated pollutants by some 95-97%, It will also use the fuel more efficiently, and result in lower CO₂ emissions.

Currently, an average urban bus emits 960g/km CO₂ (on a well to wheel basis), and 875 g/km as tailpipe emissions. For the total bus fleet in London, these tailpipe emissions add up to about 0.4 million tonnes CO₂ per year. With a hydrogen fuel cell bus, emissions would be reduced by 40% to 588 g/km (well to wheels) with zero from the tailpipe [Hart D., & Hormandinger G.,1997]. Fuel cells have added benefits of being quiet, and representing a more attractive form of transport than conventional diesel buses.

⁴Figures relate to fuel cell bus using hydrogen generated from natural gas

Table 4.1 shows tailpipe emissions from conventional, alternative fuel and fuel cell vehicles.

For Euro 3 there is no standard for SO₂ or CO₂, so these have been calculated based on 300 ppm sulphur in the fuel, and tank to wheel efficiency of 25.5%. There is very little emissions data available for fuel cell buses. Hydrogen systems will have zero emissions, and data for phosphoric acid buses indicate near-zero NO_x and very low levels of other emissions. Evaluation of actual emissions from a SPFC bus fed with reformed fuel will be important in demonstration and bus testing programmes.

Table 4.1: Tailpipe emissions from various power trains

	NO _x g/km	SO _x g/km	PM g/km	NMHC g/km	Methane g/km	CO g/km	CO ₂ g/km
EURO III standard (300 ppm sulphur)	4.4	0.19 ⁽¹⁾	0.09	0.58	N/A	1.9	875 ⁽¹⁾
Diesel (300 ppm sulphur or less)	15020	0.2-0.3	1.5	0.5-1.5	0.1	2-4	900-1200
Methanol ICE	5-15	0	0.05-1.0	3-30		1.5-3.0	600-1100
Ethanol ICE	5-20		0.05-2.0	0.1-10		2-20	690-1300
CNG ICE	1-20		0-0.05	0.5-1.3	3	0.15-25	600-960
Hydrogen ICE	0.01-1.0	0	0	0.02-0.3	0	0.06-0.4	1-8
GU 40 ft methanol fuel cell bus (IFC test results) ⁽²⁾	0		0	<0.06		0.12	
CNG fuel cell bus	0.07	0.004	0		0	0.003 ⁽³⁾	840 ⁽³⁾
Hydrogen fuel cell bus	0	0	0	0	0	0	0

(1) conversion to g/km: (g/kwh x energy use)/3.6, where energy use =16MJ/km x 20% efficiency

(2) based on data converted from g/bhp-hr allowing for 16 MJ/km

(3) based on data for large scale hydrogen production from natural gas

References: IEA AFIS 1996; F/02/00111/REP; DeLuchi, M A 1989

4. FUEL PROCESSOR MODELLING

Data from Wellman CJB, BG Technology and Johnson Matthey on fuel reformers were evaluated on their efficiency and suitability to produce hydrogen for a PEM fuel cell system for power generation in a bus. The FC system analysis comprises various elements, namely technical feasibility, system complexity, size and weight, efficiency, expected costs, etc.

To assess the technical feasibility and efficiency, heat and mass balances of a series of FC systems were simulated in Aspen. The simulations represent steady state systems, where the systems were optimised to produce 50 kWe net. The simulations are based on a number of assumptions, which are explained below.

4.1 Assumptions

A PEM fuel cell system can be divided in 5 sections, i.e. air and fuel supply, hydrogen generation, PEM fuel cell, exhaust burner, and cooling water circuit.

Air and Fuel Supply

- Inlet conditions of fuel and air are assumed to be 15°C and 1 bara.
- The efficiency of compressors and expanders are set to 65%.
- Pressure drop over heat exchangers are generally assumed to be 0.1 bar.

Hydrogen generation

- The hydrogen generation section comprises a feed preheater, reformer, catalytic CO clean-up or palladium membrane, anode fuel conditioner (condenser or humidifier, depending on the system). If necessary a high temperature shift (HTS) reactor and a low temperature shift (LTS) reactor are inserted after the reformer.
- Heat transfer is assumed to be 100%.
- The reformer and CO clean-up data are simulated according to data provided by Wellman CJB, BG Technology and Johnson Matthey
- Palladium membrane performance is based on conventional existing Palladium/Silver membranes. The hydrogen permeation is modeled according to experimental data [Ackerman F.J., Koskinas G.J.] (see Appendix B). The membrane was assumed to operate isothermally at 400°C with an in- and outlet pressure of 20 and 3.2 bara. The effect of temperature on the membrane surface area requirement was also evaluated by modeling the membrane performance at 300°C.
- The HTS reactor is assumed to be an adiabatic reactor, where the product is at equilibrium.
- The LTS reactor is assumed to be an adiabatic reactor, with a CO exit value of 0.6% (ie. about 90% of equilibrium conversion)

PEM Fuel Cell

- The fuel cell air and fuel inlet conditions are 85°C, 3 bara and fully humidified.
- Heat required to humidify the air is supplied by the fuel cell.
- The voltage efficiency is set to 50% (0.625 V/cell).

- The anode hydrogen utilisation (AHU)⁵ is assumed to be 80% for the base case calculations. System simulations have also been performed with AHU = 90%. If a palladium membrane is used in the system, the hydrogen utilisation is assumed to 100%
- The cathode stoichiometry is set to 2.

The fuel cell has a separate cooling water circuit of 1.06 kg/s. The fuel cell cooling water is cooled with the system cooling water, where the cooling requirement is based on the heat generated by the fuel cell minus the heat requirement for the cathode air humidification.

Exhaust Burner

The exhaust burner combusts all combustible components in the anode off-gas, ie. mainly hydrogen and traces of unconverted feedstock. If necessary, the burner is also used to combust additional fuel to provide the reformer and / or other units in the system with the required heat. The cathode exhaust is used as the oxygen source for the burner. This allows for the burner to be operated at elevated pressure. After heating the required system units, the burner product is expanded in an expander. The power generated by the expander contributes to the decrease in the compressor power requirement.

Cooling Water Circuit

The cooling water circuit provides cooling for the cathode product condenser, the fuel cell cooling water, and to any other unit in the system that needs it. The cooling water flow rate is 1 kg/s. It in turn is cooled by ambient air to 45°C. The air is supplied by a fan at a pressure of 1 mbarg, with an inlet temperature of 25°C. The air flow rate depends on the cooling requirement of the system and is based on an air temperature rise of 10°C.

4.1.1 Sensitivity of Assumptions

The system efficiencies are simulated based on a maximum net power output of 50 kWe. At the maximum power conditions the fuel cell efficiency is set to 50%, while the compressor/ expander efficiency are assumed to be 65%.

The fuel cell voltage efficiency at the maximum rated power output depends on the number of cells (ie. stack size), the reformate composition, the stack technology, and the operating conditions. A typical efficiency dependence on the relative fuel cell power output is shown in Figure 4.1. The fuel cell efficiency increases with decreasing power output. This is an important property of the fuel cell, when it is used for transport applications, since the maximum power load is required during a relatively short part of a drive cycle.

⁵ The fractional anode hydrogen utilisation is the inverse value of the anode stoichiometry, ie. AHU's of 80% and 90% correspond with stoichiometries of 1.25 and 1.11

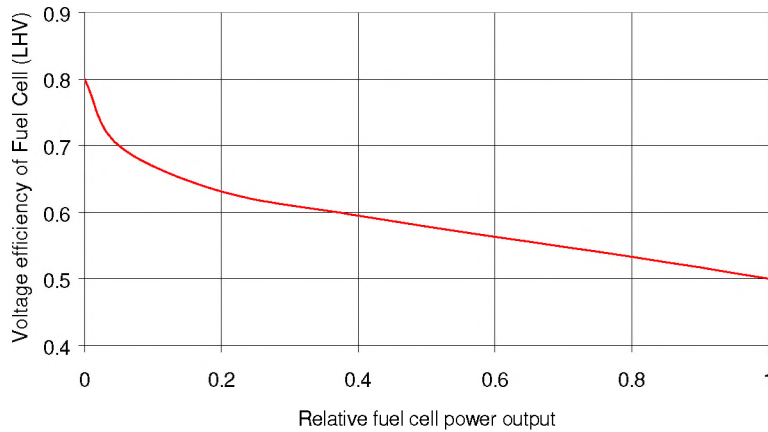


Figure 4.1: Fuel Cell efficiency vs relative power output

The compressor/ expander efficiency is also a function of power output, and generally increases with increasing load. A typical compressor/ expander efficiency curve is shown in Figure 4.2. This is a rather arbitrary curve, and may vary for the various types of compressor/ expander systems.

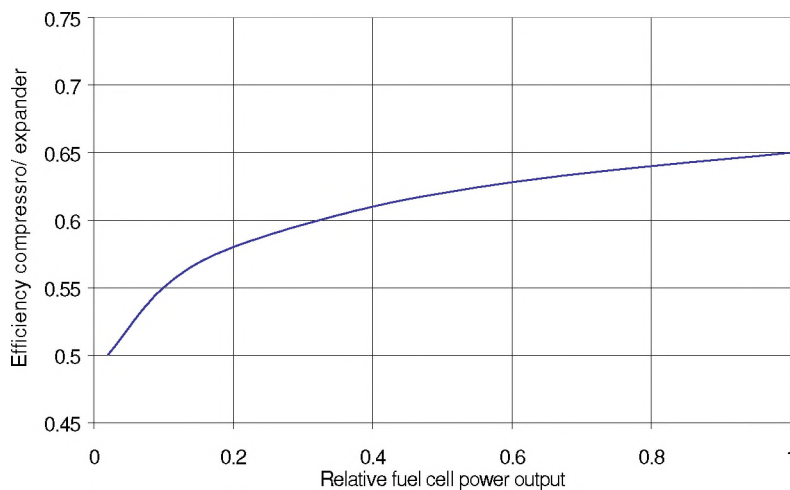


Figure 4.2: Compressor/ Expander efficiency vs relative power output

The combined effect of the increasing voltage efficiency and decreasing compressor/ expander efficiency is evaluated for System 2a, Johnson Matthey's base case system. The result is presented in Figure 4.3. This shows that the expected system efficiency increases with decreasing load. In this example the maximum NSE ranges from 30-50% of the maximum load. At 10% of the maximum load the efficiency is calculated to be the same as at 100%.

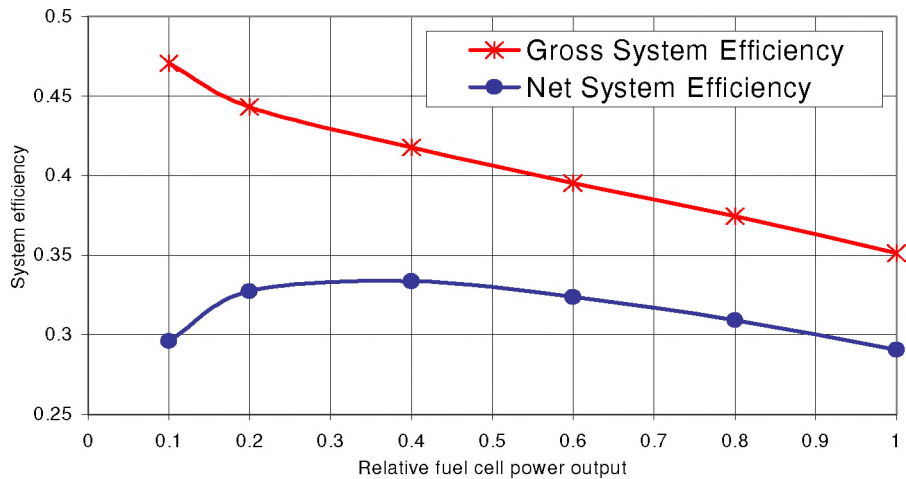


Figure 4.3: Gross and net system efficiency with varying load

Another assumption is that the heat transfer efficiency is 100%, i.e., the system does not lose any heat. Although this will never be completely true, the heat losses can be kept to a minimum through insulation of the process units. Good insulation will add to the volume of the system, but will be necessary as various system units operate at different temperatures.

4.2 Definitions

To evaluate the performance and feasibility of the various systems a number of parameters have been defined rating the systems' efficiency, size, complexity, and expected transient performance.

Efficiency

The net system efficiency (NSE) is defined as:

$$NSE = \frac{\text{net electrical power FC}}{LHV \text{ of fuel}} = \frac{50 \text{ kWe}}{\text{feed} \left(\frac{\text{mol}}{\text{s}}\right) \times LHV \left(\frac{\text{kJ}}{\text{mol}}\right)}$$

The net electrical power from the fuel cell is defined as the gross electrical power less the parasitic power requirements (see figure 4.4).

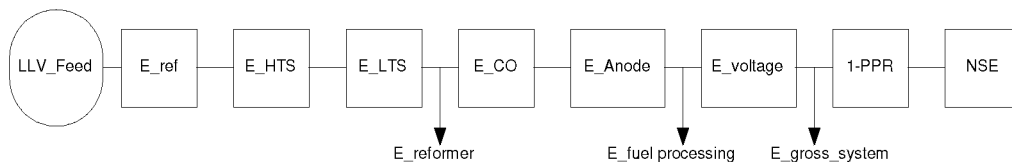


Figure 4.4: Efficiency losses in the conversion of a fuel to electrical power

The parasitic power is the sum of the power requirements for the liquid pumps, compressor(s), and radiator fan minus the power generated by the expander. To quantify the parasitic power demand of the system, the parasitic power ratio (PPR) is used.

$$PPR = \frac{\text{parasitic power demand}}{\text{gross electrical power FC}}$$

Although it is not of importance to the overall system efficiency, it is of interest to compare the efficiencies of each step in the hydrogen generation process. This allows us to assess which unit operations mainly contribute to the losses in the system (theoretical efficiencies for reforming methanol and methane are shown at the end of this Chapter). The efficiencies can be calculated by dividing the LHV of the hydrogen present in the stream after each unit by the LHV of the feed to each unit. Multiplication of all calculated efficiencies results in the net system efficiency.

Other important efficiency numbers are the reformer efficiency and the fuel processing efficiency. The reformer efficiency includes the efficiencies of the shift reactors in case they are part of the system, and is based on the total fuel feed supplied to the system. The fuel processing efficiency includes the CO clean-up efficiency and losses due to incomplete hydrogen utilisation at the anode. Table 4.1 summarises the lower and higher heating values of the feedstocks evaluated in this study.

Table 4.1		Methanol	Ethanol	Natural Gas*	Hydrogen
LHV	kJ/mol	638.51	1234.90	824.45	241.83
HHV	kJ/mol	726.53	1366.93	913.44	285.84

* Values based on natural gas composition provided by BG Technology

System Size and Complexity

The reformer, CO clean-up, and palladium membrane size are evaluated based on information provided by Wellman CJB, Johnson Matthey and BG Technology. It is beyond the scope of this project to determine the size of every unit in the system, but instead we will indicate the type and number of units required. The combination of this information will position us to distinguish the technically more feasible systems.

Dynamic performance and start-up

The dynamic performance and start-up characteristics of a fuel cell system depend on many parameters, eg. thermal mass, heat transfer properties, reaction rate, system complexity, control, etc. Dynamic performance and start-up data will be estimated based upon experience with existing reformers by the various contractors.

4.3 FC System Simulation Results

Based on the reformer and CO clean-up data provided by Wellman CJB, Johnson Matthey and BG Technology, a total of 12 system variants were simulated.

- 1) Wellman CJB Methanol Steam Reformer:
 - a Base Case
 - b anode utilisation = 0.9
 - c no expander
 - d Pd membrane CO clean up

- 2) Johnson Matthey HotSpot Reformer
 - a Base Case
 - b anode utilisation = 0.9
 - c Pd membrane CO clean up
 - d ethanol
 - e natural gas including LTS reactor
 - f natural gas without shift reactor

- 3) BG Technology Natural Gas Reformer
 - a Base Case
 - b anode utilisation = 0.9
 - c Pd membrane CO clean up

Appendix C provides details of the systems simulated, and Appendix D provides the block schemes, and simulation results of each base case simulation. A summary of the unit requirements for each system can also be found in Appendix D, Tables D.1 and D.2.

4.3.1 System simulation: Wellman CJB Results

Table 4.2 shows the calculated system efficiency results. The NSE for the base case was calculated to be 31%. The most efficient system was calculated to be system 1d, with a Pd membrane instead of a catalytic CO clean-up system. System 1b showed a significant drop in efficiency. This was due less hydrogen off gas being available to burn for heat. However, overall, it has no impact on the system efficiency.

Table 4.2: System efficiency results for Wellman CJB reformer (%)

System	1a	1b	1c	1d
Reformer	94.6	83.4	97.3	91.2
CO clean-up	99.5	99.5	99.5	88.0
Anode	80.0	90.0	80.0	100.0
Voltage	50.0	50.0	50.0	50.0
Parasitic power	83.1	83.8	75.6	86.8
NSE	31.3	31.3	29.3	34.8

However, the cost of the Pd for the membrane system alone amounts to \$76,000 - 94,000. To put this in perspective, this is 1500-1900 \$/kWe while the PGNV goal for the complete fuel processor is \$10/kWe. Although for a bus the cost target may perhaps be a little less demanding, the Pd membrane would be a very expensive system component.

4.3.2 System simulation: Johnson Matthey Results

Table 4.3. shows the calculated system efficiency results. The base case, net system efficiency was calculated to be 29.1%. By increasing the anode utilisation, the NSE rises to 32.4%. The HotSpot reformer system equipped with a membrane also shows an improved efficiency value compared to the base case. The membrane benefits the system in two ways - (i) the combined CO clean-up and anode efficiency is increased; and (ii) the parasitic power is reduced. The latter is perhaps somewhat surprising, but can be explained as follows. In system 2c the air required for the reformer is compressed to 20.5 bar, which increases the parasitic power. In return, a relatively large bleed stream from the membrane is let down in a second expander, decreasing the PPR. The net result is a higher NSE than the base case system. However, it should be realised that system 2c comprises a two-stage compressor and expander additional to the normal air compressor and expander present in the base case system. The estimated Pd cost for the membrane makes this option too expensive.

A HotSpot system fuelled with ethanol is expected to perform similarly to a methanol system, provided an effective catalyst can be developed. A separate LTS reactor may or may not be necessary, depending on the operating conditions of the reformer. The system calculations here include an LTS reactor.

As mentioned previously, the system simulations for Natural Gas HotSpot reformer are based on preliminary experimental results. With further efforts to optimise the reformer operating conditions it is expected that we will be able to increase the reformer efficiency, and hence the net system efficiency.

Table 4.3: System efficiency results for Johnson Matthey HotSpot reformers (%)

System	2a	2b	2c	2d	2e	2f
Reformer	92.6	92.6	92.6	82.8	83.3	83.3
LTS reactor	-	-	-	106.1	104.3	-
CO clean-up	94.8	94.8	79.0	97.2	96.9	91.1
Anode	80.0	90.0	100.0	80.0	80.0	80.0
Voltage	50.0	50.0	50.0	50.0	50.0	50.0
Parasitic power	82.8	82.1	87.7	83.7	81.7	79.6
NSE	29.1	32.4	32.1	28.6	27.4	24.2

4.3.3 System simulation: BG Technology Results

The BG Technology reformer distinguishes itself from Wellman CJB and Johnson Matthey's reformer by the fact that it operates on natural gas. Higher temperatures are required to reform NG, resulting in more CO in the reformat. Hence, the BG Technology systems need shift reactors to generate a suitable reformat for a PEM fuel cell system.

The results are summarised in Table 4.4. The NSE base case BG Technology reformer system was calculated to be 28.1%. Increasing the anode utilisation from 80 to 90%, improves the net system efficiency to 30.8%. Applying a Pd membrane instead of a catalytic CO clean-up is not an interesting option. Apart from the required number of membranes, the conversion of methane (natural gas) conversion is inversely dependent on the reforming pressure. A lower conversion decreases the system performance, due to excessive waste heat generated in the system. The loss in conversion at elevated pressures could possibly be minimised by more closely integrating the reformer with the membrane, like using a membrane reactor or a staged reactor system with multiple reforming and Pd membrane separation sections.

Table 4.4: System efficiency results for BG Technology reformer (%)

System	3a	3b	3c
Reformer	72.9	72.9	52.8
HTS reactor	109.6	109.6	109.3
LTS reactor	106.3	106.3	102.0
CO clean-up/ membrane	98.1	98.1	90.0
Anode	80.0	90.0	100.0
Voltage	50.0	50.0	50.0
Parasitic power	84.3	88.2	88.7
NSE	28.1	30.8	23.5

4.4 Discussion on Fuel Processor Modelling Results

4.4.1 Fuel Processing Efficiencies

Figure 4.5 shows the Reformer and CO clean-up efficiencies for all simulated systems except for the systems based on Pd membranes. The efficiencies are expressed in losses, ie. starting with a LHV of the fuel of 100%, Figure 4.5 shows the losses due to reforming (including shift reactors if they are present in the system) catalytic CO clean-up. Figure 4.3 includes reformer efficiency data of ADL's (Epyx) partial oxidation process [Mitchel, W.L., 1998]. The losses in the catalytic CO removal are estimated based on the use of Demonox for this process.

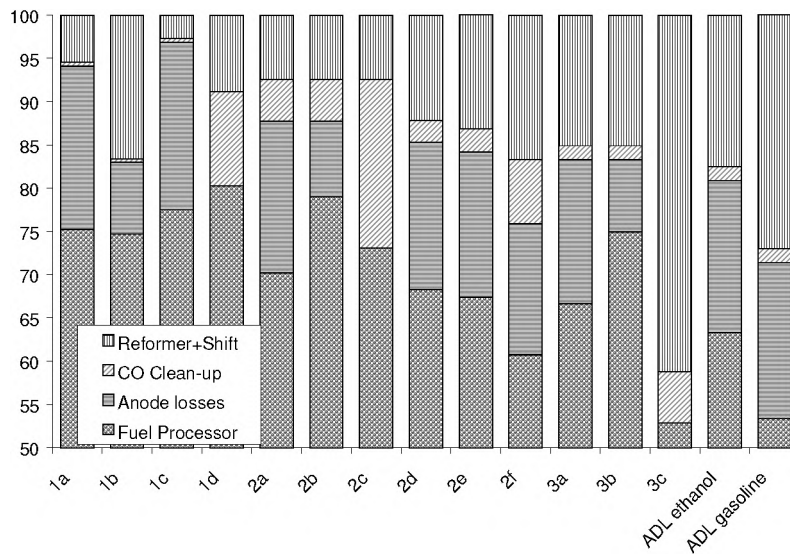


Figure 4.5: Calculated efficiencies for various fuel processors

Reforming

Figure 4.5 demonstrates that with Wellman CJB methanol steam reformer, efficiencies of 95% and higher can be reached (systems 1a and 1c). The efficiency of Johnson Matthey's methanol HotSpot reformer is calculated to be almost 93%. These efficiency values do not account for heat generated by the unutilised anode hydrogen, which is also used to provide heat for the reformer.

Comparing the performance of Johnson Matthey's HotSpot reforming of ethanol and ADL ethanol POx reformer, HotSpot reforming is expected to be a more efficient process than POx, based on the fact that HotSpot reforming is a catalytic process. ADL's POx reformer consists of two sections - partial oxidation in the gas phase followed by catalytic stage equilibrating the product. When partial oxidation is performed in the gas phase some of the oxygen fed to the system is expected to produce H₂O or CO₂ rather than CO. However, it should be noted that the HotSpot ethanol data are estimated and not based on experimental work.

BG Technology's Natural Gas reformer shows an efficiency (83-85%), similarly to the expected efficiency of a HotSpot NG reformer (83-87%). However, it is expected that HotSpot can be operated without shift reactors or with one LTS reactor, depending on whether system size and dynamic performance are more important than efficiency.

Caution should be taken while comparing reformer efficiencies operating on different fuels. In doing this the efficiency of the production of the fuel, as well as losses during fuel storage and transportation need to be taken into account.

Catalytic CO clean-up

The efficiency of the catalytic CO clean-up depends on the initial CO concentration and on the CO clean-up system itself. Data provided by Wellman CJB indicate a very efficient system. In addition the CO concentration from the reformer is very low as well (0.6%), and the efficiency of Wellman CJB's CO clean-up is calculated to be 99.5%. However, the system operates at a very low inlet temperature of 16°C. This is not a practical temperature on board a vehicle, and can not always be reached, unless a refrigeration system is installed onboard the vehicle. For a 50 kW system, the required cooling power to cool the reformat is 5-6 kW.

Johnson Matthey's catalytic CO clean-up system Demonox is designed to operate with an inlet temperature range of 130-150°C. Because it operates at higher temperatures, the efficiency is slightly less than Wellman CJB's CO clean-up. For a CO concentration of 0.6%, the CO clean-up efficiency is expected to be about 98%.

Demonox can be tailored to remove CO concentrations of up to 3%. Preferential oxidation of CO can only be performed at the expense of system efficiency. This can sometimes eliminate the need for a LTS reactor, which may make the system smaller and have a better dynamic and start-up performance.

Anode losses

For each of the three reformers, the systems were simulated with an anode utilisation of 80% and 90%. In reality the anode utilisation depends on the fuel cell design and the initial hydrogen concentration of the reformat, but at present the effect of a higher anode utilisation on the fuel cell efficiency is not well understood. Operating the fuel cell at a higher anode utilisation, will result in a lower hydrogen concentration on the anode side. Lower hydrogen concentrations may result in an increase in the mass transport resistance at the anode.

Table 4.5	Wellman CJB Methanol SR	Johnson Matthey Methanol HotSpot	BG Technology NG SR
[H ₂] wet	60.0 %	43.0%	61.3 %
flow rate	3.73 kmol/hr	5.23 kmol/hr	3.60 kmol/hr

In the three systems simulated here the hydrogen concentrations and total flow rates at the anode inlet vary. Depending on where the mass transport resistance is most predominant, a high flow rate will contribute to improved mass transfer between the gas phase and the anode catalyst layer, while a higher concentration will improve the mass transfer through the anode catalyst layer. Table 4.5 summarises the anode feeds calculated for the three base case systems.

The anode utilisation is an important factor for the *overall* system efficiency, in particular in systems where more heat is generated than required in the various process steps. JM's HotSpot and BG technology NG system both benefit significantly from a higher anode utilisation. Under the base case assumptions, both systems produce waste heat. It is also expected that ADL's partial oxidation systems benefit from a higher anode utilisation, and fuel processor efficiencies for these systems may therefore reach in the order 73% and 63% respectively.

Wellman CJB's system is expected to be more or less independent of the anode utilisation, as the base case system does not have heat to spare, although as for all systems a higher anode utilisation also means a smaller reformer, CO clean-up, shift reactors etc.

Fuel Processor

The calculated fuel processor efficiencies are summarised in Table 4.6. Comparing the methanol fuel processor efficiencies (1a-2c), the values are calculated in the range of 70-80%. This is 15-25% lower than the theoretical maximum value. In the Wellman CJB system the losses are mainly caused by the fact that the reformat is cooled to low temperatures before the CO clean-up. In Johnson Matthey's system the losses are dominated by the amount of CO in the reformat and its' removal.

Table 4.6: Calculated FP efficiencies and estimates for ADL POx reformer

1a	1b	1c	1d	2a	2b	2c	2d	2e	2f	3a	3b	3c	EtOH ADL	petrol ADL
75.3	74.7	77.5	80.3	70.2	79.0	73.1	68.3	67.4	60.8	66.6	72.8	52.9	63.4	53.4

Comparing JM's (2d) and ADL ethanol systems the efficiencies are calculated to be 68 and 63 % respectively. Both systems will become more efficient with a higher anode utilisation. Losses are mainly caused by CO and waste heat production.

Comparing the systems based on natural gas (2e-3c), the fuel processor efficiencies are calculated in the range of 60-73%. In JM's NG HotSpot systems with a LTS reactor (2e), losses are mainly caused by excess heat production. An efficiency penalty is to be paid for a simpler system without shift reactors (2f). BG NG fuel processor efficiency (3a) is expected to have an efficiency of about 67%.

The effect of a higher anode utilisation is an efficiency increase of 6%. Similar efficiency increases can also be expected for JM's NG HotSpot fuel processors operating at a higher anode utilisation. Note that the NG systems require an additional condenser or fresh water supply, since the condensate from the cathode condenser is not sufficient to make-up the reformer feed.

4.4.2 Comparison of System Efficiencies

Figure 4.6 shows the calculated efficiencies for the various systems, with systems 1a-d based on Wellman CJB's steam reformer and CO clean-up, systems 2a-f based on Johnson Matthey's HotSpot reformer, and 3a-c based on BG Technology's Natural gas reformer. Net system efficiencies of all simulated systems were calculated in the range of 23 to 35%. The NSE for the three base case systems and systems with the anode utilisation of 0.9 are summarised in Table 4.7.

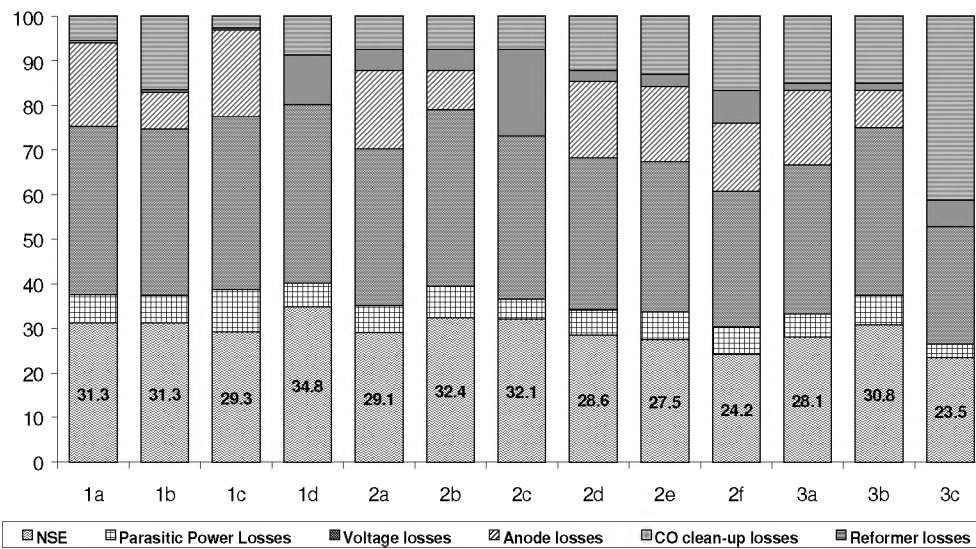


Figure 4.6: System losses and net efficiencies for all simulated systems

This table shows that the WCJB NSE is independent of the anode utilisation, and calculated to be 31.3%. JM NSE is calculated to be 29% for the base case, but increases to 34.4% with a higher anode utilisation. BG NSE are 28 and 30.8% respectively. The increase in efficiency with increasing anode utilisation, is the result of a better use of the available heat in the system, while less heat is vented to the environment. It is clear that operating with a higher anode utilisation benefits the JM and BG systems. The efficiency Wellman CJB steam reformer system will increase to at least the efficiency of Johnson Matthey’s HotSpot system through using a different CO clean-up system. The cooling and heating of the reformat before and after the CO clean-up in the proposed system limits the efficiency.

Table 4.7: NSE for base case and increased anode utilisation

	W-CJB	JM	BG Tech
Base Case	31.3	29.3	28.1
Anode Utilisation = 90%	31.3	34.8	30.8

The parasitic power losses can predominantly be ascribed to the air compressor, while the radiator fan is the second largest demander. The expander contributes positively to the losses.

Table 4.8 lists the parasitic power ratios for the simulated systems.

Disregarding the estimated PPR’s for the membrane systems (1d, 2c, 3c), the PPR is typically in the range of 16-20%. The PPR for JM’s HotSpot systems would be expected to be larger than for systems where no air is fed to the reformer. The compressor load is indeed higher (~15%). However, due to the larger flow rates through the expander, the net PPR is only marginally larger. Comparing the calculated PPR for system 1a and 1c, shows the impact of the expander. By combining the anode and cathode exhausts as expander feed, typically 30-40% of the power required by the compressor is regained by the expander.

Table 4.8: Calculated parasitic power ratios in %

1a	1b	1c	1d	2a	2b	2c	2d	2e	2f	3a	3b	3c
16.9	16.2	24.4	13.3	17.2	17.9	12.3	16.3	18.3	20.4	15.7	17.8	11.3

The calculated PPR's for the membrane systems are significantly lower than for the base case systems. This is the result of the contribution of a second expander driven by the high pressure (20 bar) membrane bleed. As mentioned earlier, the technical feasibility and costs make a membrane separator on-board a vehicle unlikely.

4.4.3 Other system considerations

System feasibility and complexity

The simulated systems vary in complexity. Complexity can be captured by the number of unit operations, and the way they connect. For example, some heat exchangers are simulated to exchange heat between one or more downstream process stream and an upstream process stream. Such unit operations are feasible under steady state operating conditions, but may become difficult to operate under varying load conditions, depending on the system's response time. However, in order to reach higher system efficiencies the systems need to be better integrated.

Comparing the base case systems, the Wellman CJB and Johnson Matthey system would be of a similar complexity. Wellman CJB's system has the advantage that no air is needed in the reformer, which makes for a simple compressor. Disadvantage of this system is that the reformat stream is cooled against the methanol feed, and subsequently cooled to very low temperatures (preferably < 20°C, but in the model simulations to 50°C). The resulting system includes several multi-stream heat exchangers. As mentioned earlier, it is unknown what the effect of a higher operating temperature on Wellman CJB's CO clean-up has.

The BG Technology systems require shift reactors. Although shift reactors are reasonably elementary, they are generally fairly large. Additionally, they do not function until they have reached a certain temperature, and will invariably impact negatively on the dynamics and start-up of the system.

Systems including Pd membranes to separate the hydrogen from the other products in the reformat stream are not feasible from a cost standpoint. The Pd cost alone was estimated to be in the range of 1500-2500 \$/kWe. However, estimations were based on conventional unsupported Pd membranes. Progress is being made in the development of supported Pd membranes with Pd layers a factor 15 to 20 lower than the conventional type. This may perhaps still be too expensive for transport applications, but for stationary fuel cell systems this cost is conceivable. In particular, a steam reformer Pd membrane combination may yield high system efficiencies, while the system remains simple.

Combining a HotSpot reformer with a Pd membrane is also expected to yield good system efficiencies, but at a cost of a more complex system. A NG steam reformer is not very compatible with a Pd membrane separation system, since the equilibrium conversion of methane decreases significantly with pressure. Hence the reformer would need to be operated at very high temperatures, which is undesirable from a materials standpoint.

The expected sizes of a reformer (including anode off-gas/ fuel burner) and CO clean-up for the three different reformers are summarised in Table 4.9. This provides an idea of the size and volume of the main fuel processor system, including the fuel reformer, CO removal and anode off-gas/ fuel burner. Most reformers built to date are prototypes or lab test units. Such units are not usually designed and built to optimise weight and size, but for ease of testing and data gathering. The values in Table 4.9 are based on different levels of system development, ranging from extrapolated laboratory data, to prototypes. Targets are also included to give an indication of the desired reductions in size weight and cost. Hence, the numbers in Table 4.9 may vary substantially once several scaled-up versions have been built.

Table 4.9: Size, weight, costs for fuel processing system¹ (50 kW net output)

FP System	Power density kg/kW	Specific Power litre/kW	Cost £/kW
W-CJB, processor estimate based on 10 kW breadboard system	12	12	150
W-CJB, processor target based on targets for Joule 50 kW	2.5	2.5	25
JM, processor estimate based on 20 kW prototype CAPRI	2.8	11	600
JM, processor target based on 20 kW prototype CAPRI	1.5	3	35-40
BG reformer estimate ²	0.4	0.35	230
BG processor estimated target	1.9	3.5	?

¹ Fuel processor and CO clean up only, excluding compressor, pipes, valves, controls etc

² These values were provided by BG Tech for reformer only without insulation

³ Estimate for fuel processor size and weight based on BG Tech reformer plus JM CO clean-up and shift reactors.

Wellman CJB provided weight, volume, and cost *estimates* based on breadboard experience for a reformer plus CO clean-up, and on deliverable targets for the Joule project. With respect to the latter projection a 50 kW reformer plus CO cleanup system would weigh 125 kg and take up 125 litre.

Johnson Matthey has built a 20 kW methanol reformer for the CAPRI project, so size and costs are based on this *practical* experience. This reformer is currently being tested at ECN and will subsequently be integrated in a VW Golf. This system includes a HotSpot reformer, a Demonox CO clean-up, and a catalytic afterburner. The projected size is still rather large, but a considerable amount of the volume is the result of volume

between units, rather than the actual unit sizes. The weight of this system is high, but largely over-engineered like prototypes tend to be.

It is expected that with the CAPRI experience Johnson Matthey's methanol HotSpot system can be substantially improved. The specific weight is projected to <3 litre/kW, while the power density is expected to 1.5 kg/kW or lower.

BG Technology provided weight and volume *estimates* for the reformer alone, without including insulation. The dimensions of the BG Technology reformer are expected to be 34x26x20 cm, with a weight of about 20 kg. A crude estimate is made for the size and weight of the fuel processor system, including shift reactors and CO clean-up.

To complete the system, heat exchangers, valves, actuators, controls, pumps, compressor/ expander, piping and insulation need to be added. The total system size and volume should therefore expected to be considerably larger than the projected numbers in Table 4.9 (see also section 5.2). Table 4.10 identifies the main components of the fuel processor system.

Table 4.10: Estimated system units

System	Wellman CJB (MeOH)	JM (MeOH)	BG (NG)	JM (NG)
liquid pump	4	4	3	3
compressor	1	1	2	1
expander	1	1	1	1
reformer	1	1	1	1
shift reactors	0	0	2	0
CO clean-up/ membrane	1	1	1	1
catalytic burner	1	1	1	1
vaporiser	1	1	1	1
condenser	1	2	3	3
heat exchanger (l/l)/(g/l)/(g/g)	1/3/2	1/2/0	1/3/0	1/2/1
fan	1	1	1	1
Total number of units	18	16	20	16

Dynamic performance and start-up

Dynamic performance and start-up times depend on many factors and are hard to estimate. Start-up times are a function of the total thermal mass in the system, the required operating temperatures, as well as system control. The PEM fuel cell start-up time has proven to be relatively fast, producing >90% of the expected power within seconds upon feeding suitable reformat. The rate determining step in the start-up process is therefore the time it takes to produce a reformat suitable for the fuel cell. This depends on the reformer and the CO clean-up. Partial oxidation reformers are generally self-starting and can therefore be expected to produce reformat faster than steam reformers. Steam reformers first need to be heated to a certain operating temperature before they can start producing reformat, or heat is generated in a separate reactor and transferred to the reformer. With the more recent plate reactor designs this start-up time will be decreased, but these reactors are still in a development phase.

Once reformat is produced, the CO must be removed. Start-up time for CO clean up depends on the clean-up system and the CO content in the reformat. If only a little CO is produced during start-up, a catalytic system can be run from ambient by burning some of the hydrogen to bring the system to its operating temperature. On the other hand, if the CO content in the reformat is much higher than under steady state conditions, start-up of the clean-up may be delayed due to the catalyst poisoning properties of CO.

Palladium membranes do not function below 250°C, and should really be heated to above 300°C before they can start operating properly. Similarly, shift reactors also require a certain operating temperature at which the catalyst becomes active. Membranes and shift reactors will slow down the system start-up time.

Factors that impact on the dynamic performance of a system are more difficult to pinpoint. Minimising the system's volume (reactor and tubing) and weight generally optimises response times. However, since the response times of the different unit operations vary, good system control is required based on reliable measurable system parameters.

Wellman CJB describe that their 10 kW breadboard would produce suitable reformat in 15 minutes while it could take up to 2 hours before "steady state" was reached. However this system was not optimised for start-up, the catalyst bed-depth being too large. A better designed packed bed should start up in minutes - depending whether it is heated by direct catalytic combustion, by convective heat transfer from combustion products, or indirectly via a heat transfer medium.

The target start-up time for the plate reactor reformer in the Joule project is 5 seconds to produce a usable reformat. Within this project Wellman CJB are able to get to reforming temperatures in less than a minute, but this is still in a testing and evaluation stage.

Johnson Matthey has achieved start-up times of ~ 10 minutes with a 5 kW HotSpot reformer plus Demonox, where the system was not controlled but started with the feed setting as during steady state operation. With the reformer itself start-up times of ~ 50 seconds are achieved, once the feed is vaporised. In both cases the start-up time includes the time it requires to pump fluids to the reformer. It is expected that the start-up time of the system can easily be reduced to 30-60 seconds.

The HotSpot reformer can be started under self-starting partial oxidation conditions. As soon as the temperature reaches a certain temperature, the feed can be changed to "normal" operating conditions. One of the characteristics of the HotSpot reformer is that it produces very little CO during start-up. Hence it is expected that the CO clean-up system start-up time will be minimal. It is the aim within the CAPRI project to produce a reformat suitable for the fuel cell at all times, even though the initial hydrogen content may be relatively low.

BG Technology notes that there is a compromise between fast start-up and reformer life time. Although the construction of the reformer will allow it to heat very rapidly, this may happen at the expense of thermal fatigue. BG Technology suggests that a start-up

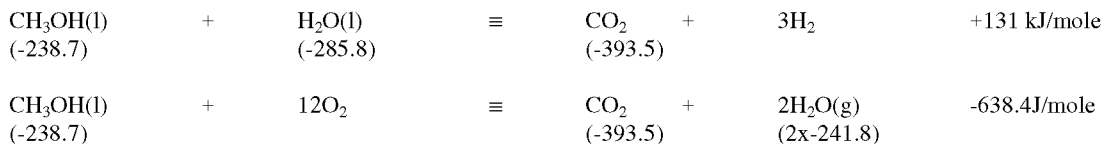
of 10 minutes to reach 100% throughput may provide a reasonable compromise between start-up and life time.

With regard to the transient response of the reformer, BG Technology expects there will be no substantial change in reformer product composition if the changes are smooth. It was suggested that a significant load change of 50% should be achievable within one minute. Note that the estimates for the transients and start-up do not take the shift reactors into consideration.

Theoretical efficiencies

On-board a vehicle heat required for fuel steam reforming will be generated through oxidation of the same fuel. If available, part of the heat load may come from other sources, like heat from anode exhaust burner. Heat from the fuel cell is not useful to the system, because it generated at too low a temperature. In this study the fuel processor efficiency is subdivided in reformer efficiency, CO clean-up efficiency, and anode utilisation (see Figure 4.2)

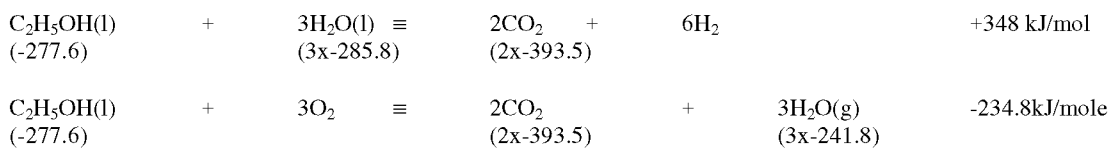
For methanol the theoretical efficiency can be calculated based on the steam reforming and combustion reactions, where it is assumed that the reactants are liquids, while the combustion product is in the vapour phase (values between parentheses correspond to the heat of formation in kJ/mole).



From the heats of reaction, it can be calculated that 0.205 (=131/638.4) mole of methanol needs to be combusted, to provide enough heat to reform 1 mole of methanol. The theoretical efficiency of the methanol reforming process can therefore be calculated as:

$$\textit{Theoretical efficiency CH}_3\text{OH reforming} = \frac{3 \cdot \text{LHV of H}_2}{1.205 \cdot \text{LHV of methanol}} \cdot 100\% = 94.3\%$$

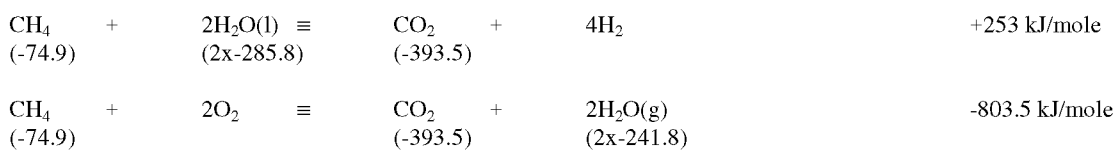
Similar calculations can be performed for ethanol and methane. For ethanol the theoretical efficiency can be calculated based on the partial oxidation combined with shift and combustion reactions, where it is assumed that the reactants are liquids, while the combustion product is in the vapour phase.



From the heats of reaction, it can be calculated that 0.28 (=348/1234.8) mole of ethanol needs to be combusted, to provide enough heat to reform 1 mole of ethanol. The theoretical efficiency of the ethanol reforming process can therefore be calculated as:

$$\textit{Theoretical efficiency C}_2\text{H}_5\text{OH reforming} = \frac{6 \cdot \text{LHV of H}_2}{1.28 \cdot \text{LHV of ethanol}} \cdot 100\% = 91.8\%$$

For methane the above reactions can be written as follows.



From the heats of reaction, it can be calculated that 0.315 (=253/803.5) mole of methane needs to be combusted, to provide enough heat to reform 1 mole of methane. The theoretical efficiency of the methane reforming process can therefore be calculated as:

$$\textit{Theoretical efficiency CH}_4 \textit{ reforming} = \frac{4 \cdot \text{LHV of H}_2}{1.315 \cdot \text{LHV of methane}} \cdot 100\% = 91.6\%$$

For each fuel the maximum fuel processor efficiency is calculated to be 91-95%. In practice, the efficiency will be lower as a result of the production of CO and unutilised heat, i.e. available heat in exhaust streams or cooling with cooling water circuit, as well as water to fuel feed ratio larger than stoichiometrically required.

5. CONCLUSIONS OF PHASE 1

The decision about which reformer to take forward to Phase 2 of the project was based on a number of criteria. These include:

- Fuel processor system performance
- Fuel processor system complexity
- Suitability for use on a vehicle
- Projected size and weight of fuel processing system
- On board fuel storage volume, and refuelling times
- Ease of fuel processing
- Processor developmental status (research, pilot scale, prototype, demonstration)
- Fuel cost implications

All the simulated systems are expected to both reach efficiencies of about 30% at full power output (see Table 5.1).

Table 5.1: Net system efficiencies of reformer systems

	Base case	Anode utilisation 0.9	Pd membrane
Wellman CJB	31.3%	31.3%	34.8%
JM Methanol	29.1%	32.4%	32.1%
BG Technology	28.1%	32.1%	23.5%

The most efficient system was calculated to be Wellman CJB's with a palladium membrane instead of catalytic CO clean up. However, due to the high cost of the Pd required in these systems (£2400-4000/kWe), they can be disregarded for transport applications. Thin film supported palladium membranes may offer a lower cost alternative, but at £120-200/kWe even these are probably too expensive. Johnson Matthey's system, including catalytic CO clean-up is reasonably efficient and can be tailored for various reformat streams. WCJB's system, using catalytic CO clean up shows slightly higher net efficiency than the Johnson Matthey system. This is due to the very high efficiencies of WCJB's catalytic CO cleanup. However, this operates at very low inlet temperatures that cannot always be reached on board a vehicle unless refrigeration is used. BG Technology NG reformer is expected to reach slightly lower net efficiencies, but is still comparable to the methanol reformers.

The issue of weight differentiates the reformers more widely at present. Based on *current design*, the Wellman CJB reformer for a 50kW system would weigh 460 kg more than the Johnson Matthey methanol reformer (see Table 3.9). At the time of writing this report, no data was available for the size or volume of a *near term* BG Technology system. However, *target weights* are quite similar for all three reformers, ranging from 1.5-2.5 kg/kW. If projected targets are met, then there will be little to chose based on fuel processors only. However, estimates for the fuel processor size and weight is not enough. It is not until a system is actually built, including pipes, compressors, tubing, valves, insulation controls etc that a better estimate can be made. Chapter 6 attempts to do this for a methanol HotSpot FCS hybrid bus, based on experience of building a 20kW system for the CAPRI project.

The critical commercial criterion was cost. The main factors (capital cost, fuel cost and maintenance cost) could not be estimated with sufficient accuracy to distinguish between the reformer choices. This can only be provided from production ready prototypes and field trials. However, all the reformers could potentially improve on diesel and alternative fuelled internal combustion engines, and hydrogen fuelled fuel cell buses on the grounds of running cost, if maintenance costs are low and fuels such as methanol and natural gas do not carry heavy duties.

There appears to be little to choose between the reformer systems on performance, operational or commercial criteria. However, it became apparent during the course of the study that neither the Wellman CJB methanol reformer nor the BG Natural Gas reformer was sufficiently developed to provide comprehensive data for the study. In many cases performance, size, weight and cost data have been inferred or projected from laboratory or model calculations. The consequence was that, while the JM Hotspot data was also relied on assumptions in some respects, it was the only reformer that had been developed to the stage of working prototype and hence it was chosen for the second phase design study. When the other reformers are further developed, they could also prove to be suitable candidates for a fuel cell powered hybrid bus.

Of all the commercial factors considered, cost was the most important to bus operators. This is not just the initial capital investment, but the bus lifecycle costs. When commercialising a fuel cell bus, consideration will need to be given to the cost of fuel, maintenance costs, expected bus lifetime, and interest on bus capital cost. However, many assumptions have to be made at this point. For example, the choice and cost of fuel is not certain. At present, many organisations are opting for methanol fuel – it is liquid and easy to handle, and is generally considered one of the “easiest” fuels to reform. However, methanol is not a transport fuel, and is therefore not yet subject to road fuel duty.

Based on efficiency predictions from the modelling, the cost of methanol to the bus operator would need to be £0.17 per litre (compared to current diesel cost of £0.26 per litre) to give similar fuel cost per km of bus use. The average price of methanol (as a chemical not a fuel) was about £0.13 per litre (pre-tax) in 1998. If subjected to the same duty as diesel for bus operators, then methanol would cost in the region of £0.175/litre. All reformer choices can potentially reduce the fuel cost, compared to diesel or natural gas ICE's, and hydrogen fuelled fuel cell buses.

Maintenance schedules are also unknown. Only estimates can be made at present. Fuel cell buses will most likely need less engine-based maintenance than conventional buses as there are fewer moving parts, causing less vibration. A fuel cell bus is projected to have a life of about 15 years (compared to 12 for a diesel bus). For this lifetime, it is anticipated that the fuel cell will need replacing twice.

Taking the *complete lifecycle* costs into account, it has been estimated that a methanol fuel cell hybrid bus would cost about the same as a diesel bus. This of course is based on many assumptions and variables, and it will be some time before the economics of fuel cell buses can be made more definitive.

6. POWER TRAIN SPECIFICATIONS AND DETAILED SYSTEM DESIGN

Thoreb AB and Scania have developed a hybrid bus comprising a conventional internal combustion engine and a series of batteries. This bus is used as the basis for the models of the FCS in Phase 2. Focussing on an existing operational hybrid bus removes uncertainty and allows the design study to concentrate on key FCS issues.

Although some problems were experienced with the exhaust system and traction inverter, of the Thoreb/Scania bus, it has proven a success, in that it operates well and shows good driveability. However, in terms of fuel economy it performs slightly worse than a conventional diesel bus and does not contribute to the overall reduction of emissions. Since fuel cells have been identified as clean, quiet and highly efficient power generators, a FCS hybrid bus may offer the solution to urban public transportation.

In this chapter, a more detailed study is undertaken to understand the power flow in the current hybrid bus. By simulating various FCS power supply scenarios, the power demands on the batteries can be determined. The max FCS power output and battery capacity are optimised for a range of FCS dynamic responses. Upon determining the optimum FCS and battery size, the overall powertrain size and weight can be estimated. In addition, more detailed specifications of the FCS components are provided in section 6.4.

6.1 Fuel Cell System Dynamic Response

This section primarily discusses the power demands on the fuel cell system. First, the bus power requirements were analysed during a drive cycle (as measured on the Thoreb/Scania bus) distinguishing between the power supplied by the batteries and the ICE. Secondly, the FCS power supply was simulated as a function of various input variables, allowing the gap between the FCS and the ICE power supply to be assessed. This gap analysis formed the basis of the FC hybrid bus power requirements for the various FCS power supply scenarios. The model simulations form the framework for the design of a hybrid FCS bus, optimising the battery and FCS size within the constraints of the FCS performance.

6.1.1 Drive cycle power measurements

Appendix E describes the hybrid bus built by Thoreb and Scania. Thoreb provided raw data on the power flows of this bus. These data include measurements over two drive cycles, one of approximately 15 minutes, and one of about 3 hours. During these drive cycles the power produced by the generator from the ICE, the power charge/ discharge of the battery, and the total power demand were recorded every second. The total power demand is the sum of the power demand by the traction inverter, the power steering, the DC-DC converter, and the air compressor. Table 6.1 shows some characteristics of the two drive cycles.

Table 6.1: Average values over bus drive cycle

Drive Cycle Characteristics	unit	Drive Cycle I	Drive Cycle II
Total Energy Demand	kWh	7.02	63.87
Net Energy Consumption	kWh	6.57	60.23
Maximum Power Demand	kW	107.23	109.0
Average Power Demand	kW	26.2	20.3
Drive Cycle Time	hrs:min:sec	0:15:03	2:58:28
Maximum Speed	km/h	40.75	52.23
Average Speed	km/h	16.60	15.33

For Drive Cycle I the average power demand was calculated to be 26 kW, while the total energy demand was 7.02 kWh. The contribution of regenerative braking was calculated to be -0.45 kWh (6.4%), such that the net energy consumption was 6.6 kWh. For Drive Cycle II the average power demand was calculated 20 kW. The total energy demand in this drive cycle was 63.9 kWh, of which 5.7% was regained by regenerative braking.

The above drive cycles are representative for inner-city buses measured by Thoreb in Sweden. The average power demand can differ substantially from 18-40kW, but over this flat inner city route the average speed is 15 km/h with an average power demand of 20-25 kW. The most representative standardized test cycle for inner city buses, the Braunschweig cycle is slightly more demanding than the cycles considered here with an average power of ~30 kW, and an average speed ~23 km/h.

Figure 6.1 shows the total power demand as well as the power supply from the ICE and power charge and discharge by the batteries for Drive Cycle I. Note that when the battery power flow is positive, the batteries are charged; a negative value means power discharge. It can be seen that during the first 3 minutes of the drive cycle and between 11-13 mins in the drive cycle the generator is switched off. While driving through zero emission zones the bus is powered by the batteries only. The battery state-of-charge (SOC) is shown with the units on the secondary y-axis. On the bottom of Figure 6.1 the bus speed is displayed

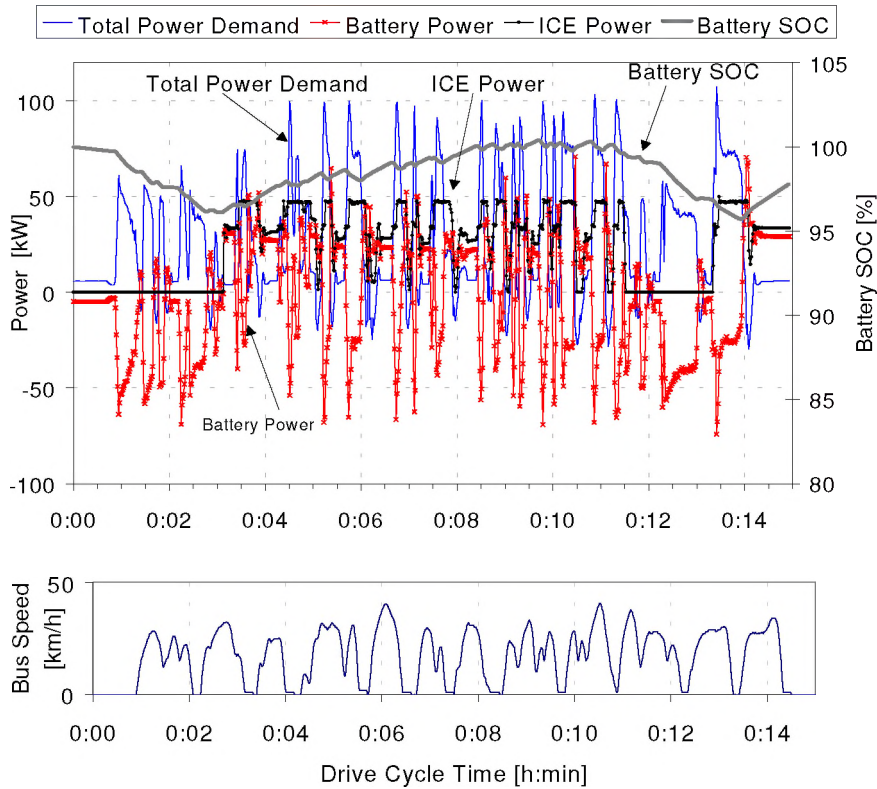


Figure 6.1: Power demand/supply in present hybrid bus (drive cycle I)

6.1.2 FCS requirements in FC hybrid bus: simulation input variables and output parameters

Simulation input variables

The total power demand measurements of the current hybrid bus were used to investigate the dynamic requirements of the FCS, with the FCS replacing the ICE. In this initial study the following assumptions were made:

- the total power demand is the same for the FC bus as for the ICE bus (this may be different if the weight of the FC bus differs from the ICE bus)
- unlike the ICE, the FCS follows the load rather than operates at various set-points
- the FCS does not produce emissions and does not need to shut-off during a zero-emission zone
- the discrepancy between power demand and power generated by the FCS is delivered instantaneously by the battery system, i.e. the battery functions as a load leveler

The variables considered in the simulations to study the effect of various FCS power supply scenarios are summarised in Table 6.2.

A	= FCS power turn up rate	kW/s	S	= min power step size FCS	kW/s
D	= FCS power turn down rate	kW/s	SOC _{max}	= max SOC (→FCS off)	%
Max	= maximum net FCS power	kW	SOC _{min}	= min SOC (→FCS on)	%
Min	= minimum net FCS power	kW	Capacity	= rated battery energy	kWh

Simulation output parameters

For a certain set of input variables, a series of output values are calculated for the battery and the FCS. These values are compared to the current ICE bus. For a direct replacement of the ICE with a FCS in the current bus the demands on the batteries are the most important, and it is necessary to understand whether the batteries can handle the power requirements, leveling the load with the FCS. In addition a number of output parameters for the ICE generator and the FCS are calculated. The most important output values are summarised in Table 6.3.

Table 6.3: Calculated output values for the batteries and the ICE or FCS

Battery	ICE or FCS
Net energy supply kWh	Total energy supply kWh
Average power discharge kW	Average power supply kW
Average power charge kW	Average power turn-up rate kW/s
Maximum power discharge kW	Average power turn-down rate kW/s
Maximum power charge kW	Maximum power turn-up rate kW/s
Average power discharge %/s	Maximum power turn-down rate kW/s
Maximum power discharge %/s	Fraction of drive cycle at 0 power %
Minimum SOC %	Fraction of drive cycle at Min power %
Maximum SOC %	Fraction of drive cycle at Max power %

6.1.3 Simulation Results

The output values were evaluated over the given drive cycles for various input values. The input variables for the first series of calculations are given in Table 6.4.

Table 6.4: Input variables considered in FCS power supply scenarios

A = 1 - 100 kW/s	S = Max/100 kW/s
D = -A kW/s	SOC _{max} = 99 %
Max = 20 - 110 kW	SOC _{min} = 80 - 95 %
Min = 0 - 50 kW	Capacity = 25.9 - 0 kWh

The simulations were carried out for both drive cycles, and similar trends were found. The discussion here will be illustrated with the results for drive cycle I. In the simulations it was intended to first find the extremes of the system, followed by more realistic intermediate values.

1. If the FCS turn down rates was as low as 1 kW/s, will the current batteries be able to handle this?
2. How fast does the FCS need to respond to satisfy the bus power demands by a FCS alone?
3. What are the demands for the battery and FCS capacity for intermediate acceleration values?

Table 6.5 summarizes some of the calculated output values for various sets of input values, allowing comparison of the power demands on the batteries in the ICE bus and the FCS bus.

1. Slow Dynamic Response

It was found that with a dynamic response of 1 kW/s, the FCS is very slow compared to the change in power demand of the bus. With a minimum value of 5 kW (Min), the maximum power (Max) output of 50 kW is reached, for less than 1% of the drive cycle. If the maximum FCS power values is reduced to 40 or 30 kW this increases only slightly to 2.5% and 6% respectively. Also, under these operating conditions the system would never need to switch off, and actually loses battery power. The steady decline of the battery SOC under these conditions is the result of the fact that the FCS tries to follow load. By the time it gets to a substantial output, the demand has already decreased again. So, the FCS output decreases until the next load peak, where it increases again. However, the battery charge during low power demand is less than the battery discharge during high power demand. Figure 6.2 shows the power supply by the FCS and the battery, as well as the total power demand and the battery SOC, for $A = 1$ kW/s, $D = -1$ kW/s, $Max = 50$ kW, $Min = 5$ kW, $SOC_{max} = 99\%$, $SOC_{min} = 80\%$, and $S = Max/100$.

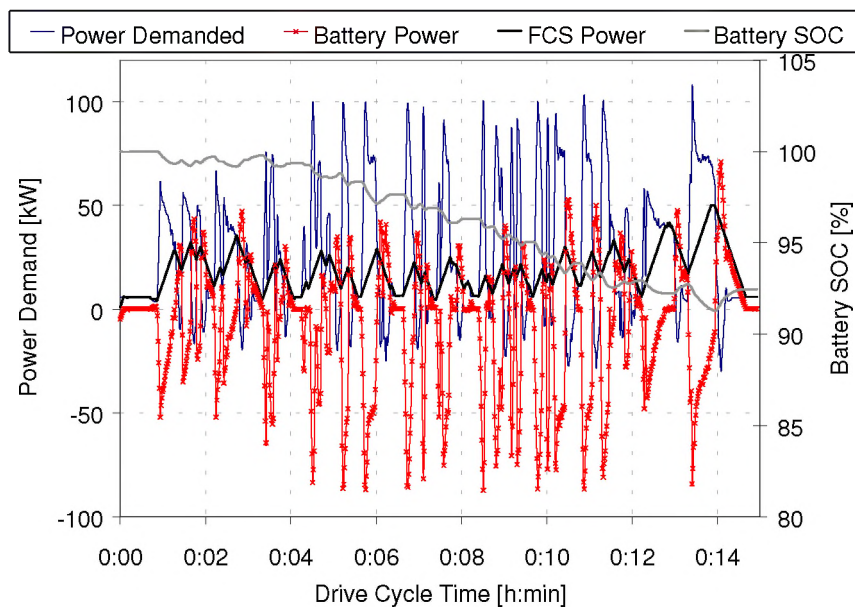


Figure 6.2: Simulated power supply in FCS bus
 $A = 1$ kW/s, $D = -1$ kW/s, $Max = 50$ kW, $Min = 5$ kW

The decline in battery SOC can be prevented by increasing the value of the SOC_{min} ; e.g. instead of 80% this could be raised to 95%. In that case the FCS system will become more or less a slave of the battery system as soon as SOC_{min} is reached, trying to keep the batteries charged rather than follow the bus power demand.

Table 6.5: Simulation results for various FCS power supply scenarios.

Input variables		ICE	FCS								
A	[kW/s]	0	1	1	1	1	2	5	10	20	55
D	[kW/s]	0	-1	-1	-1	-1	-2	-5	-10	-20	-55
Max	[kW]	0	27	35	50	50	37	45	55	60	110
Min [kW]		0	27	20	5	5	15	5	3	3	0
S	[kW/s]	0	0.27	0.35	0.5	0.5	0.37	0.45	0.55	0.6	0.5
SOC min	[%]	0	80	80	80	95	95	95	95	95	95
SOC max	[%]	0	99	99	99	99	99	99	99	99	100
Time 10%-90% Power ^a	[s]	∃1.3	21.6	28	40	40	14.8	7.2	4.4	2.4	1.6
Acceleration	[%/s]	∃60	3.7	2.9	2	2	5.4	11.1	18.2	33.3	50
Batteries											
Number	[-]	10	10	10	10	10	10	8	6	5	10
Rated capacity	[kWh]	25.9	25.9	25.9	25.9	25.9	25.9	20.7	15.5	13.0	25.9
Net energy supply	[kWh]	-0.58	-0.68	-0.87	-2.03	-1.02	-1.08	-0.99	-0.57	-0.33	0.45
Average discharge	[kW]	-28.05	-30.33	-28.12	-32.17	-29.82	-25.85	-19.15	-11.96	-7.59	-0.23
Average charge	[kW]	24.54	23.14	20.20	14.44	17.81	17.13	11.24	7.19	5.16	3.21
Maximum discharge	[kW]	-74.23	-86.55	-84.55	-87.34	-87.34	-80.23	-79.39	-67.90	-57.70	-22.85
Maximum charge	[kW]	70.77	56.87	57.88	70.87	77.45	64.87	74.87	48.53	39.22	29.87
Minimum SOC	[%]	95.69	95.83	95.41	90.97	94.61	94.75	93.89	95.93	97.08	100.00
Maximum SOC	[%]	100.37	99.99	99.99	99.99	99.99	99.99	100.00	100.08	100.37	101.72
SOC start of cycle	[%]	100.00	99.99	99.99	99.99	99.99	99.99	100.00	100.00	100.00	100.00
SOC end of cycle	[%]	97.77	97.37	96.62	92.16	96.07	95.82	95.21	96.32	97.48	101.72
Average Discharge rate	[%/s]	-0.030	-0.033	-0.030	-0.034	-0.032	-0.028	-0.026	-0.021	-0.016	0.000
Max Discharge rate	[%/s]	-0.080	-0.093	-0.091	-0.094	-0.094	-0.086	-0.106	-0.121	-0.124	-0.025
ICE or FCS											
Total energy supply	[kWh]	5.83	5.89	5.70	4.54	5.55	5.49	5.58	6.00	6.24	7.01
Average power supply	[kW]	24.22	24.94	24.09	18.15	22.20	21.87	22.23	23.91	24.89	27.97
Maximum power supply	[kW]	49.88	27.00	35.00	50.00	50.00	37.00	45.00	55.00	60.00	107.00
Average power acc	[kW/s]	1.88	0.99	1.00	0.99	0.99	1.98	4.20	6.22	8.64	9.89
Average power dec	[kW/s]	-1.91	-1.00	-1.00	-0.98	-0.98	-1.94	-4.05	-5.66	-7.12	-7.27
Maximum power acc	[kW/s]	30.29	1.00	1.00	1.00	1.00	2.00	5.00	10.00	20.00	55.00
Maximum power dec	[kW/s]	-33.83	-1.00	-1.00	-1.00	-1.00	-2.00	-5.00	-10.00	-20.00	-55.00
Frac of drive cycle 0 power	[%]	5.97	6.08	5.97	0.44	0.44	7.74	4.98	4.65	8.85	15.15
Frac of drive cycle at Min	[%]	-	76.00	22.01	1.22	1.22	24.34	9.07	8.19	6.86	15.15
Frac of drive cycle at Max	[%]	22.23	76.00	9.29	0.66	1.77	14.16	15.82	14.82	17.92	0.00

^a 2000 PNGV target for transient response time is 20 seconds (time from 10% to 90% of rated power)

With a dynamic response of 1 kW/s the FCS system is far from being able to follow load, so operating the FCS at a constant load could be considered. The maximum power of the FCS system operating in this mode should be slightly higher than the average power demand, to ensure the batteries will not be drained. The average power demand during drive cycle I was 26.2 kW (Table 6.1), and therefore values of Min = Max = 27 kW would be reasonable. Figure 6.3 shows that when constant power of 27 kW is supplied by the FCS, the battery SOC limits are fulfilled.

In practice the average power demand over a drive cycle would not be exactly known, and in fact, even for a particular route, will change slightly on a daily basis depending on the outside conditions and number of passengers. Hence, it would be more flexible to build a power train with a fuel cell system operating with Min = 20 kW and Max = 35 kW, for a FCS with limited dynamic response capabilities.

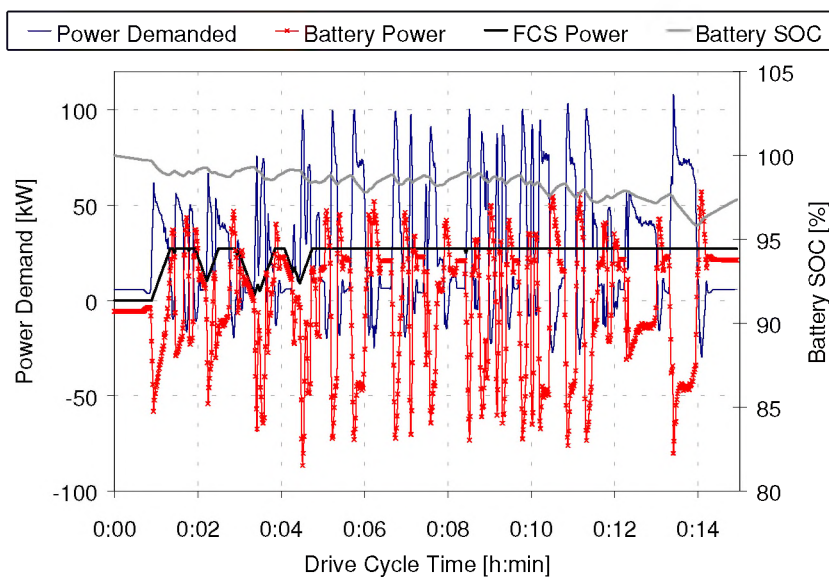


Figure 6.3: FCS semi-constant power supply scenario
 $A = 1 \text{ kW/s}$, $D = -A$, $\text{Max} = 27 \text{ kW}$, $\text{Min} = 27 \text{ kW}$

2. Fast Dynamic Response – Fuel-cell-only bus

For a FCS-only bus, the necessary acceleration of a FCS to completely follow load can easily be determined by increasing the value for the dynamic response (A). At some value for A the FCS energy supply will match the demand, while the battery power supply is reduced to zero. Note that with the data used here, the battery charge will not reach zero, due to regenerative braking. The maximum FCS power supply needs to be increased to cover the full load, which was determined to be about 110 kW, whereas the minimum power should be zero.

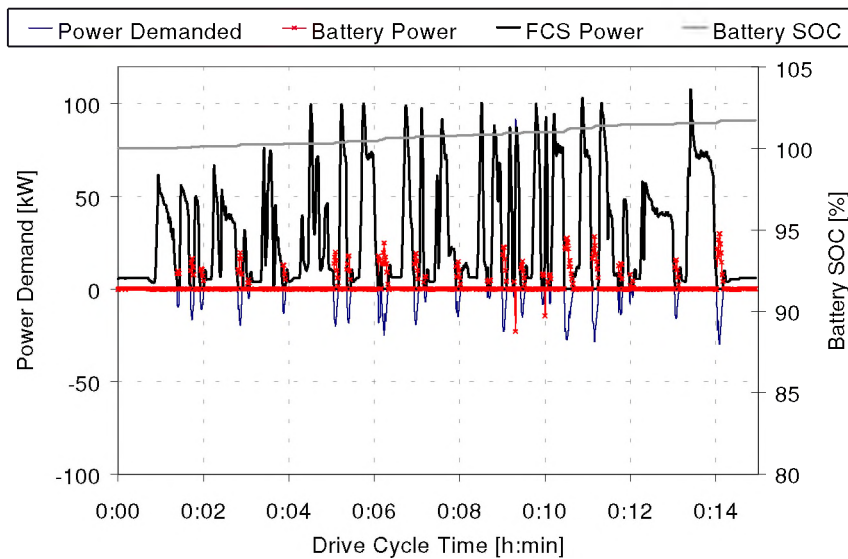


Figure 6.4: FCS-only, completely load following.
 $A=55 \text{ kW/s}$, $D=-A$, $\text{Max}=110 \text{ kW}$, $\text{Min}=0 \text{ kW}$, $S=0.5 \text{ kW/s}$

Figure 6.4 shows the result for FCS with a dynamic response of 55 kW/s. It can be seen that there are two very small spikes (9.5 and 10 minutes) where the battery delivered energy (0.3% of the total energy demand). Further decrease of A increases these spikes, and other small spikes appear. Hence, for a FC only bus to have the same driving characteristics as the current hybrid ICE bus the FCS acceleration needs to be at least 55 kW/s.

3. Intermediate Dynamic Response

Having investigated the extremes of the FCS's dynamic response of 1 kW/s and 55 kW/s, the power demand and supply was also studied for 2, 5, 10, and 20 kW/s. In each case, the battery capacity and FCS Max and Min were determined according to the following guidelines.

- $\text{SOC}_{\min} = 95\%$, $\text{SOC}_{\max} = 99\%$, $S = \text{Max}/100$
- FCS operates at Max during ~15% of the drive cycle
- By varying Min, the drive cycle time of FCS operating at zero power is minimized.
- Battery capacity is determined by comparing the average and maximum discharge rate expressed in %/s. In the ICE bus the average power supply is 0.03 %/s, while the maximum discharge rate is 0.08 %/s [74.23/93240*100%]. The batteries however can supply at least 100 to 120 kW [0.11-0.13%/s], if it does not occur too often. Table 6.5 shows the results for each intermediate acceleration value, assessed within the constraint of the maximum discharge <0.13 %/s.

With increasing FCS dynamic response, the battery capacity (number of batteries) can be decreased, but the required maximum FCS power output needs to be increased. At the same time, the average power charge and discharge become substantially lower as the FCS becomes more load following. It is preferable to use the batteries as little as possible, since every time energy is stored and released there is a small efficiency penalty. The impact of the battery/ FCS capacity versus the FCS dynamic response on total system size and weight will be discussed in Section 6.3.5.

In the present ICE hybrid bus the ICE is switched off during braking when the regenerative energy is charging the batteries. This is necessary to protect the batteries from overheating by the sudden power charge. Intuitively, it would be expected that regenerative braking in a FCS hybrid bus might cause a problem if the FCS does not shut down like the ICE. However, the data calculated here do not support this as the maximum charge rate was found to be similar or smaller than in the ICE bus. The average charge rate was always calculated to be smaller for the FCS hybrid bus.

6.2 Hybrid System Size

6.2.1 Scania/ Thoreb Hybrid Bus Power Train

A schematic representation of the power train in this bus is displayed in Figure 6.5. The shaded boxes (ICE and Generator) are to be replaced with a FCS. The other system units remain by and large the same. Depending on the dynamic response of the FCS, the battery capacity can be reduced.

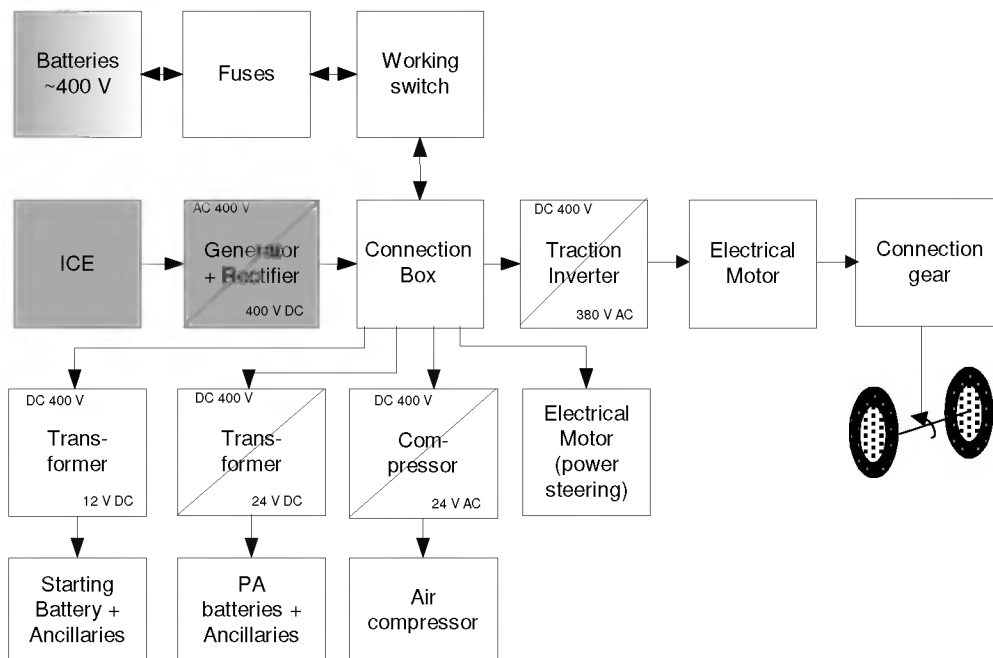


Figure 6.5 : Power train lay-out in Scania/ Thoreb Hybrid bus

The present hybrid bus, including 66 passengers, averaging 70 kg each, weighs 17,800 kg - 1000 kg more than a conventional bus. Almost half (45%) of the power train weight in the hybrid bus is due to the batteries. Table 6.6 shows a breakdown of the weight of the various power train components versus the conventional bus.

Table 6.6: Power train component weight in kg

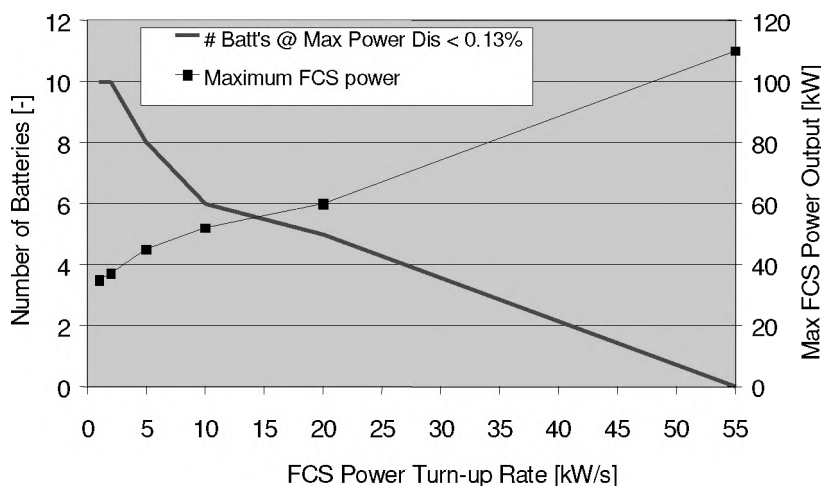
	ICE hybrid bus	Conventional Diesel
ICE	250	800
Generator	150	-
Batteries	1000	-
Inverter	130	-
Electrical motor	500	-
Connection gear	250	400
Total	2280	1200

The weight of some of the components in the hybrid bus, in particular the generator and the inverter, could be reduced by a factor 2 or 3 using more up-to-date technology. For the batteries however, only a moderate improvements in weight is expected for a future hybrid bus.

6.2.2 FCS Hybrid Bus

In section 6.1 it was determined that for a FCS with a limited dynamic response the current battery capacity seems adequate, i.e. the power demands on the batteries are found to be similar for the FC bus compared to the ICE bus. As the FCS dynamic response increases it was found that the average discharge rate decreased significantly (see Table 6.6), indicating that less battery capacity is required. However, the maximum discharge rate decreased less steeply. This is considered an important parameter, as frequent high discharges will decrease the battery lifetime.

The battery capacity was optimised for a series FCS dynamic response values, keeping the maximum discharge rate below 0.13%/s in each. Figure 6.6 shows the estimated FCS capacity and the required number of batteries as a function of the FCS power turn-up rate.

**Figure 6.6:** Battery and FCS capacity vs FCS acceleration

The objective of replacing the ICE in the current hybrid bus was to create an efficient zero-emission vehicle. The vehicle should also have a respectable driving range, without giving up space or increasing the weight.

Scania evaluated the available weight and volume for the FCS in the hybrid bus, including 1000 kg batteries. They established that a volume of 1000 litre (1 m³) is acceptable for the FCS (stack plus reformer), which should weigh no more than 1000 kg. If the number of batteries can be reduced in the FCS hybrid bus, the FCS could possibly weigh more, although this may cause problems with the weight distribution. The batteries occupy about 1m³, and are placed on the roof. Battery capacity reduction will not result in more available space for the FCS as the latter would be placed in the rear of the bus and not on the roof.

The FCS specific power is based on Johnson Matthey's fuel processor technology, derived from our work in the CAPRI project. For this project we have built a 16 kWe net (20 kWe gross) methanol processor. The fully integrated system, including FC and controls occupies most of the luggage space of the VW Golf (about 0.57m³). The weight of the system is estimated to be about 300 kg. Table 6.7 lists the CAPRI system size and weight (See also table 3.8).

Table 6.7: FCS power density and specific power based on Capri (net system power)

	Power density (kW/liter)	Specific power (kW/kg)
Stack	0.20	0.16
FP	0.033	0.08
FCS	0.028	0.053

As the CAPRI system is the first of its kind, one would expect that the size and weight of a future FCS of the same kind could be reduced in size by at least a factor 2. Hence perhaps more realistic values to work with are 0.05 kW/litre and 0.1 kW/kg.

In Table 6.8 the power train weight and volume are estimated as a function of the FCS acceleration, where the FCS weight and volume are based on extrapolated Capri data. For comparison, the first column shows the size and weight of the current ICE/generator and the batteries.

Table 6.8: Estimated Hybrid System Weight [kg] and Volume [liter]

ICE/FCS acceleration (kW/s)	<i>ICE</i>	1	2	5	10	20	55
Number of batteries	<i>10</i>	10	10	8	6	5	0
Maximum power (kW)	<i>~50</i>	35	37	45	55	60	110
Battery volume	<i>1000</i>	1000	1000	800	600	500	0
FCS/ICE volume	<i>200</i>	700	740	900	1100	1200	2200
Total Volume	<i>1200</i>	1700	1740	1700	1700	1700	2200
Battery weight	<i>1000</i>	1000	1000	800	600	500	0
FCS/ICE (+ generator) weight	<i>400</i>	350	370	450	550	600	1100
Total weight	<i>1400</i>	1350	1370	1250	1150	1100	1100
FCS Specific Power:	0.1 kW/kg, 0.05 kW/liter (based on net power output)						

The table indicates that the total system weight does not vary much with the FCS power turn-up rate, although a small weight reduction is projected for FCS hybrid bus. The volume of the FCS hybrid bus is estimated to be 500 litre larger than the ICE hybrid, but weigh less. The volume of the FCS itself is estimated to be 700 litres for a 35 kWe

system and 1200 litres for a 60 kW system. The latter just exceeds the target set by Scania, which was 1000 litres.

Figures 6.7 and 6.8 show the system size and weight based on Capri data, versus the current ICE hybrid bus. Figure 6.7 shows that the total battery and FCS volume, based on the Capri estimates, is expected to be greater than the current system volume. However, if the FCS power density can be improved the total system size is expected to be similar at the lower acceleration values, since the power density of FCS is now similar to that of the ICE. For higher FCS acceleration values, the system size is projected reduce significantly.

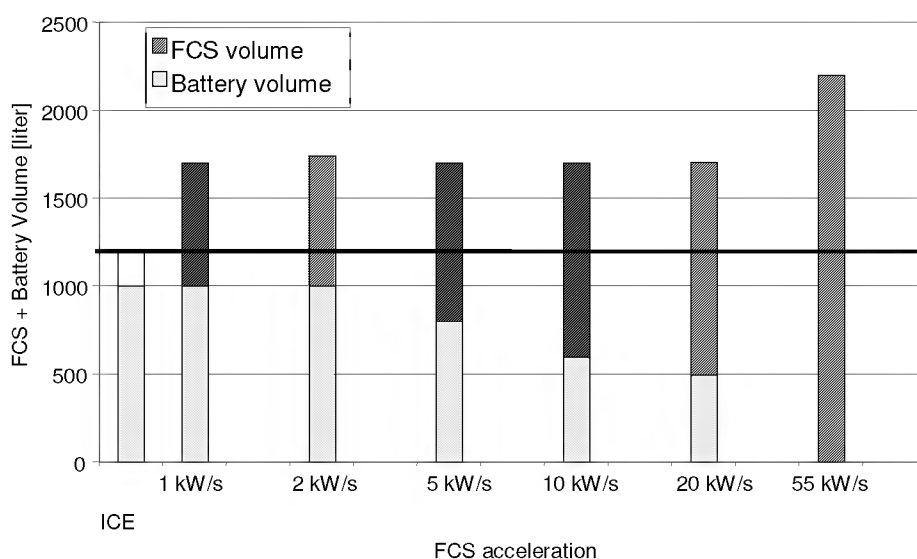


Figure 6.7: FCS and battery volume based on extrapolated Capri values

Figure 6.8 indicates that with the projected FCS specific power based on Capri, the total system weight is expected to be similar or slightly smaller than the current system. Again if the FCS specific power can be improved, significant weight reductions can be expected.

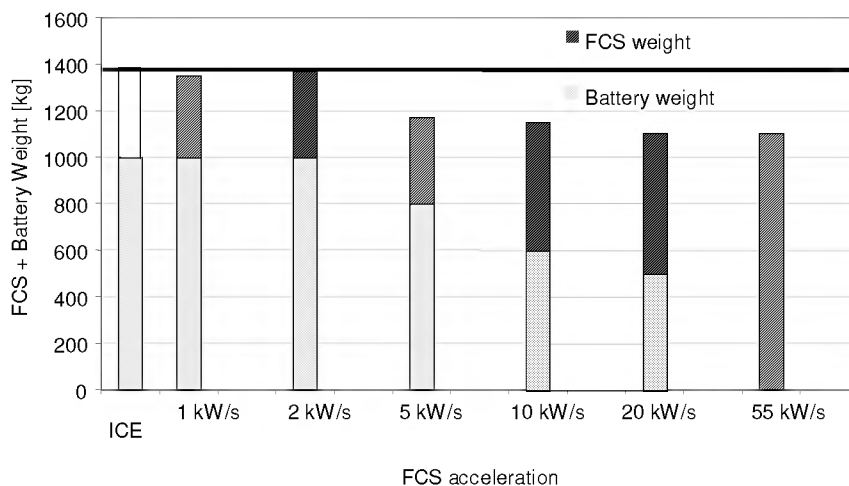


Figure 6.8: FCS and Battery weight based on extrapolated Capri values

6.2.3 Choice of FCS and Battery capacity

Only a few fuel cell systems including fuel processors have been built to date, so there is little information on their dynamic behavior. Different groups may have quoted the dynamic response of a single component, but this does not give the full picture. Also, at present a lot of the work is done in the laboratories, with fuel supply systems that would not be used in a real vehicle.

The fuel cell itself is expected to respond more or less instantaneously with varying load. Johnson Matthey's HotSpot reformer and Demonox systems have shown good load following characteristics, but have never been subjected to major load changes on a second to second basis.

James Larkin (of Georgetown University which has demonstrated FCS hybrid buses using methanol), has found that a FCS dynamic response of about 20%/s could be achieved [Larkins J, Sept 1998]. However, more reasonable values would be in the range of 10%/s. This translates into 5 kW/s for a 50 kWe system. Without knowing the dynamic response, it is difficult to map out the capacity of the FCS and the batteries. However, based on the above guidelines a 5kW/s, 50 kWe (net) FCS seems reasonable, while maintaining a similar battery capacity. If the FCS possess slower dynamics, the FCS is somewhat oversized for the drive cycles considered here, but the batteries will be able to deal with the power demands placed on them. On the other hand, if the FCS demonstrates a dynamic response of 10%/s, the battery capacity may be reduced.

6.3 Fuel Cell System Start-up Time

In Section 6.1 the dynamic requirements of the FCS were evaluated. In this study it was assumed that the system was warm at all times. The FCS system is only shut-down during the drive cycle, in order to prevent overcharging the batteries. Typical shut-down times were found to be 5 to 20 seconds, during which a well insulated system will not lose to much heat. Experience with JM's methanol HotSpot reformer confirms that shutting down the system for 30-60 seconds should present no problems.

The start-up time of the system depends upon two steps, first, the methanol/water feed has to be vaporised, then the reformer has to generate hydrogen. Once the feed is vaporised, JM's HotSpot reformer will produce a hydrogen-rich stream suitable for the fuel cell within 1 minute. Vaporisation of the methanol/ water mixture takes about 2 minutes. It can be accomplished by:

- Heat of combustion, through burning methanol in the anode off-gas burner
- Electrical heating, drawing power from the battery

6.3.1 FCS Start-up Using Heat from Methanol Combustion

The first strategy is followed in the Capri project, and we successfully generated hydrogen within 2 minutes after starting combustion of methanol in the catalytic burner. During this time the vehicle will be battery powered by the batteries.

The same approach could be followed in the hybrid bus. The power flow over drive cycle 1 is shown in Figure 6.9 for a conservative FCS start-up time of 3 minutes. Note that in drive cycle I the bus idles about 50 seconds and then starts driving. The impact of the power demand on the battery state-of-charge is moderate, as it drops only to 95%.

Figure 6.9 shows that a FCS start-up time of about 3 minutes should cause no problems for the batteries. If it were acceptable to have the bus idle about two minutes instead of 50 seconds before starting to drive, the impact on batteries would be significantly smaller.

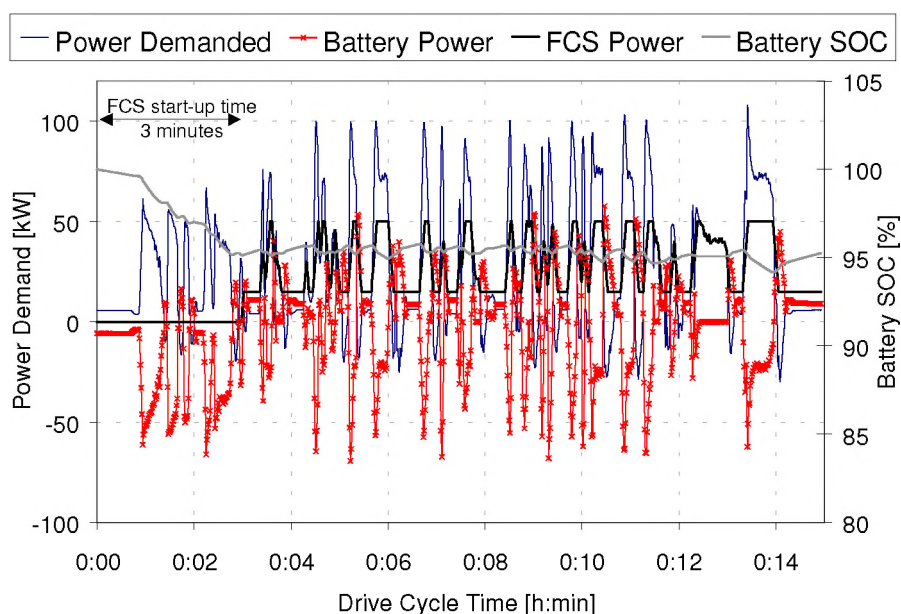


Figure 6.9: Power flow in FCS hybrid bus during drive cycle I with 3 minute FCS start-up, using heat generated by methanol combustion in the anode off-gas burner. A = 5 kW/s, D = -5 kW/s, Max = 50 kW, Min = 15 kW, 8 Batteries

6.3.2 FCS Start-up Using Electrical Heating

The second start-up approach, using battery power to first heat the evaporator and then vaporise the methanol/water feed, will have a more substantial impact on the batteries. Assuming we start the FCS under 25% of the full load of 50 kW, the following estimate for the battery power demand during start-up can be made.

- Energy to heat-up the evaporator 660 kJ (extrapolated from measurements on single HotSpot reactor)
- Energy to vaporise methanol/ water feed during 1 minute = 1.02 MJ

If an efficiency of 90% for converting electricity to heat is assumed, the evaporator can be heated in 2 minutes with a power requirement of 6.1 kW. Subsequently, when the evaporator is warm, the fuel processor feed needs to be vaporised during 1 minute, which consumes 19 kW. Figure 6.10 shows what the effect is of utilising battery energy to start-up the system.

Although the impact on the batteries is more severe during a start-up using electrical heat, it would probably still be possible. However, if it were acceptable to idle two or three minutes before starting to drive, the initial battery power consumption would be relatively small, as the required energy is estimated to be 2.5 % of the batteries' rated capacity (1.87 MJ / 74.6 MJ (= 8 batteries) *100%).

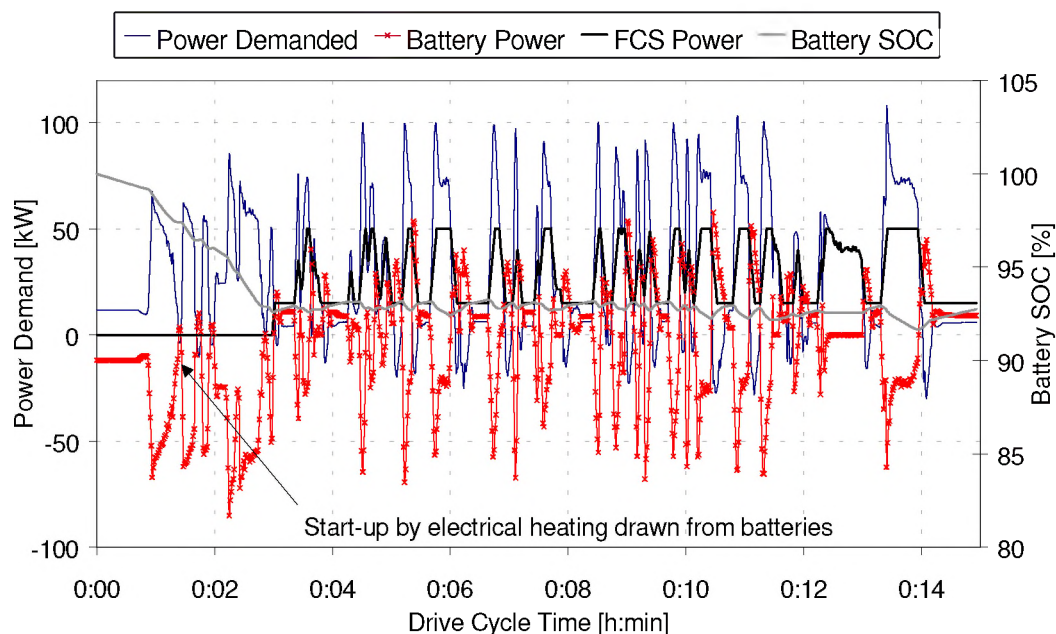


Figure 6.10:Power flow in FCS hybrid bus during drive cycle I with 3 minute FCS start-up, using battery power to vaporise the feed.
 A = 5 kW/s, D = -5 kW/s, Max = 50 kW, Min = 15 kW, 8 Batteries

6.4 Fuel Cell System Specifications

During Phase 1 of this study, various fuel processing options were investigated. A combination of technical and commercial factors led to the choice of a Johnson Matthey HotSpot methanol fuel processor (See Section 3). In this section the system component specifications will be discussed, based on a JM methanol fuel processor.

Figure 6.11 shows a process flow diagram including all unit operations. This diagram represents Johnson Matthey's base case system as is described in Chapter 3 and Appendix D. JM's methanol fuel processor is indicated by the shaded area, which has the requirements outlined below. The specifications of the unit operations will be outlined for a 50 kW net system.

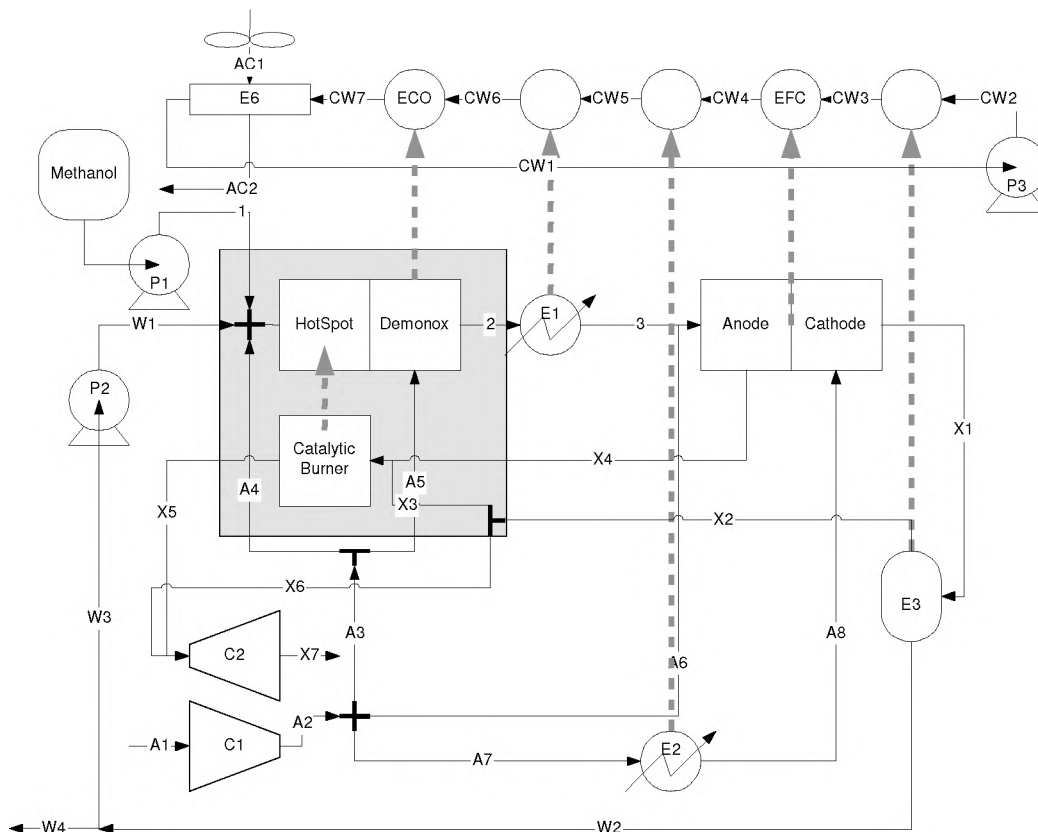


Figure 6.11: Fuel cell system including HotSpot methanol fuel processor

6.4.1 Fuel cell stack

As part of the CAPRI project a 20 kW gross (16 kW net) fuel cell system is currently being assembled. The system includes two 10 kW stacks, which together take up 80.3 litre and weigh 100 kg. This corresponds with 0.25 kW/litre and 0.2 kW/kg. The CAPRI stacks are not state-of-the-art: Ballard MK7 series stacks are capable of 1 kW/litre and 1 kW/kg. Hence, reasonable stack targets for the hybrid bus would be a power density of at least 0.5 kWe/litre and a specific power of at least 0.5 kWe/kg.

The stack needs to be designed to operate on a reformat with ~50% hydrogen, 30% N₂, 20% CO₂, and a CO level of # 50 ppm. To get good system efficiency with a methanol reformer, the anode hydrogen utilisation should be at least 80%, but preferably 85-90%. The average cell voltage should be at least 0.68 V at maximum power, 0.75 V at 50% power output, and 0.8 V at 25% power output. Table 6.9 summarises the fuel cell requirements.

Table 6.9: Fuel Cell stack specifications

Power Output ^a	kWe	60	Anode utilisation	%	>80 ^b
Specific power	kWe/kg	0.5	CO in reformat	ppm	50
Power density	kWe/litre	0.5	Δ P over FC	bar	<0.2
Pressure	bar	3-1.5	Cell voltage @ 100%	V	0.68
Temperature	EC	85-65	Cell voltage @ 50%	V	0.75
[H ₂] _{reformat dry}	%	50	Cell voltage @ 25%	V	0.8

^a The maximum FC power required is estimated to be 60 kWe gross for a 50 kWe net FCS, assuming a parasitic power of 20%.

^b The anode utilisation should be at least 80%, but preferably 85-90%

6.4.2 Fuel Processor Requirements

The following feeds and exhausts for the fuel processor are shown in Figure 6.11.

- 1 controlled methanol feed for the HotSpot reformer (1)
- 2 controlled air feed for the HotSpot reformer (A4)
- 3 controlled water feed for the HotSpot reformer (W1)
- 4 controlled air feed for the CO removal section (A5)
- 5 anode exhaust for the catalytic burner (X4)
- 6 cathode exhaust for the catalytic burner (X2)
- 7 cooling for the CO removal section (ECO)

Effective management of heat is important in a fuel cell system. The fuel processor has the following cooling requirements (see figure 6.11)

- 1 reformat before anode (E1)
- 2 compressed air for the cathode (E2)
- 3 cathode exhaust to a temperature at which sufficient water condenses to feed the reformer section (E3)
- 4 fuel cell; heat generated ~ to power generated (EFC).
- 5 cooling water radiator (E6).

The cooling has been simulated as a series operation. In the real system it could be considered to have parallel streams to reduce the flow rate and the pressure drop over a single unit. The heat exchanger duties are shown in table 6.10.

Table 6.10: Heat exchanger duties and temperatures (C = coolant, P = process stream)

Heat exchanger	Unit	E3	EFC	E2	E1	ECO	E6
Duty	kW	18.73	62.1	8.6	4.3	10.3	104.3
Coolant Medium		water	water	water	water	water	Air
Coolant Flow	kg/s	1	1	1	1	1	7.6
Process Flow	kg/s	0.071	-	0.070	0.025	0.025	1
T _{C-in}	EC	45	49.2	62.9	64.8	65.5	25
T _{C-out}	EC	49.2	62.9	64.8	65.5	68	38.6
T _{P-in}	EC	85	85	205	160	170	68
T _{P-out}	EC	58	85	85	85	160	45

6.4.3 Parasitic Power Requirements

The fuel processor system included compressors and expanders which impose a parasitic power demand.

- 1 compressor to compress air to the system to 3.2 bar, slightly above the FC operating pressure (C1).
- 2 expander fed by burner exhaust, reduces the load of the compressor (C2).
- 3 methanol pump (P1)
- 4 water pump (P2)
- 5 cooling water re-circulation pump (P3)
- 6 radiator fan

Table 6.11 gives the required pump and compressor specifications

Table 6.11: Pump and compressor specifications

Pump/compressor	Unit	P1	P2	P3	C1	C2
Duty	kW	0.011	0.006	0.348	15.85	-6.90
Process Flow	g/s	8.6	5.7	1000	80.8	88.4
Process medium		CH ₃ OH	water	water	air	exhaust
P _{in}	bar	1	1	1	1	2.4
P _{out}	bar	4	4	2	3.2-3.5	1
T _{in}	EC	15	58	45	15	245
T _{out}	EC	15.3	58.2	45.1	205	176

6.5 Hybrid Bus Component Dimensions and Costs

In section 6.2.2, it was estimated that the overall FCS specific power and volumetric power density (net power) would be about 0.1 kW/kg and 0.05 kW/litre, for a fully integrated system. For a 50kW (net) system, 60kW gross would be required, assuming parasitic power of 17%. The FCS would therefore occupy 1.0m³, and weigh 500kg. This meets the target on size, and weight is well within limits. Weight is the more critical issue, as more power train weight means fewer passengers can be carried. However, when the complete drivetrain is taken into account, including the batteries and fuel tank,

then the estimate for the methanol fuel cell system is comparable to diesel ICE bus on both a volume and weight basis. Tables 6.12 and 6.13 show refined estimates for volumes and weights of a fuel cell hybrid power train, based on 50kW net power and turn-up rate of 5kW/s (10%/s). These estimates are within the targets outlined in Section 2.4.

Table 6.12: Volume of methanol fuel cell power train (m³)

Component	Diesel ICE	FC Target	FC Estimate
FCS/ICE	2.2	1.0	1.0
Battery	N/A	1.3	0.8
Electric Motor	N/A	0.5	0.25
Fuel Tank	0.3 ¹	0.55 ²	0.2 ³
TOTAL	2.5	3.35	2.25

¹260l fuel, plus 10% extra tank volume. This would give diesel range of about 580km
²based on about 2x diesel volume
³for 250 km range. Includes 10% extra fuel. Lower margin fuel tank possible because of battery backup

Table 6.13: Weight of methanol fuel cell power train (kg)

Component	Diesel ICE	FC Target	FC Estimate
FCS/ICE	1200	520 ¹	500
Battery	N/A	1000	800
Electric Motor	N/A	200	200
Fuel Tank (full)	380 ²	480 ³	180 ⁴
TOTAL	1580	2200	1680

¹ based on total of 2000kg less batteries and fuel tank
²@3kg fuel per kg tank.
³ based on 500 l methanol
⁴ for 250 km range. Includes 10% extra fuel.

The diesel bus currently carries a fuel tank which is oversized, and would give a range of about 580km if all the fuel carried was used. The estimates for the methanol hybrid bus are based on a range of 250km, plus 10% extra fuel capacity. The fuel cell hybrid system does not need such a generous margin, as the batteries could act as power back up in an emergency. Scania's target weight for a fuel cell bus would be no more than 300-500g heavier than a conventional diesel bus (see section 2.4). If no weight savings can be made elsewhere in the bus, then the FCS power train would be restricted to about 2000kg. However the estimates for FCS come within this 2000kg limit.

Table 6.14 gives a detailed estimate of the costs, including a breakdown of individual power train components. Again, this is based on a 60kW(gross) / 50kW (net) system, with an acceleration rate of 5kW/s.

Table 6.14: Estimated power train costs

Component	Duty	Cost (£)
FC Stack	60 kW (gross)	18,000 ¹
Fuel Processor	60 kW (gross)	6,000 ²
Batteries	20.7 kWh	10,000
Electric Motor	150 kW	12,000
Inverter	150kW, 400V DC to AC	15,000 ³
Compressor	16kW, 81g/sec	
Expander	-7kW, 90g/sec	600 ⁴
Management system		12,000 ⁵
Other		1,400
TOTAL		75,000

¹ based on £300/kW, at production of several hundred per year
² based on £100/kW, at production of several hundred per year
³ based on £100/kW
⁴ based on estimates for mass produced compressor/expander system for transport [Arthur D Little Inc, 1998]
⁵ estimate based on production of several hundred a year, using Thoreb/Scania PTMS cost of £20,000 as basis

A conventional 12m bus costs about £115,000. Of this, approximately £20,000 is drivetrain cost, and £95,000 chassis cost.

The fuel cell bus costing estimates that the drivetrain would cost £75,000. If the FCS drivetrain is incorporated in a conventional chassis, the overall cost will be in the region of £170,000. Alternative fuel buses, with an ICE, cost in the order of £140,000 for LPG and £155,000 for CNG. The cost of power conditioning systems was investigated by Collinson et al in ETSU report F/03/00064/REP. A target of about £100/kW_e was identified. If costs of the inverter and fuel management can be further reduced, then the fuel cell bus will be more in line with other alternative buses. The components of the bus fuel cell engine should benefit from the later introduction of fuel cells for cars, and the costs would be expected to drop further.

7. CONCLUSIONS OF PHASE 2

FCS Dynamic Requirements

The dynamic requirements of a FCS for the hybrid FC bus were investigated covering a range of FCS dynamic responses. For a slow FCS dynamic response of 1 or 2 kW/s (2-4%/s) it is more sensible to operate the FCS at semi-constant load, rather than load following. In this operation mode the FCS power output varies between a maximum and a minimum (e.g. 35 and 20 kW), dictated by the batteries rather than the total power demand. However, such a strategy can only be implemented if the relevant battery parameters can be measured and translated reliably into a value for the battery SOC.

The simulations show that the current battery capacity is sufficient for a direct replacement of the ICE with a FCS with a dynamic response of 2-4%/s (50-25 seconds to reach 100% output). A maximum power output of such a FCS of 35-40 kWe net would be adequate, based on the drive cycles considered here.

For a FC only bus, in the drive cycles considered, the dynamic response of the FCS needs to be at least 55 kW/s (50%/s), while the maximum FCS power needs to be 110 kW to cover the full power range.

Battery/FCS trade off

For a FCS with a dynamic response of 5-10 kW/s (10-20%/s), the simulations showed that battery capacity can probably reduced by 20-40%. The maximum power of such a system should be about 45-55 kWe. It was found that for a dynamic response of 5kW/s, 50 kWe (net) FCS seems reasonable, with a small reduction in battery capacity. If the FCS possesses a slower dynamic response, the FCS is somewhat oversized for the drive cycles considered here, but the batteries will be able to deal with the power demands placed upon them.

FCS Start-up

Starting-up the system with combustion heat by burning methanol in the anode off-gas burner has been applied in real tests. It has been demonstrated that a fuel cell suitable reformat can be generated in less than 3 minutes. During these the 3 minutes no additional power is drawn from the batteries. The 3 minutes start-up time imposes no problems for the batteries in drive cycle I, where the bus starts driving after 50 seconds. In reality, this time can probably be improved to 2 minutes or less.

An estimate of the electrical heat requirements during start-up showed that the amount of electrical energy is about 2.5 % of the batteries' rated capacity. If electrical heating is used during start-up, it is probably better to idle the bus for 2 minutes, while the FCS is started, before driving away.

System Size and Cost

From the models of a methanol fueled FCS, and using estimates of weight and volume based on a 20kW prototype, the FCS power train would be of equivalent weight and volume to a diesel ICE power train. Using costs based on several hundred units per year, the fuel cell hybrid bus would be about 48% more than a conventional diesel bus. The three most expensive components are the stack, the inverter and the powertrain management system. It is widely believed that the bus market will benefit in the longer term from the entry of fuel cells into the car mass market. This will lead to cost reductions in these major components. However, the lifecycle costs, normalised per km, are projected to be the same for the methanol fuel cell and a diesel ICE bus.

8. REFERENCES

Ackerman, F.J., Koskinas, G.J., Permeation of Hydrogen and Deuterium through Palladium-Silver Alloys, *Journal of Chemical and Engineering Data*, Vol 17, No 1, 1972, p51-55.

Arthur D Little Inc, "Advanced Fuel Cells for Transportation Applications. (Development of Compressor/Expander for Fuel Cells in Transportation Applications)". Final Report to DoE, DE-AC08-96NV11982, February 10, 1998.

Bechtold R. L., *Alternative Fuels Guidebook*, 1997.

BG Technology, Datasheets for Mercedes Sprinter Van, 1998.

Clean Fuels Report, p70-72, June 1998.

Collinson, A., Howson, D., Morgan, T., *Power Systems Considerations for use in Fuel Cell Generation Plant*, ETSU F/03/00064/REP, 1995.

European Energy Report, p16, 29 Jan, 1999.

Julen, K., Thoreb Private Communication, August 1998.

Hart, D., Private Communication, Nov 1998.

Hart, D., Hormandinger, G., ETSU F/02/00111/REP/1, *Initial Assessment of the Environmental Characteristics of Fuel Cells and Competing Technologies: Volume 1*, 1997.

Larkins J, Fuel Cell Technology Conference, London, Sept 15-16, 1998.

Larkins, J. T., Private Communication, Dec 1998.

Mitchel, W.L., "CO Clean up and Fuel Cell Performance on Gasoline/Ethanol Fuel Processor Reformate". Presented at Fuel Cells for Transportation TOPTEC Meeting, March 18-19, Cambridge MA, 1998.

Pedersen, P-L., Private Communication, Apr 1998.

Wimmer, B, Georgetown University, Private Communication, November 1998.

APPENDIX A: FUEL ISSUES

METHANOL / ETHANOL

Availability/ Infrastructure

Methanol and ethanol are both alcohol fuels, which have been used in internal combustion engines for some time now.

Methanol is mainly used in the USA, in cars and trucks / buses. Most cars can run on a mixture of methanol and gasoline (85% vol methanol). Trucks and buses use methanol with a small amount of additives. Methanol has received more attention than ethanol. It is seen as the more promising alternative fuel, because of environmental advantages, costs, and the variety of feedstocks from which it can be made.

If Flexible Fuel Vehicles (FFV's) are used, infrastructure vehicles can be introduced gradually. Methanol dispensing stations provide either M85 or M100.

Methanol can be readily produced using well proven technology. In 1995, the US alone produced 6.5 billion litres [Bechtold R.L., 1997]. The main producers of methanol are Methanex (Canada) and Statoil in Europe. Methanex is a world leading supplier of methanol as a logistic fuel to the transit industry, including the supply of M100 to over 300 fleet buses in the US, and methanol blends to SL Buss in Stockholm. Methanex has confirmed its interest in supplying methanol to a fuel cell demonstration bus.

Like other alternative fuels, the infrastructure does not exist for methanol. However, the methanol industry is ready to commit to the methanol infrastructure over the next ten years [Schmidt P., Feb 1998].

Storage and Handling

As methanol is a liquid fuel, the storage and dispensing is largely similar to gasoline. It is easy to handle and no sophisticated compression equipment is required.

Methanol is toxic, and can be absorbed by the skin. However, exposure studies in the US (where it is becoming more widely used) have shown that methanol does not cause harm in the quantities that would accumulate in the body from exposure to refuelling vapours or from unburned methanol in the exhaust [Bechtold, R.L. 1997]. Methanol is generally considered to be a safer fuel than gasoline, because it is less likely to ignite, and if it does, it releases only about 20% of the heat of a gasoline fire.

However, methanol is a very polar liquid that is completely miscible with water. When water is present, methanol becomes more corrosive. This is largely because water serves as an electrolyte, and so corrosion can set in. If storage tanks are fully wetted with methanol, then this problem is not so bad. [Schmidt P., Feb 1998]. Although stainless steel is the best materials for methanol tanks, pipes and components, mild steel can be used so long as no water is present. Non-anodised aluminium should be avoided, but even anodised aluminium will eventually corrode. Methanol is also very aggressive

to most elastomers. Teflon is least affected, and elastomers with a high fluorine content have been shown to be acceptable [Bechtold R. L., 1997].

Storage tanks and piping can be made from stainless steel, carbon steel, or fiberglass. Methanol tanks placed underground must have secondary containment in the USA. Methanol is hygroscopic. When in contact with air or groundwater alcohols attract, and absorb, water. Fixed roof tanks with internal floating covers should be used to store the alcohols. The tanks should be watertight [Owen, K., Coley, T., 1995].

Like tanks, dispensers for methanol must be made from steel, cast iron or stainless steel components. Other parts will have to be nickel coated. The most durable methanol filters have used nylon filter elements and methanol compatible glue [Bechtold R. L., 1997].

Economics

The costs of methanol are dependent on the market price of oil, because it is used as an energy source in the production of methanol, and because gasoline and diesel are competing fuels. Taxes and subsidies also play an important role.

The market prices of methanol fluctuated between \$0.09 and \$0.37 (US) per litre between 1990-1995 due to increase in demand and decrease in supply. The energy content of 1.7 gallons of methanol is equivalent to 1 gallon of petrol. The Californian Energy Commission has estimated that in 2010, the price for M85 (on an energy equivalent basis) will be \$0.28/l, compared to \$0.32 for petrol and \$0.27 for diesel [Cadwaller, S., Donovan, N., 1995] .

In addition to the costs of the fuel, the distribution and vehicle costs should be taken into account. Costs will include the construction of fuel dispensers, and new fuel handling equipment, removal of dirt dissolved in the alcohol, lining of storage tanks and alcohol resistant plastics. It is important that high grade methanol is used, as low grade methanol can contain formic acid which adds to the corrosion problems. [Agneton, B, Nov 1997].

In the USA this is estimated to be \$600 per bus, based on a 170 bus fleet [Chandler, K., et al, 1996]. In the UK, it is anticipated that the distribution of methanol and ethanol will cost the same as gasoline, per litre, but with additional costs for lining storage tanks [IEA/AFIS, 1996]. Due to the lower energy content of alcohols, the distribution of methanol and ethanol is 70% and 30% more expensive than gasoline per MJ. However, this will be offset buy the increased efficiency of fuel cells engines.

Reforming Issues

Liquid methanol is easily reformed into a hydrogen rich gas stream and has favourable weight and volume power densities. Carbon monoxide is a by-product of methanol reforming so the gas stream must pass through a clean-up stage before entering the fuel cell.

Ethanol

Availability / Infrastructure

Recently, ethanol has been tested in the USA, Canada and Europe as a fuel for buses. Sweden is one of the few countries with an ambitious project to find new bio-based fuels. The Swedish Transport and Communications Research Board (KFB) has had a development and demonstration project running since 1991. As part of this study, 32 ethanol powered buses are being run in Stockholm. The operator Stockholm Transport (SL) has been pleased with the results of the trial. SL has now decided to phase out all diesel buses in favour of ethanol and hybrid buses. SL aims to have 300 ethanol buses running by 2000. Elsewhere in Sweden, a total of another 300 ethanol buses are being demonstrated. [1]

The main problem facing the large scale use of ethanol as a transport fuel is the amount of land required for growing the feedstock. On the whole, Japan and Europe do not have the space and the US could not supply more than 20-30% of its transport energy requirements [IEA, 1995]. Brazil is an exception to this rule however. In 1989, almost 20% of all Brazilian transport used ethanol fuel, and in the same year, 90% of all new vehicles were alcohol fuelled. However, recently, confidence in alcohol fuel has dropped due to shortages. In 1994, only 10% of new vehicles were alcohol fuelled [Cadwaller, S., Donovan, N, 1995]

Storage and Handling

Ethanol has similar storage and handling requirements as methanol. However, it is not so corrosive and materials such as aluminium can be used. Like methanol, Teflon is the least affected elastomer, and those with a high fluorine content are acceptable. Other elastomers can be used with ethanol so long as they have been proven to be compatible. Ethanol is completely miscible with water and the presence of water (particularly from salted roads or contaminants) can make ethanol corrosive [Bechtold R. L., 1997].

Swebus has now got several years experience in handling ethanol fuelled buses. In terms of vehicle maintenance, injector nozzle blockages are a problem, but routine ultrasound cleaning each month solves this.

To fuel 16 buses, Swebus installed a 45m³ tank, which is filled weekly. This cost 1.1m SEK to build and install, although it could be done for around 400,000-600,000 SEK. [Danielson, H, Nov 1997]

The tanks should be kept away from buildings (more than 25m) and buses must be filled outside. It has been found that filling an ethanol bus takes 6-7 minutes more than diesel.

Regulations regarding ethanol include making sure storage is secure, and satisfying the drug authority that fuel is not being consumed by anyone other than the bus! To do this, detailed records are kept, but this is the same for all buses. When installing ethanol in Stockholm, the biggest problem encountered was with the fire authorities.

Swebus has not encountered any problems with fuel handling by drivers or mechanics.

The ethanol fuel tank onboard the bus holds 375 litres. This give a range of 460km. The daily route may be up to 450km. Standard diesel fuel tanks hold 250l. [Danielson, H.1997]

Economics

The City of Helsingborg is very interested in environmental issues. It supports Swebus Helsingborg to undertake environmental projects. As a result, Swebus Helsingborg has experience in running ethanol ICE buses. (Without this financial suport, diesel would be the preferred fuel). It has been operating 16 ethanol buses (29% of its total fleet) over the past two and a half years. Each bus has run on average 6,500 km per month (80,000km per year).

Running costs for a conventional diesel engine are about 2SEK per km. Running costs on ethanol is more than twice that of diesel. Per unit of energy ethanol has been put at 5-6x gasoline. Table A1 compares the costs for buses run at Swebus Helsingborg.

Fuel	Fuel cost	Fuel consumption	Bus manufacturer
Diesel	1.9 Kr/km	4.3Kr/l (£0.33/l)	5 litres / 10km Mercedes (12 m)
Ethanol	3.9 Kr/km	4.8Kr/l (£0.38/l)	8.2 litres / 10km Scania

By 2001, Swebus estimates its buses will be running a total of 9.5 million km per year. Fuel costs and efficiency is therefore of major concern.

In theory fuel consumption with ethanol should be 1.7x diesel. In practice it is more like 2x diesel. For cars, ethanol is much better, with fuel consumption similar to petrol.

Apart from Sweden, ethanol tends to be rejected by European countries because of its higher cost. Per unit of energy, ethanol is five times more expensive than gasoline.

BTL, a Swedish truck and haulage company have been involved in a KFB (Swedish government) funded project to evaluate ethanol fuelled trucks. Technically the project has not encountered any problems. However, the trucks had not yet run for 100,000

miles which is when problems are usually encountered. The fuel injectors did tend to corrode and therefore leak. This meant they had to be replaced after 50,000 miles. BTL are continuing to test one bus.

Reforming Issues

Johnson Matthey has looked into the reforming of ethanol [Carpenter, I.W., Golunski, S.E. 1998]. A number of problems were found when reforming ethanol via partial oxidation and autothermal reactions.

- poor efficiency arising from the low selectivity with which ethanol forms hydrogen
- need for intermittent catalyst regeneration to remove deposited carbon
- need for a complicated clean up unit to remove the range of organic by products formed, as well as CO.

NATURAL GAS

Availability/ Infrastructure

Compressed natural gas (CNG) vehicles are on the market today. One litre of diesel compares to about 3.35 litres of CNG at 200 bar. As CNG is stored under pressure, and has a lower energy content than diesel, larger, heavier tanks are required for the same range. Therefore, CNG is not suitable for long distance haulage lorries.

Liquid Natural Gas (LNG) is used to a certain extent. With LNG, less space is required to store the same amount of energy as CNG. The disadvantage is the complicated refuelling procedure, requiring low temperatures. Also, the energy investment in treating, transporting and compressing LNG is greater than CNG.

There are currently over one million natural gas vehicle in use in the world. Italy and Argentina each have about 250,000 natural gas vehicles, and the former Soviet Union about 315,000. [Cadwallader, S and Donovan, N, 1995,] [Carslaw , D., Fricker, N., 1995]

Germany has the best developed NG bus market in terms of city coverage, and number of buses. 220 buses operate in Germany (Nov 1996). By the end of 1996, Sweden had 140 buses running on NG. The fleet in Malmo (114 buses) is the largest in Europe.

In 1994, the UK had some 300 natural gas vehicles, (buses and cars) and there are eight fast-fill refuelling stations.

Storage and Handling

To use natural gas as a vehicle fuel, it must be either compressed or liquified so that sufficient amounts of energy can be stored onboard. Pipeline gas is delivered at below 5psi. To achieve the high pressures for on-board storage, the gas is compressed in multiple stages (usually four). Natural gas presents few materials compatibility problems. The materials used in compressors are usually cast iron, steel and aluminium. Piping is usually seamless stainless steel.

Natural gas refuelling facilities must be located away from public streets and places, railways, and other refuelling dispensers. CNG refuelling can be fast-fill or slow-fill. In slow-fill systems, several vehicles are connected to the output of the compressor at one time. In fast fill, enough CNG is stored so vehicles can be refuelled one after the other.

All operators would expect to receive compressed gas, ready for refuelling on their premises.

Economics

A natural gas bus has lower efficiency than a diesel bus in urban traffic. The main reason for this is the comparatively lower efficiency of the otto type engine process. The energy utilisation for natural gas is about 20% from the fuel to performed transportation work.

The main drawback of NG buses is their high purchase cost, and higher operating cost.

Natural gas produces lower levels of carbon dioxide, nitric oxides and particulates during combustion, than diesel. Measured in units of energy, combustion of natural gas in an Otto engine gives carbon dioxide emissions comparable to a diesel engine. The proportion of liquid hydrocarbons, which contribute to the formation of ground level ozone is reduced, but emissions of methane increase. The natural gas engine tends to be quieter than diesel, due to lower compression. Natural gas is considered to complement diesel in local and regional traffic. Its use can improve the local environment and health in areas with traffic congestion. However, natural gas does not greatly reduce emissions of fossil carbon dioxide. A limitation of natural gas is that the composition, and therefore quality, varies. The methane content can range from 80-98%.

Reforming Issues

A compact on-board natural gas reformer is being developed by BG Technology. However, at the time of writing this report, this reformer is believed to be at least two years away from prototype demonstration.

Compressed Hydrogen

Although abundant, hydrogen is not readily available in its uncombined form in nature. When burned in an internal combustion engine, it produces no CO or CO₂, and only small amounts of HC and NO_x. Hydrogen is produced by cracking hydrocarbon fuels, or by the electrolysis of water. It is generally used as a vehicle fuel in the liquid form. However, this requires specialised insulated tanks. Even as compressed gas, rather than liquid, the handling problems and subsequent huge investment in the infrastructure make it only feasible in the long term [Cadwallader, S and Donovan, N, 1995]

A problem with hydrogen fuelled combustion engines, is the limited range, and the weight reducing the number of passengers which can be carried. For example, 88.8 pounds of hydrogen stored at 300 bar in aluminium tanks will weigh 2.2tonnes, and give a range of 125 miles. The weight means that only 70, not 100 passengers could be carried [Daimler Benz High Tech Report 1995]. Another method is to use metal hydrides. Here, a bus with around 160 cubic meters of hydrogen stored as hydrides had a range of 100 miles [FT Automotive Analyst, June 1997].

Availability / Infrastructure

Storage and Handling

Hydrogen is a gas, and is supplied in a compressed or liquid form. For the purposes of this report, we will only consider compressed hydrogen.

Refuelling a hydrogen combustion engine bus can be done in seven minutes. This will store enough hydrogen for a range of 125 miles. On board the vehicle, hydrogen is stored in tanks within the roof-space.

[Daimler Benz High Tech Report ,1995]

Economics

Used in a fuel cell hybrid configuration, with system efficiency of 40%, hydrogen consumption by an urban bus would be around 9m³/10km⁶. The cost of purchasing hydrogen in bottles is currently about £1.70/nm³, or £15.30 /10km. However, these figures are probably higher than costs for hydrogen as a fuel.

⁶ Normal m³

Table A2: Summary of Alternative Fuels

Fuel	Storage & Handling	Health & Safety	Energy Density ⁽¹⁾	Reformer
Compressed Hydrogen	Supplied as gas in compressed form. Stored in steel, aluminium or composite tanks at 300 bar	Flammability range 4-75 volume % in air Burns without visible flame in air	Requires 20 times the storage volume of gasoline if stored as compressed gas at 300 bar. Added to this is the packing inefficiency of cylindrical tanks	Not required
CNG	Compressed to 240, 300 or 360 bar. Stored in cylindrical tanks on vehicle If utility supply is used, complicated refuelling system including (1) dryer, (2) compressor, (3) cascade (to deliver as much CNG as possible before pressure decreases and slows refuelling rate), (4) dispenser Fast flow dispensers are expensive	Flammability range 5-15 volume % in air Burns with a visible flame Lighter than air, escapes into atmosphere if there is a leak	240 bar - 4.5 times storage volume of gasoline 300 bar - 3.7 times 360 bar - 3.0 times. Added to this is the packing inefficiency of cylindrical tanks	Being developed by BG Technology. Still at development stage Prototype will be developed in 2-3 years

Methanol	Liquid fuel, similar to gasoline to handle. Some materials compatibility issues	Flammability range 7.3-36 volume % in air Burns with an invisible flame in air However, less prone to produce flammable vapour than gasoline, and releases only 20% of the heat of gasoline when ignited Corrosive in the presence of water Soluble in water Toxic, can be absorbed through skin - prolonged exposure not recommended	Requires about 2 times the storage volume of gasoline	Being developed by JM and Wellman CJB JM – 20kW prototype built WCJB – prototypes / development
Ethanol	Liquid fuel, similar to gasoline to handle. Some materials compatibility issues, but fewer than methanol	flammability range 4.3-19% in air Flame difficult to see in daylight Less susceptible to ignite than gasoline Soluble in water	Requires 1.5 time storage volume of gasoline	Evaluated by JM. Feasibility demonstrated. Also being developed by Epyx.

⁽¹⁾ Only based on comparison of energy density. Engine efficiency will vary also, and so more or less fuel will be required to travel a set distance
[Bechtold, RE, 1997; IEA/AFIS, December 1996]

APPENDIX B: PALLADIUM MEMBRANE

Instead of catalytically removing the carbon monoxide from the reformat to make the reformat suitable for the fuel cell, a palladium membrane can be used. One advantage of a membrane is that the product from the membrane is pure hydrogen. Assuming that the fuel cell anode can be operated dead-ended, the anode utilisation is then 100%.

Disadvantages of a Pd membrane are its operating conditions. The Pd membrane needs an operating temperature of at least 250-300°C, which makes this unit less suitable if a quick start-up is required. In order to recover most of the hydrogen from the reformat, high upstream pressures are required. This makes Pd membrane less suitable for partial oxidation or autothermal reforming systems where air is fed to the reformer, and the hydrogen fraction in the reformat is generally lower than for steam reformers.

Palladium silver alloys are well known for their capability of separating hydrogen from other components. The hydrogen dissociates at the metal surface and diffuses through the metal, provided there is a partial pressure gradient. The permeation rate is a function of the alloy temperature, the diffusion pathlength, the membrane surface area, and the hydrogen partial pressure difference, and can generally be expressed by equation B1.

$$F_{H_2} = A \cdot \exp\left(\frac{-E}{RT}\right) \cdot \frac{a}{t} \cdot \left((Y_{H_2}^{up} P_{up})^{0.5} - (Y_{H_2}^{down} P_{down})^{0.5} \right) \quad \text{Eq. B1}$$

F_{H_2}	=	H_2 flow through membrane	mol/s
A	=	constant	mol/s.m.Pa ^{0.5}
E	=	constant	J/mol
R	=	gas constant: 8.314	J/mol.K
T	=	temperature	K
a	=	membrane area	m ²
t	=	membrane thickness	m
$Y_{H_2}^{up}$	=	upstream hydrogen molfraction	-
$Y_{H_2}^{down}$	=	downstream molfraction	-
P_1	=	upstream pressure	Pa
P_2	=	downstream pressure	Pa

The membranes evaluated in this study are commercially available by Johnson Matthey or Engelhard. The tubes are made of 75wt% Pd and 25wt% Ag, with an alloy density of 11.638 kg/litre. The length of a single tube is 5.82 m, while the thickness is 124.46 µm. The in- and outside diameter are 1.02 and 1.27 mm. Hence the effective (log mean) area is calculated to be 0.021 m². A single membrane coil contains about 22.8 grams of Pd. At present the palladium price is about 11,600 \$/kg, resulting in a Pd only cost of 264 \$/membrane.

In the system studies here, for each scenario the number of membranes required was calculated based on the following assumptions.

$$\begin{aligned}
 P_1 &= 20 \text{ bar} \\
 P_2 &= 3.2 \text{ bar} \\
 Y_{H_2} &= 1 \\
 T &= 300 \text{ or } 400^\circ\text{C}
 \end{aligned}$$

The membrane performance was calculated by assuming that the flow through the membrane can be described by plug flow behaviour and is operated isothermally.

Because the reformat contains other components, the maximum fraction of hydrogen that can be retrieved from the reformat mixture is limited by the operating pressures and reformat hydrogen fraction. The maximum retrievable hydrogen fraction, ie. hydrogen product flow from membrane divided by the hydrogen flow in the feed to the membrane, can be calculated by the equation B2.

$$H_{2, \text{ maximum recoverable}} = \frac{1 - \frac{P_2}{P_1 \cdot Y_{g0}}}{1 - \frac{P_2}{P_1}} \quad \text{Eq. B2}$$

For example, if the reformat hydrogen concentration is 75%, $H_{2, \text{ maximum recoverable}}$ is 93.7%.

Figure B1 shows the H_2 fraction recovered along the length of the Pd membrane for a series of reformat feed rates. It can be seen that with a feed rate of 1 litre a min, the maximum recoverable hydrogen is reached within 2 meters. With a feed rate of 6 litres/min, only 70% of the hydrogen is recovered. The ideal flow rate in this case would be 3-3.5 litres, such that almost all recoverable hydrogen is recovered. Figure B.2 shows the impact of temperature on the hydrogen diffusion through the Pd membrane.

APPENDIX C: SYSTEM SIMULATIONS

C1 - Wellman CJB methanol reformer and CO clean-up

Data provided by Wellman CJB

Wellman CJB's reformer operates on a 54 wt% methanol mixture with water. The data provided is based on a electrically heated catalyst bed (1.24 litre). The feed is pumped to 4 bara and vaporised and superheated to about 300°C. The catalyst bed temperature is typically in the range of 220-250°C. The methanol conversion was estimated to be 99%. The dry reformer product consists of 74.6% H₂, 24.5% CO₂, 0.65% CO, 0.25% methanol.

The reformer product is cooled to 16°C, before it is fed to the CO clean-up reactor. The latter consists of 4 beds, each 1 inch diameter and 1 meter long. Air is fed to the CO clean-up reactor, to match an O₂:CO ratio of 0.74. The outlet concentration of CO was measured to be 2 ppm.

System Simulation: Base Case (system 1a, see Appendix D, figure D.1)

Methanol is pumped to pressure and split into two streams. One stream is fed to a catalytic burner (15 mol%), while the other is partially vaporised by heat exchange from the reformer product. Water is pumped to pressure and mixed with the partially preheated methanol to be vaporised and superheated. The vapour mixture is then fed to the reformer. Heat for both the feed preheater and the reformer is supplied by the hot exhaust gases from the catalytic burner.

Wellman CJB provided data for the CO clean-up to operate at an inlet temperature of 16°C. Operating temperatures of 16°C are not realistic for a car, since the lowest temperature achievable depends on the temperature of the cooling water. The cooling water in its turn is determined by the surrounding air temperature. The lowest cooling water temperature is assumed to 45°C, while the reformat is cooled to 50°C (instead of 16°C). It is unknown what the consequences are of this higher temperature (and higher water concentration in the reformat) on the performance of Wellman CJB's CO clean-up system.

The cooled reformat product is fed with air to the cooled CO clean-up reactor. The CO clean-up product, at 85°C, is humidified before entering the anode. In the anode 80% of the hydrogen is reacted to produce electricity. The remaining hydrogen and other rejected gases are fed to the catalytic burner. The catalytic burner oxidises all combustible components, using the cathode reject air. The burner product is used to heat the reformer, before it is expanded in the expander.

On the cathode side, air is compressed to 3.2 bar and humidified. The wet air is fed to the cathode, where half of the oxygen reacts with the hydrogen. The cathode reject gas

is cooled with cooling water to a temperature low enough to condense the appropriate amount of water to be recycled to the reformer. The vapour product from the condenser is used as the oxidant supply to the burner. The NSE of the Wellman CJB base case system was calculated to be 31.3%.

System Simulations: variations to Base Case

Three system variations were simulated in addition to the Base Case. A summary of the unit requirement for each system can be found in Appendix D, table D.2.

In **system 1b**, the anode hydrogen utilisation was set to 90% instead of 80%. As a result the heat generated from hydrogen in the catalytic burner is less and more methanol (25 mol%) needs to be fed to the burner to still supply the reformer with sufficient heat. The result of a more efficient anode is a less efficient reformer. Hence varying the anode utilisation has little to no effect on the net system efficiency (31.3%)

The expander in the system requires a high enough inlet temperature such that the vapour does not condense during expansion. In the base case system it was found that an inlet temperature of at least 150°C was necessary to prevent condensation, and the methanol feed to the catalytic burner was adjusted. In **system 1c** it was evaluated whether the net impact of the expander is positive, by simulating a system without an expander. This system demonstrated a more efficient reformer (12.5 mol% methanol to catalytic burner), but the PPR increased by 6%. The net result was a less efficient system, NSE = 29.3%. On the other hand, system 1c does not have an expander, nor the coupling to the compressor or control that comes with it.

The third variation to the system was the implementation of a palladium membrane instead of a catalytic CO clean-up reactor, **system 1d**. Since Wellman CJB do not have high pressure performance data of their steam reformer, it was assumed that the performance at 20 bar is equal to that of 4 bar.

In this system the reformer product is not cooled against the methanol feed, but instead it is heated to the membrane operating temperature. The Pd membrane is evaluated for two operating temperatures, i.e. 300 and 400°C. More detailed information on the performance of the membrane is provided in Appendix B. It is assumed that the membrane operates isothermally, and does not diffuse (leak) any other components than hydrogen. After the membrane, the hydrogen flow is heated to 85°C, while the bleed is expanded in an extra expander before entering the catalytic burner. The burner requires slightly more methanol than in the base case (16-18 mol%) to provide the other units in the system with heat. Although, the reformer is less efficient, the efficiency over the membrane and anode is now higher, resulting in a higher fuel processing efficiency. The NSE calculated for membrane operating temperatures of 300 and 400°C are 35.3 and 34.8%. The membrane requirements for this system are summarised in Appendix D, Table D.1.

Data provided by Johnson Matthey

Johnson Matthey's HotSpot reformer was originally developed to generate hydrogen from methanol by the combining partial oxidation and steam reforming over a single catalyst bed. More recently we have also evaluated this concept for other fuels [Carpenter, I. & Golunski, S.,1998]

In this study, three systems based on Johnson Matthey's methanol HotSpot reformer will be evaluated. In addition, the use of ethanol and natural gas as a fuel are also investigated. Micro-scale reactor test with ethanol were not very promising, ie. with the series of catalysts that were tested we achieved relatively low hydrogen concentrations, while significant coking occurred. Hence, the real data achieved in the above work is not very suitable for this study. Instead, the simulated system is based on how we would expect ethanol to reform if coking were absent or negligible.

Catalyst testing has also been conducted in HotSpot methane reforming. Although, by far not as well developed as methanol, initial results look promising. System simulations with Natural Gas in this work are based on results obtained with methane on a 1 kWe scale. It is assumed that Natural Gas performs similar to methane. This is a reasonable assumption, since methane is the most stable component in NG and it can therefore be expected that the higher hydrocarbons present in NG will convert more easily than methane.

Johnson Matthey's methanol HotSpot reformer is fed with methanol, water and air. The molar ratio during steady state operation is typically $\text{CH}_3\text{OH}:\text{H}_2\text{O}:\text{O}_2 = 1:1.18:0.2$. The CO in the reformer product is removed in Johnson Matthey's catalytic CO clean-up system, Demonox. The dry product from Demonox contains 52% H_2 (44% wet) and less than 10 ppm CO.

System Simulation: Base Case (system 2a, see Appendix D, figure D.2)

Methanol and water are pumped to pressure, and fed together with air to the HotSpot reformer preheat section. Heat required to fully vaporise the feed is delivered from the reformer and the catalytic burner. The reformer product and air are fed to Demonox (CO clean-up). The product from Demonox is cooled to the fuel cell operating temperature. The reformat is fully saturated. The rejected hydrogen and other non-reacting components in the reformat are fed to the catalytic burner.

On the cathode side the air is compressed to 3.2 bar, where the air for HotSpot and Demonox is compressed further in an additional compressor to 3.5 bar. The amount of air required for the fuel processor unit is relatively small (13.6%). The cathode air is humidified and fed to the cathode, where half of the oxygen reacts with the hydrogen. The cathode reject gas is cooled with cooling water to a temperature low enough to condense the appropriate amount of water to be recycled to the reformer. The vapour

product from the condenser is used as the oxidant supply to the burner. The burner product is, after preheating the reformer preheat section, expanded in an expander. The NSE of the Johnson Matthey HotSpot base case system is calculated to be 29.1%

System Simulation: variations to base case

In **system 2b** the anode utilisation was set to 90% instead of 80%. This improves the system efficiency with 3.4%, provided the heat from Demonox is used in the HotSpot preheat section. The increase in efficiency is because less heat is wasted in the system, and the rejected anode hydrogen is still sufficient to provide the HotSpot preheat section with heat. No further changes to the system are necessary.

Johnson Matthey's HotSpot reformer was also simulated in combination with a palladium membrane in **system 2c**. Johnson Matthey has no data available on the performance of HotSpot at elevated pressure in the range of 20 bar. Hence in the simulation here, the performance is assumed the same as at 3.5 bar.

The air for the reformer in system 2c is compressed to 20.5 bar in a two stage compressor with inter-stage cooling, additional to the normal compressor present to compress air to 3.2 bar. The reformer product is heated to the membrane operating temperature of 300 or 400°C (see Table D.3, Appendix D). The membrane hydrogen product is cooled and fed to the anode, while the bleed gas is expanded in an extra expander. The gains from this second expander result in a lower parasitic power for this system than the base case.

System 2d simulates the expected performance of Johnson Matthey's HotSpot reformer operating on ethanol. It is assumed that ethanol behaves similarly as methanol in the reformer, although the reformer is expected to operate at a higher temperature. As a result of the higher operating temperature, the CO content in the reformat is expected to be too high and a LTS reactor is inserted in the system before Demonox. The NSE was estimated to be 28.6%.

System 2e and 2f simulate fuel cell systems based on HotSpot reforming natural gas. The NG composition is assumed to be the same as data by BG Technology supplied for this project. Experimental results have indicated that we can obtain fairly low CO concentrations from HotSpot operating with methane. Therefore, the system was evaluated with and without a LTS reactor. The LTS reactor will increase the efficiency of the system, but also increase the size, dynamics, and complexity of the system. Table D4 in Appendix D lists the expected required unit operation for the various systems. The NSE for systems 2e and 2f were calculated to be 27.4 and 24.2.

C3 - BG Technology Natural Gas reformer

Data provided by BG Technology

BG Technology's reformer generates hydrogen from Natural Gas in a heat exchange reactor. On one side of the heat exchanger, NG is reformed, while on the other side NG is combusted to provide the heat to drive the steam reforming reaction. Two sets of reformer operating data were provided by BG Technology. The first set is for a natural gas reformer operating at a pressure of about 3.5 bar on the steam reformer side, while the second set of data is based on a steam reforming pressure of 20.5 bar. In both cases the combustion side inlet pressure is 1.4 bar.

Natural gas and superheated steam at 170°C ($\text{CH}_4:\text{H}_2\text{O}$ ratio = 1:3.32) are fed to the reformer side at 3.5 bara, while air and natural gas ($\text{CH}_4:\text{O}_2$ ratio = 1:3.05) are fed to the combustion side at 1.4 bara. The reformat product exits the reformer at 400°C, containing 75.5% H_2 (dry), 13.2% CO, 9.3% CO_2 , and 1.6% residual methane. The conversion is approximately 93%. The combustion product leaves the reformer at 180°C, where all hydrocarbons are fully converted.

Similarly, natural gas and saturated steam ($\text{CH}_4:\text{H}_2\text{O}$ ratio = 1:3.32) are fed to the reformer side at 20.5 bara, while air and natural gas ($\text{CH}_4:\text{O}_2$ ratio = 1:4.58) are fed to the combustion side at 1.4 bara. Methane steam reforming conversion is inversely proportional to pressure. At 20.5 bar, the methane conversion is expected to be 56.3%. Hence the dry reformat product now contains 67.5% H_2 , and 12.6% remaining CH_4 .

System Simulation: Base Case (system 3a, see figure D.3 in Appendix D)

Water is pumped to pressure, and superheated with heat from the catalytic burner. Natural Gas is delivered from the pressurised storage tank to both the reforming and combustion side of the reformer. Air is compressed in a separate compressor to supply air to the combustion side. The reformer product is shifted in two consecutive shift reactors. Both the HTS and LTS reactor are assumed to operate adiabatically. After the HTS reactor the reformat is cooled to 200°C, while after the LTS reactor, the reformat is cooled to suitable temperature for Demonox (~150°C). After Demonox the reformat is cooled to 85°C and fed to the anode.

The anode reject gas is combusted in a catalytic burner using the cathode off-gas. The burner product is, after generating steam for the reformer, expanded in an expander. The expander product is cooled to produce enough condensate water for the water recycle stream. The condensate of the cathode condenser is not sufficient to supply the reformer. Like in the previous systems, the air for the cathode is compressed to 3.2 bar and humidified before it is being fed to the fuel cell. The NSE for the BG natural gas reformer base case is calculated to be 28.1%.

System Simulation: variations to Base Case

Two variations of the base case system were evaluated for the BG reformer. In **system 3b** the anode utilisation was set to 90% instead of 80%. This improves the system efficiency with 2.7%, provided the heat from the cooler after the LTS reactor and from Demonox is used to contribute to raise the superheated steam for the reformer. The increase in efficiency is result of the fact that less heat is wasted in the system, and the combined heat from the cooler, Demonox, and the catalytic burner are sufficient to raise the steam. No further changes to the system are necessary.

In **system 3c** the possibility of a Pd membrane instead of a catalytic CO clean-up is evaluated. With the high pressure data provided by BG, the hydrogen concentration after the LTS reactor was calculated to be 45.4%. This low value is the result of the low conversion and the high water to carbon feed ratio. The maximum fraction of hydrogen that can be removed would then be 78%. This is already lower than the base case anode hydrogen utilisation.

However, if the reformat is first cooled to knock out the majority of the water and then heated and fed to the membrane, a higher hydrogen recovery can be expected. In the system here, the reformat is cooled to 100°C resulting in a reformat with a hydrogen concentration of 69%. The maximum hydrogen recovery is now > 90%. The results for the membrane are summarised in Appendix D, Table D.5.

The NSE for the membrane system was calculated to be 23.5%, significantly lower than the base case system. This is by and large due to the lower methane conversion. The unconverted methane from the steam reformer is combusted in the catalytic burner, producing more heat than required in the system.

APPENDIX D: ASPEN MODELS

D1 -Wellman CJB methanol steam reformer system

Table D.1: Membrane requirements for Wellman CJB reformer system 1d

Reformate feed conditions		Membrane	300°C	400°C
H ₂ frac	0.657	number	357	290
flow rate (mol/min)	49.503	actual H ₂ recovered	0.88	0.88
H ₂ max recoverable	0.90	Pd cost (\$)	94,300	76,600

Table D.2: Units required for Wellman CJB systems

System	1a	1b	1c	1d
liquid pump	4	4	4	4
compressor	1	1	1	1
expander	1	1	0	2
reformer	1	1	1	1
shift reactors	0	0	0	0
CO clean-up/ membrane	1	1	1	1
catalytic burner	1	1	1	1
evaporator	1	1	1	1
condenser	1	1	1	1
heat exchanger (l/l)/(g/l)/(g/g) ¹	1/3/2	1/3/2	1/3/2	1/3/1
fan	1	1	1	1
Total number of units	18	18	17	18

¹ l = liquid phase, g = gas phase

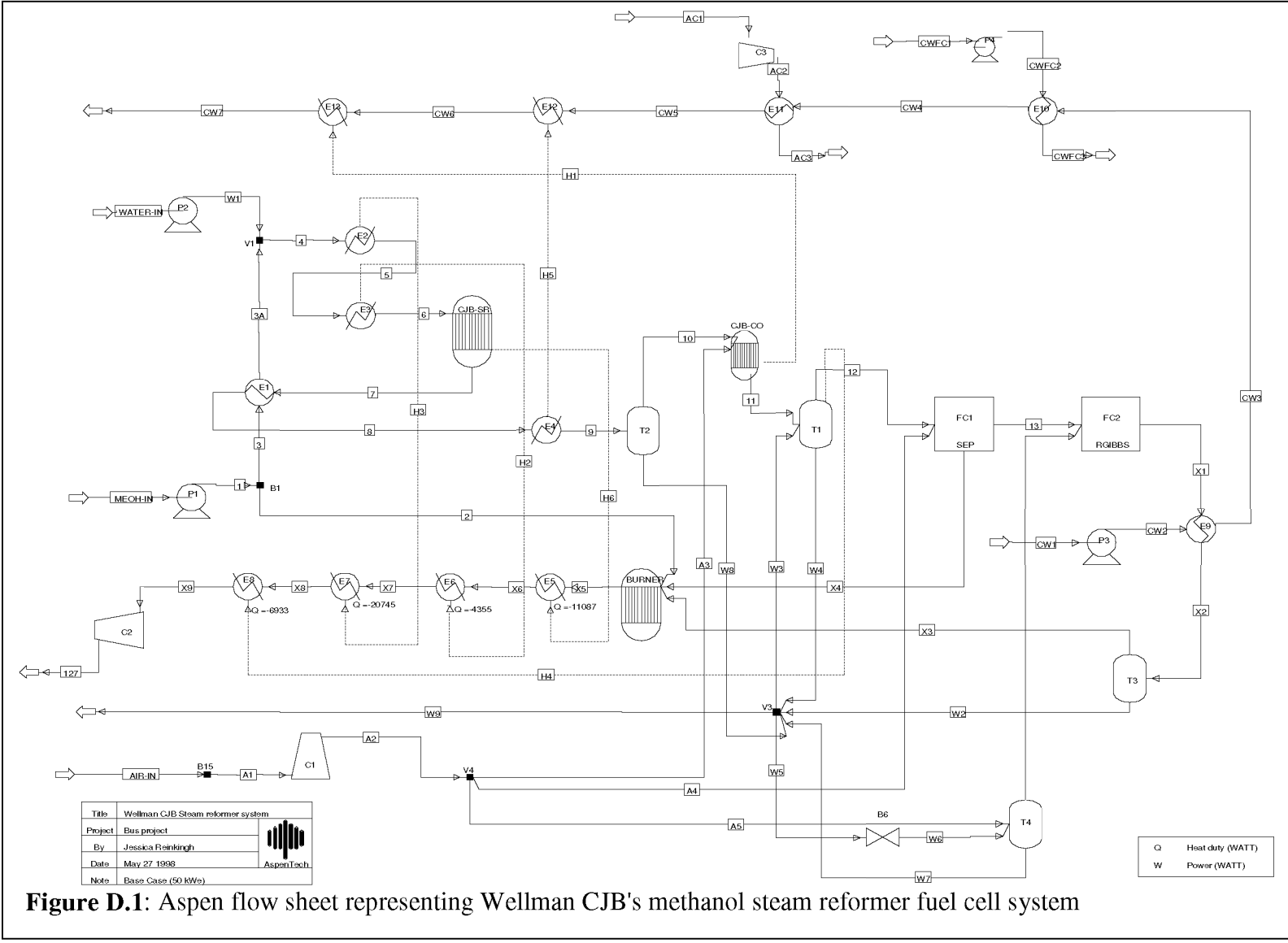


Figure D.1: Aspen flow sheet representing Wellman CJB's methanol steam reformer fuel cell system

Stream Tables Wellman CJB Base Case system

Data file created by ASPEN PLUS Rel. 9.3-1 on
 22:17:35 Wed May 27, 1998
 Run ID: CJB_3

Stream	MEOH-IN	1	2	3	3A	4	5	6
From		P1	B1	B1	E1	V1	E2	E3
To	P1	B1	BURNER	E1	V1	E2	E3	CJB-SR
Phase	LIQUID	LIQUID	LIQUID	LIQUID	MIXED	LIQUID	VAPOR	VAPOR
Mole Flow MOL/MIN								
MEOH	15.01	15.01	2.25	12.76	12.76	12.76	12.76	12.76
H2O	0.00	0.00	0.00	0.00	0.00	19.14	19.14	19.14
H2	0.00	0.00	0.00	0.00	0.00	0.00	0.00	0.00
CO2	0.00	0.00	0.00	0.00	0.00	0.00	0.00	0.00
CO	0.00	0.00	0.00	0.00	0.00	0.00	0.00	0.00
O2	0.00	0.00	0.00	0.00	0.00	0.00	0.00	0.00
N2	0.00	0.00	0.00	0.00	0.00	0.00	0.00	0.00
Total Flow MOL/MIN	15.01	15.01	2.25	12.76	12.76	31.90	31.90	31.90
Total Flow KG/SEC	0.01	0.01	0.00	0.01	0.01	0.01	0.01	0.01
Total Flow L/MIN	0.59	0.59	0.09	0.50	22.05	0.97	270.65	412.35
Temperature C	15.00	15.27	15.27	15.27	101.92	107.00	128.25	308.00
Pressure BAR	1.00	4.00	4.00	4.00	3.90	3.90	3.80	3.70
Vapor Frac	0.00	0.00	0.00	0.00	0.22	0.00	1.00	1.00
Liquid Frac	1.00	1.00	1.00	1.00	0.78	1.00	0.00	0.00
Density KG/CUM	811.15	810.83	810.83	810.83	18.54	773.85	2.78	1.83
Average MW	32.04	32.04	32.04	32.04	32.04	23.63	23.63	23.63

Data file created by ASPEN PLUS Rel. 9.3-1 on
 22:17:35 Wed May 27, 1998
 Run ID: CJB_3

Stream	7	8	9	10	11	12	13
From	CJB-SR	E1	E4	T2	CJB-CO	T1	FC1
To	E1	E4	T2	CJB-CO	T1	FC1	FC2
Phase	VAPOR	VAPOR	MIXED	VAPOR	VAPOR	VAPOR	VAPOR
Mole Flow MOL/MIN							
MEOH	0.13	0.13	0.13	0.11	0.11	0.11	0.00
H2O	6.88	6.88	6.88	1.75	1.95	11.10	0.00
H2	37.53	37.53	37.53	37.53	37.34	37.34	29.87
CO2	12.26	12.26	12.26	12.26	12.63	12.63	0.00
CO	0.37	0.37	0.37	0.37	0.00	0.00	0.00
O2	0.00	0.00	0.00	0.00	0.00	0.00	0.00
N2	0.00	0.00	0.00	0.00	1.04	1.04	0.00
Total Flow MOL/MIN	57.16	57.16	57.16	52.02	53.08	62.23	29.87
Total Flow KG/SEC	0.01	0.01	0.01	0.01	0.01	0.01	0.00
Total Flow L/MIN	724.67	573.25	448.05	436.68	509.91	616.62	298.69
Temperature C	245.00	125.00	55.00	50.00	85.00	85.00	87.15
Pressure BAR	3.40	3.30	3.20	3.20	3.10	3.00	3.00
Vapor Frac	1.00	1.00	0.92	1.00	1.00	1.00	1.00
Liquid Frac	0.00	0.00	0.08	0.00	0.00	0.00	0.00
Density KG/CUM	1.04	1.31	1.68	1.51	1.37	1.40	0.20
Average MW	13.18	13.18	13.18	12.70	13.17	13.88	2.02

Data file created by ASPEN PLUS Rel. 9.3-1 on
 22:17:35 Wed May 27, 1998
 Run ID: CJB_3

Stream	AIR-IN	A1	A2	A3	A4	A5	A6	AC1	AC2	AC3
From		B15	C1	V4	V4	V4	T4		C3	E11
To	B15	C1	V4	CJB-CO	FC1	T4	FC2	C3	E11	
Phase	VAPOR	VAPOR	VAPOR	VAPOR	VAPOR	VAPOR	VAPOR	VAPOR	VAPOR	VAPOR
Mole Flow MOL/MIN										
MEOH	0.00	0.00	0.00	0.00	0.00	0.00	0.01	0.00	0.00	0.00
H2O	1.97	1.40	1.40	0.01	0.01	1.37	31.05	0.00	0.00	0.00
H2	0.00	0.00	0.00	0.00	0.00	0.00	0.00	0.00	0.00	0.00
CO2	0.00	0.00	0.00	0.00	0.00	0.00	0.00	0.00	0.00	0.00
CO	0.00	0.00	0.00	0.00	0.00	0.00	0.00	0.00	0.00	0.00
O2	42.85	30.41	30.41	0.28	0.26	29.87	29.87	3166.67	3166.67	3166.67
N2	161.20	114.40	114.40	1.04	0.97	112.38	112.38	11916.67	11916.67	11916.67
Total Flow MOL/MIN	206.02	146.21	146.21	1.33	1.24	143.63	173.32	15083.33	15083.33	15083.33
Total Flow KG/SEC	0.10	0.07	0.07	0.00	0.00	0.07	0.08	7.25	7.25	7.25
Total Flow L/MIN	4932.12	3500.21	1816.10	16.54	15.46	1784.10	1715.08	373704.00	373478.00	386779.00
Temperature C	15.00	15.00	204.59	204.59	204.59	204.59	85.00	25.00	25.12	35.40
Pressure BAR	1.00	1.00	3.20	3.20	3.20	3.20	3.00	1.00	1.00	1.00
Vapor Frac	1.00	1.00	1.00	1.00	1.00	1.00	1.00	1.00	1.00	1.00
Liquid Frac	0.00	0.00	0.00	0.00	0.00	0.00	0.00	0.00	0.00	0.00
Density KG/CUM	1.20	1.20	2.31	2.31	2.31	2.31	2.72	1.16	1.17	1.13
Average MW	28.75	28.75	28.75	28.75	28.75	28.75	26.91	28.85	28.85	28.85

Data file created by ASPEN PLUS Rel. 9.3-1 on
 22:17:35 Wed May 27, 1998
 __70Run ID: CJB_3

Stream	CW1	CW2	CW3	CW4	CW5	CW6	CW7	CWFC1	CWFC2	CWFC3
From		P3	E9	E10	E11	E12	E13		P4	E10
To	P3	E9	E10	E11	E12	E13		P4	E10	
Phase	LIQUID									
Mole Flow MOL/MIN										
MEOH	0.00	0.00	0.00	0.00	0.00	0.00	0.00	0.00	0.00	0.00
H2O	3333.33	3333.33	3333.33	3333.33	3333.33	3333.33	3333.33	3561.79	3561.79	3561.79
H2	0.00	0.00	0.00	0.00	0.00	0.00	0.00	0.00	0.00	0.00
CO2	0.00	0.00	0.00	0.00	0.00	0.00	0.00	0.00	0.00	0.00
CO	0.00	0.00	0.00	0.00	0.00	0.00	0.00	0.00	0.00	0.00
O2	0.00	0.00	0.00	0.00	0.00	0.00	0.00	0.00	0.00	0.00
N2	0.00	0.00	0.00	0.00	0.00	0.00	0.00	0.00	0.00	0.00
Total Flow MOL/MIN	3333.33	3333.33	3333.33	3333.33	3333.33	3333.33	3333.33	3561.79	3561.79	3561.79
Total Flow KG/SEC	1.00	1.00	1.00	1.00	1.00	1.00	1.00	1.07	1.07	1.07
Total Flow L/MIN	61.75	61.76	62.02	62.72	61.65	61.73	61.75	68.73	68.73	67.98
Temperature C	46.60	46.63	50.89	61.66	45.00	46.23	46.58	85.00	85.01	75.00
Pressure BAR	1.00	1.60	1.50	1.30	1.20	1.10	1.00	1.00	1.20	1.00
Vapor Frac	0.00	0.00	0.00	0.00	0.00	0.00	0.00	0.00	0.00	0.00
Liquid Frac	1.00	1.00	1.00	1.00	1.00	1.00	1.00	1.00	1.00	1.00
Density KG/CUM	972.44	972.41	968.19	957.43	974.02	972.81	972.46	933.60	933.59	943.90
Average MW	18.02	18.02	18.02	18.02	18.02	18.02	18.02	18.02	18.02	18.02

Data file created by ASPEN PLUS Rel. 9.3-1 on
 22:17:35 Wed May 27, 1998
 Run ID: CJB_3

Stream	WATER-IN	W1	W2	W3	W4	W5	W6	W7	W8	W9
From		P2	T3	V3	T1	V3	B6	T4	T2	V3
To	P2	V1	V3	T1	V3	B6	T4	V3	V3	
Phase	LIQUID	LIQUID	LIQUID	MIXED	LIQUID	MIXED	LIQUID	LIQUID	LIQUID	MIXED
Mole Flow MOL/MIN										
MEOH	0.00	0.00	0.00	0.00	0.00	0.01	0.01	0.00	0.02	0.01
H2O	19.14	19.14	53.98	10.00	0.85	33.32	33.32	3.65	5.12	20.28
H2	0.00	0.00	0.00	0.00	0.00	0.00	0.00	0.00	0.00	0.00
CO2	0.00	0.00	0.00	0.00	0.00	0.00	0.00	0.00	0.00	0.00
CO	0.00	0.00	0.00	0.00	0.00	0.00	0.00	0.00	0.00	0.00
O2	0.00	0.00	0.00	0.00	0.00	0.00	0.00	0.00	0.00	0.00
N2	0.00	0.00	0.00	0.00	0.00	0.00	0.00	0.00	0.00	0.00
Total Flow MOL/MIN	19.14	19.14	53.98	10.00	0.85	33.33	33.33	3.65	5.14	20.28
Total Flow KG/SEC	0.01	0.01	0.02	0.00	0.00	0.01	0.01	0.00	0.00	0.01
Total Flow L/MIN	0.36	0.36	1.01	0.19	0.02	0.62	0.62	0.07	0.10	0.38
Temperature C	60.00	60.17	55.00	56.72	85.00	56.72	56.71	85.00	50.00	56.72
Pressure BAR	1.00	4.00	2.70	2.70	3.00	2.70	3.20	3.00	3.20	2.70
Vapor Frac	0.00	0.00	0.00	0.00	0.00	0.00	0.00	0.00	0.00	0.00
Liquid Frac	1.00	1.00	1.00	1.00	1.00	1.00	1.00	1.00	1.00	1.00
Density KG/CUM	959.10	958.92	964.10	962.22	933.22	962.22	962.25	933.59	967.42	962.22
Average MW	18.02	18.02	18.02	18.02	18.03	18.02	18.02	18.02	18.06	18.02

Data file created by ASPEN PLUS Rel. 9.3-1 on
 22:17:35 Wed May 27, 1998
 Run ID: CJB_3

Stream	X1	X2	X3	X4	X5	X6	X7	X8	X9	127
From	FC2	E9	T3	FC1	BURNER	E5	E6	E7	E8	C2
To	E9	T3	BURNER	BURNER	E5	E6	E7	E8	C2	
Phase	MIXED	MIXED	VAPOR	MIXED	VAPOR	VAPOR	VAPOR	VAPOR	VAPOR	VAPOR
Mole Flow MOL/MIN										
MEOH	0.00	0.00	0.00	0.11	0.00	0.00	0.00	0.00	0.00	0.00
H2O	60.94	60.94	6.96	11.11	30.27	30.27	30.27	30.27	30.27	30.27
H2	0.00	0.00	0.00	7.47	0.00	0.00	0.00	0.00	0.00	0.00
CO2	0.01	0.01	0.01	12.63	15.01	15.01	15.01	15.01	15.01	15.01
CO	0.00	0.00	0.00	0.00	0.00	0.00	0.00	0.00	0.00	0.00
O2	14.92	14.92	14.92	0.26	7.90	7.90	7.90	7.90	7.90	7.90
N2	112.38	112.38	112.38	2.02	114.40	114.40	114.40	114.40	114.40	114.40
Total Flow MOL/MIN	188.26	188.26	134.27	33.60	167.57	167.57	167.57	167.57	167.57	167.57
Total Flow KG/SEC	0.08	0.08	0.06	0.01	0.08	0.08	0.08	0.08	0.08	0.08
Total Flow L/MIN	1535.63	1305.04	1354.95	277.48	4955.40	4501.20	4326.49	3056.50	2699.79	5208.10
Temperature C	85.00	55.00	55.00	87.15	615.53	501.85	456.29	231.61	153.66	101.04
Pressure BAR	3.00	2.80	2.70	3.00	2.50	2.40	2.35	2.30	2.20	1.00
Vapor Frac	0.82	0.71	1.00	0.83	1.00	1.00	1.00	1.00	1.00	1.00
Liquid Frac	0.18	0.29	0.00	0.17	0.00	0.00	0.00	0.00	0.00	0.00
Density KG/CUM	3.08	3.62	2.77	3.03	0.94	1.04	1.08	1.53	1.73	0.90
Average MW	25.09	25.09	27.94	24.99	27.83	27.83	27.83	27.83	27.83	27.83

D2 - Johnson Matthey HotSpot reformer system

Table D.3: Membrane requirements for Johnson Matthey system 2c

Reformate feed conditions		Membrane	300°C	400°C
H ₂ frac	0.50	number	590	482
flow rate (mol/min)	71.7	actual H ₂ recovered	0.79	0.79
H ₂ max recoverable	0.81	Pd cost (\$)	155,839	127,313

Table D.4: Units required for Johnson Matthey systems

System	2a	2b	2c	2d	2e	2f
liquid pump	4	4	4	4	3	3
compressor (+ booster)	1	1	2*	1	1	1
expander	1	1	2	1	1	1
reformer	1	1	1	1	1	1
shift reactors	0	0	0	1	1	0
CO clean-up/ membrane	1	1	1	1	1	1
catalytic burner	1	1	1	1	1	1
vaporiser	1	1	1	1	1	1
condenser	2	2	1	3	3	3
heat exchanger (l/l)/(g/l)/(g/g)	1/2/0	1/2/0	1/5/1	1/2/1	1/3/1	1/2/1
fan	1	1	1	1	1	1
Total number of units	16	16	21	19	18	16

* 1 single stage and 1 two stage compressor

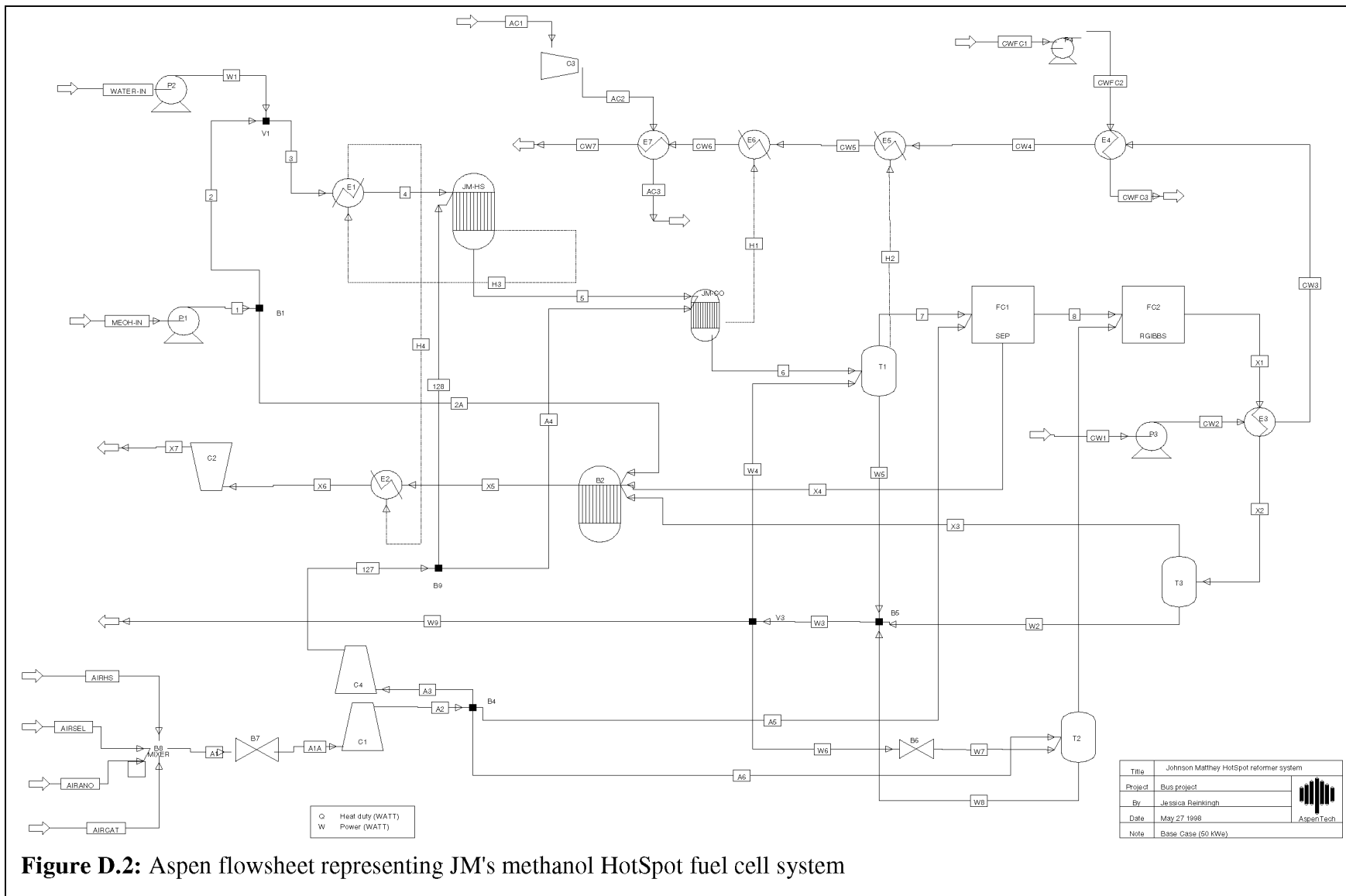


Figure D.2: Aspen flowsheet representing JM's methanol HotSpot fuel cell system

Stream Tables Johnson Matthey Methanol Reformer Base Case system

Data file created by ASPEN PLUS Rel. 9.3-1 on 09:39:39
 Thu May 28, 1998
 Run ID: JMHS_2

Stream	MEOH-IN	1	2	2A	3	4	5	6	7	8
From		P1	B1	B1	V1	E1	JM-HS	JM-CO	T1	FC1
To	P1	B1	V1	B2	E1	JM-HS	JM-CO	T1	FC1	FC2
Phase	LIQUID	LIQUID	LIQUID	LIQUID	LIQUID	VAPOR	VAPOR	VAPOR	VAPOR	VAPOR
Mole Flow MOL/MIN										
MEOH	16.15	16.15	16.15	0.00	16.15	16.15	0.16	0.16	0.16	0.00
H2O	0.00	0.00	0.00	0.00	19.15	19.15	11.16	13.21	15.56	0.00
H2	0.00	0.00	0.00	0.00	0.00	0.00	39.47	37.43	37.43	29.94
CO2	0.00	0.00	0.00	0.00	0.00	0.00	14.72	15.74	15.74	0.00
CO	0.00	0.00	0.00	0.00	0.00	0.00	1.02	0.00	0.00	0.00
O2	0.00	0.00	0.00	0.00	0.00	0.00	0.00	0.00	0.00	0.00
N2	0.00	0.00	0.00	0.00	0.00	0.00	12.20	17.96	17.96	0.00
CH4	0.00	0.00	0.00	0.00	0.00	0.00	0.25	0.25	0.25	0.00
Total Flow MOL/MIN	16.15	16.15	16.15	0.00	35.30	35.30	78.98	84.74	87.09	29.94
Total Flow KG/SEC	0.01	0.01	0.01	0.00	0.01	0.01	0.02	0.03	0.03	0.00
Total Flow L/MIN	0.64	0.64	0.64	0.00	1.00	289.95	909.23	1029.59	862.54	299.39
Temperature C	15.00	15.27	15.27	15.27	24.85	126.60	170.00	180.00	85.00	87.17
Pressure BAR	1.00	4.00	4.00	4.00	4.00	3.90	3.20	3.10	3.00	3.00
Vapor Frac	0.00	0.00	0.00	0.00	0.00	1.00	1.00	1.00	1.00	1.00
Liquid Frac	1.00	1.00	1.00	1.00	1.00	0.00	0.00	0.00	0.00	0.00
Density KG/CUM	811.15	810.83	810.83	810.83	859.22	2.97	1.44	1.47	1.81	0.20
Average MW	32.04	32.04	32.04	32.04	24.43	24.43	16.56	17.92	17.92	2.02

Data file created by ASPEN PLUS Rel. 9.3-1 on

09:39:39 Thu May 28, 1998

Run ID: JMHS_2

Stream	AIRANO	AIRCAT	AIRHS	AIRSEL	A1	A2	A3	A5	A6	A7
From					B8	C1	B4	B4	B4	T2
To	B8	B8	B8	B8	B7	B4	C4	FC1	T2	FC2
Phase	VAPOR	VAPOR	VAPOR	VAPOR	VAPOR	VAPOR	VAPOR	VAPOR	VAPOR	VAPOR
Mole Flow MOL/MIN										
MEOH	0.00	0.00	0.00	0.00	0.00	0.00	0.00	0.00	0.00	0.00
H2O	0.00	0.00	0.00	0.00	0.00	0.00	0.00	0.00	0.00	31.12
H2	0.00	0.00	0.00	0.00	0.00	0.00	0.00	0.00	0.00	0.00
CO2	0.00	0.00	0.00	0.00	0.00	0.00	0.00	0.00	0.00	0.00
CO	0.00	0.00	0.00	0.00	0.00	0.00	0.00	0.00	0.00	0.00
O2	0.37	29.94	3.24	1.53	35.08	35.08	4.77	0.37	29.94	29.94
N2	1.38	112.64	12.20	5.76	131.98	131.98	17.96	1.38	112.64	112.64
CH4	0.00	0.00	0.00	0.00	0.00	0.00	0.00	0.00	0.00	0.00
Total Flow MOL/MIN	1.74	142.58	15.44	7.29	167.06	167.06	22.73	1.74	142.58	173.70
Total Flow KG/SEC	0.00	0.07	0.01	0.00	0.08	0.08	0.01	0.00	0.07	0.08
Total Flow L/MIN	41.70	3413.77	369.78	174.51	3999.76	2076.89	282.62	21.65	1772.61	1718.92
Temperature C	15.00	15.00	15.00	15.00	15.00	204.96	204.96	204.96	204.96	85.00
Pressure BAR	1.00	1.00	1.00	1.00	1.00	3.20	3.20	3.20	3.20	3.00
Vapor Frac	1.00	1.00	1.00	1.00	1.00	1.00	1.00	1.00	1.00	1.00
Liquid Frac	0.00	0.00	0.00	0.00	0.00	0.00	0.00	0.00	0.00	0.00
Density KG/CUM	1.21	1.21	1.21	1.21	1.21	2.32	2.32	2.32	2.32	2.72
__Average MW	28.85	28.85	28.85	28.85	28.85	28.85	28.85	28.85	28.85	26.91

Data file created by ASPEN PLUS Rel. 9.3-1 on
 09:39:39 Thu May 28, 1998
 Run ID: JMHS_2

Stream	CW1	CW2	CW3	CW4	CW5	CW6	CW7	CWFC1	CWFC2	CWFC3
From		P3	E3	E4	E5	E6	E7		P4	E4
To	P3	E3	E4	E5	E6	E7		P4	E4	
Phase	LIQUID									
Mole Flow MOL/MIN										
MEOH	0.00	0.00	0.00	0.00	0.00	0.00	0.00	0.00	0.00	0.00
H2O	3333.33	3333.33	3333.33	3333.33	3333.33	3333.33	3333.33	3515.53	3515.53	3515.53
H2	0.00	0.00	0.00	0.00	0.00	0.00	0.00	0.00	0.00	0.00
CO2	0.00	0.00	0.00	0.00	0.00	0.00	0.00	0.00	0.00	0.00
CO	0.00	0.00	0.00	0.00	0.00	0.00	0.00	0.00	0.00	0.00
O2	0.00	0.00	0.00	0.00	0.00	0.00	0.00	0.00	0.00	0.00
N2	0.00	0.00	0.00	0.00	0.00	0.00	0.00	0.00	0.00	0.00
CH4	0.00	0.00	0.00	0.00	0.00	0.00	0.00	0.00	0.00	0.00
Total Flow MOL/MIN	3333.33	3333.33	3333.33	3333.33	3333.33	3333.33	3333.33	3515.53	3515.53	3515.53
Total Flow KG/SEC										
Total Flow KG/SEC	1.00	1.00	1.00	1.00	1.00	1.00	1.00	1.06	1.06	1.06
Total Flow L/MIN										
Total Flow L/MIN	61.65	61.65	61.91	62.59	62.63	62.81	61.65	67.84	67.84	67.10
Temperature C										
Temperature C	45.00	45.03	49.02	59.66	60.23	63.06	45.00	85.00	85.01	75.00
Pressure BAR										
Pressure BAR	1.00	1.60	1.50	1.30	1.20	1.10	1.00	1.00	1.20	1.00
Vapor Frac										
Vapor Frac	0.00	0.00	0.00	0.00	0.00	0.00	0.00	0.00	0.00	0.00
Liquid Frac										
Liquid Frac	1.00	1.00	1.00	1.00	1.00	1.00	1.00	1.00	1.00	1.00
Density KG/CUM										
Density KG/CUM	974.02	973.98	970.04	959.44	958.87	956.02	974.02	933.60	933.59	943.90
Average MW										
Average MW	18.02	18.02	18.02	18.02	18.02	18.02	18.02	18.02	18.02	18.02

Data file created by ASPEN PLUS Rel. 9.3-1 on
 09:39:39 Thu May 28, 1998
 Run ID: JMHS_2

Stream	WATER- IN	W1	W2	W3	W4	W5	W6	W7	W8	W9
From		P2	T3	B5	V3	T1	V3	B6	T2	V3
To	P2	V1	B5	V3	T1	B5	B6	T2	B5	
Phase	LIQUID	LIQUID	LIQUID	MIXED	MIXED	LIQUID	MIXED	LIQUID	LIQUID	MIXED
Mole Flow MOL/MIN										
MEOH	0.00	0.00	0.00	0.00	0.00	0.00	0.00	0.00	0.00	0.00
H2O	19.15	19.15	53.12	57.15	3.33	0.98	34.17	34.17	3.05	19.65
H2	0.00	0.00	0.00	0.00	0.00	0.00	0.00	0.00	0.00	0.00
CO2	0.00	0.00	0.00	0.00	0.00	0.00	0.00	0.00	0.00	0.00
CO	0.00	0.00	0.00	0.00	0.00	0.00	0.00	0.00	0.00	0.00
O2	0.00	0.00	0.00	0.00	0.00	0.00	0.00	0.00	0.00	0.00
N2	0.00	0.00	0.00	0.00	0.00	0.00	0.00	0.00	0.00	0.00
CH4	0.00	0.00	0.00	0.00	0.00	0.00	0.00	0.00	0.00	0.00
Total Flow MOL/MIN	19.15	19.15	53.12	57.15	3.33	0.98	34.17	34.17	3.05	19.65
Total Flow KG/SEC	0.01	0.01	0.02	0.02	0.00	0.00	0.01	0.01	0.00	0.01
Total Flow L/MIN	0.35	0.35	1.00	1.07	0.06	0.02	0.64	0.64	0.06	0.37
Temperature C	45.00	45.17	57.49	59.44	59.44	85.00	59.44	59.43	85.00	59.44
Pressure BAR	1.00	4.00	2.70	2.70	2.70	3.00	2.70	3.20	3.00	2.70
Vapor Frac	0.00	0.00	0.00	0.00	0.00	0.00	0.00	0.00	0.00	0.00

Liquid Frac	1.00	1.00	1.00	1.00	1.00	1.00	1.00	1.00	1.00	1.00
Density KG/CUM	974.02	973.85	961.61	959.64	959.64	933.22	959.64	959.66	933.60	959.64
Average MW	18.02	18.02	18.02	18.02	18.02	18.03	18.02	18.02	18.02	18.02

Data file created by ASPEN PLUS Rel. 9.3-1 on
 09:39:39 Thu May 28, 1998
 Run ID: JMHS_2

Stream	X1	X2	X3	X4	X5	X6	X7	AC1	AC2	AC3
From	FC2	E3	T3	FC1	B2	E2	C2		C3	E7
To	E3	T3	B2	B2	E2	C2		C3	E7	
Phase	MIXED	MIXED	VAPOR	MIXED	VAPOR	VAPOR	VAPOR	VAPOR	VAPOR	VAPOR
Mole Flow MOL/MIN										
MEOH	0.00	0.00	0.00	0.16	0.00	0.00	0.00	0.00	0.00	0.00
H2O	61.06	61.06	7.94	15.56	31.80	31.80	31.80	0.00	0.00	0.00
H2	0.00	0.00	0.00	7.49	0.00	0.00	0.00	0.00	0.00	0.00
CO2	0.00	0.00	0.00	15.74	16.15	16.15	16.15	0.00	0.00	0.00
CO	0.00	0.00	0.00	0.00	0.00	0.00	0.00	0.00	0.00	0.00
O2	14.97	14.97	14.97	0.37	10.86	10.86	10.86	3333.33	3333.33	3333.33
N2	112.64	112.64	112.64	19.34	131.98	131.98	131.98	12523.33	12523.33	12523.33
CH4	0.00	0.00	0.00	0.25	0.00	0.00	0.00	0.00	0.00	0.00
Total Flow MOL/MIN	188.68	188.68	135.55	58.89	190.78	190.78	190.78	15856.67	15856.67	15856.67
Total Flow KG/SEC										
Total Flow L/MIN	1539.20	1331.05	1378.19	535.26	4140.53	3232.70	6716.59	392864.00	392627.00	407029.00
Temperature C	85.00	58.00	57.49	87.17	379.20	216.18	150.50	25.00	25.12	35.72
Pressure BAR	3.00	2.80	2.70	3.00	2.50	2.40	1.00	1.00	1.00	1.00
Vapor Frac	0.82	0.72	1.00	0.91	1.00	1.00	1.00	1.00	1.00	1.00
Liquid Frac	0.18	0.28	0.00	0.09	0.00	0.00	0.00	0.00	0.00	0.00
Density KG/CUM	3.08	3.56	2.74	2.90	1.29	1.65	0.79	1.16	1.17	1.12
Average MW	25.09	25.09	27.87	26.33	27.93	27.93	27.93	28.85	28.85	28.85

D3 - British Gas NG reformer system

Table D.5: Membrane requirements for British Gas system 3c

Reformate feed conditions		Membrane	300°C	400°C
H ₂ frac	0.69	number	350	276
flow rate (mol/min)	47.0	actual H ₂ recovered	0.90	0.90
H ₂ max recoverable	0.92	Pd cost (\$)	92,447	72,901

Table D.6: Units required for British Gas Natural Gas reformer systems

System	3a	3b	3c
liquid pump	3	3	3
compressor	2	2	2
expander	1	1	2
reformer	1	1	1
shift reactors	2	2	2
CO clean-up/ membrane	1	1	1
catalytic burner	1	1	1
Vaporiser	1	1	1
Condenser	3	3	2
Heat exchanger (l/l)/(g/l)/(g/g)	1/3/0	1/2/1	1/5/1
Fan	1	1	1
Total number of units	20	20	23

Stream Tables British Gas Natural Gas Base Case system

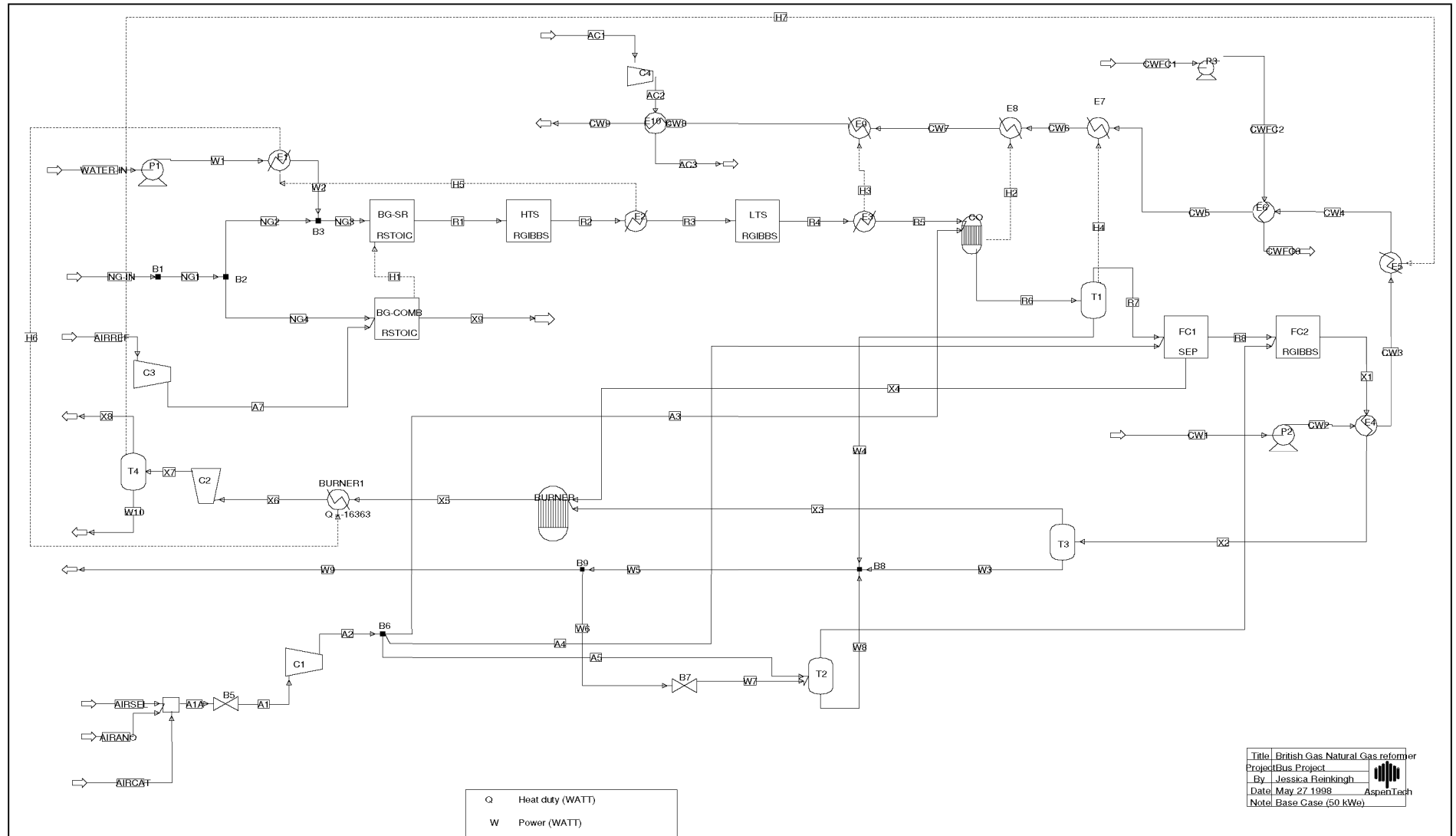


Figure D.3: Aspen flowsheet representing BG Tech's natural gas fuel cell system

Data file created by ASPEN PLUS Rel. 9.3-1 on
 23:31:20 Wed May 27, 1998
 Run ID: BGNG_2

Stream	NG-IN	NG1	NG2	NG3	NG4	R1	R2	R3	R4
From		B1	B2	B3	B2	BG-SR	HTS	E2	LTS
To	B1	B2	B3	BG-SR	BG-COMB	HTS	E2	LTS	E3
Phase	VAPOR	VAPOR	VAPOR	MIXED	VAPOR	VAPOR	VAPOR	VAPOR	VAPOR

Mole Flow MOL/MIN

CH4	6.29	12.15	9.25	9.25	2.89	0.66	0.66	0.66	0.66
C2	0.22	0.43	0.33	0.33	0.10	0.00	0.00	0.00	0.00
C3	0.05	0.09	0.07	0.07	0.02	0.00	0.00	0.00	0.00
C4	0.02	0.04	0.03	0.03	0.01	0.00	0.00	0.00	0.00
C5	0.01	0.01	0.01	0.01	0.00	0.00	0.00	0.00	0.00
H2O	0.00	0.00	0.00	30.84	0.00	17.28	14.18	14.18	11.96
H2	0.00	0.00	0.00	0.00	0.00	32.21	35.31	35.31	37.53
CO2	0.01	0.01	0.01	0.01	0.00	3.95	7.05	7.05	9.27
CO	0.00	0.00	0.00	0.00	0.00	5.68	2.58	2.58	0.36
O2	0.00	0.00	0.00	0.00	0.00	0.00	0.00	0.00	0.00
N2	0.12	0.23	0.18	0.18	0.06	0.18	0.18	0.18	0.18
Total Flow MOL/MIN	6.72	12.96	9.88	40.72	3.09	59.96	59.96	59.96	59.96

Total Flow KG/SEC

Total Flow KG/SEC	0.00	0.00	0.00	0.01	0.00	0.01	0.01	0.01	0.01
Total Flow L/MIN	44.26	85.43	65.08	382.94	20.35	1058.95	1167.48	748.55	833.06
Temperature C	15.00	15.00	15.00	130.52	15.00	406.35	464.15	200.00	244.80
Pressure BAR	3.60	3.60	3.60	3.50	3.60	3.20	3.15	3.15	3.10
Vapor Frac	1.00	1.00	1.00	1.00	1.00	1.00	1.00	1.00	1.00
Liquid Frac	0.00	0.00	0.00	0.00	0.00	0.00	0.00	0.00	0.00
Density KG/CUM	2.60	2.60	2.60	1.89	2.60	0.68	0.62	0.97	0.87
Average MW	17.13	17.13	17.13	17.80	17.13	12.09	12.09	12.09	12.09

Data file created by ASPEN PLUS Rel. 9.3-1 on
 23:31:20 Wed May 27, 1998
 Run ID: BGNG_2

Stream	R6	R7	R8	WATER-IN	W1	W2	W3	W4	W5
From	CO	T1	FC1		P1	E1	T3	T1	B8
To	T1	FC1	FC2	P1	E1	B3	B8	B8	B9
Phase	VAPOR	MIXED	VAPOR	LIQUID	LIQUID	VAPOR	LIQUID	LIQUID	LIQUID
Mole Flow MOL/MIN									
CH4	0.66	0.66	0.00	0.00	0.00	0.00	0.00	0.00	0.00
C2	0.00	0.00	0.00	0.00	0.00	0.00	0.00	0.00	0.00
C3	0.00	0.00	0.00	0.00	0.00	0.00	0.00	0.00	0.00
C4	0.00	0.00	0.00	0.00	0.00	0.00	0.00	0.00	0.00
C5	0.00	0.00	0.00	0.00	0.00	0.00	0.00	0.00	0.00
H2O	12.68	10.71	0.00	30.84	30.84	30.84	45.97	1.97	47.94
H2	36.81	36.81	29.45	0.00	0.00	0.00	0.00	0.00	0.00
CO2	9.63	9.63	0.00	0.00	0.00	0.00	0.00	0.00	0.00
CO	0.00	0.00	0.00	0.00	0.00	0.00	0.00	0.00	0.00
O2	0.00	0.00	0.00	0.00	0.00	0.00	0.00	0.00	0.00
N2	2.21	2.21	0.00	0.00	0.00	0.00	0.00	0.00	0.00
Total Flow MOL/MIN	61.99	60.01	29.45	30.84	30.84	30.84	45.97	1.97	47.94
Total Flow KG/SEC	0.01	0.01	0.00	0.01	0.01	0.01	0.01	0.00	0.01
Total Flow L/MIN	778.23	594.86	294.45	0.57	0.57	318.54	0.85	0.04	0.89
Temperature C	180.00	85.00	87.18	45.00	45.15	170.00	49.57	85.00	51.03
Pressure BAR	3.00	3.00	3.00	1.00	3.60	3.50	2.70	3.00	2.70
Vapor Frac	1.00	1.00	1.00	0.00	0.00	1.00	0.00	0.00	0.00
Liquid Frac	0.00	0.00	0.00	1.00	1.00	0.00	1.00	1.00	1.00
Density KG/CUM	1.03	1.28	0.20	974.02	973.87	1.74	969.50	933.60	968.05
Average MW	12.89	12.72	2.02	18.02	18.02	18.02	18.02	18.02	18.02

Data file created by ASPEN PLUS Rel. 9.3-1 on
 23:31:20 Wed May 27, 1998
 Run ID: BGNG_2

Stream	W6	W7	W8	W9	W10	CWFC1	CWFC2	CWFC3	CW4
From	B9	B7	T2	B9	T4		P3	E6	E5
To	B7	T2	B8			P3	E6	E6	E6
Phase	LIQUID	LIQUID	MISSING	LIQUID	LIQUID	LIQUID	LIQUID	LIQUID	LIQUID
Mole Flow MOL/MIN__									
CH4	0.00	0.00	0.00	0.00	0.00	0.00	0.00	0.00	0.00
C2	0.00	0.00	0.00	0.00	0.00	0.00	0.00	0.00	0.00
C3	0.00	0.00	0.00	0.00	0.00	0.00	0.00	0.00	0.00
C4	0.00	0.00	0.00	0.00	0.00	0.00	0.00	0.00	0.00
C5	0.00	0.00	0.00	0.00	0.00	0.00	0.00	0.00	0.00
H2O	21.67	21.67	0.00	26.28	4.76	3478.53	3478.53	3478.53	3333.33
H2	0.00	0.00	0.00	0.00	0.00	0.00	0.00	0.00	0.00
CO2	0.00	0.00	0.00	0.00	0.00	0.00	0.00	0.00	0.00
CO	0.00	0.00	0.00	0.00	0.00	0.00	0.00	0.00	0.00
O2	0.00	0.00	0.00	0.00	0.00	0.00	0.00	0.00	0.00
N2	0.00	0.00	0.00	0.00	0.00	0.00	0.00	0.00	0.00
Total Flow MOL/MIN	21.67	21.67	0.00	26.28	4.76	3478.53	3478.53	3478.53	3333.33
Total Flow KG/SEC	0.01	0.01	0.00	0.01	0.00	1.04	1.04	1.04	1.00
Total Flow L/MIN	0.40	0.40	0.00	0.49	0.09	67.12	67.12	66.39	62.16
Temperature C	51.03	51.02	0.00	51.03	53.50	85.00	85.01	75.00	53.00
Pressure BAR	2.70	3.20	0.00	2.70	1.00	1.00	1.20	1.00	1.60
Vapor Frac	0.00	0.00	0.00	0.00	0.00	0.00	0.00	0.00	0.00
Liquid Frac	1.00	1.00	0.00	1.00	1.00	1.00	1.00	1.00	1.00
Density KG/CUM	968.05	968.06	0.00	968.05	965.60	933.60	933.59	943.90	966.10
Average MW	18.02	18.02	0.00	18.02	18.02	18.02	18.02	18.02	18.02

Data file created by ASPEN PLUS Rel. 9.3-1 on
 23:31:20 Wed May 27, 1998

Run ID: BGNG_2

Stream	AIRANO	AIRCAT	AIRREF	AIRSEL	A1	A1A	A2	A3	A4	A5
From					B5	B4	C1	B6	B6	B6
To	B4	B4	C3	B4	C1	B5	B6	CO	FC1	T2
Phase	VAPOR	VAPOR	VAPOR	VAPOR	VAPOR	VAPOR	VAPOR	VAPOR	VAPOR	VAPOR
Mole Flow MOL/MIN										
CH4	0.00	0.00	0.00	0.00	0.00	0.00	0.00	0.00	0.00	0.00
C2	0.00	0.00	0.00	0.00	0.00	0.00	0.00	0.00	0.00	0.00
C3	0.00	0.00	0.00	0.00	0.00	0.00	0.00	0.00	0.00	0.00
C4	0.00	0.00	0.00	0.00	0.00	0.00	0.00	0.00	0.00	0.00
C5	0.00	0.00	0.00	0.00	0.00	0.00	0.00	0.00	0.00	0.00
H2O	0.00	0.00	0.00	0.00	0.00	0.00	0.00	0.00	0.00	0.00
H2	0.00	0.00	0.00	0.00	0.00	0.00	0.00	0.00	0.00	0.00
CO2	0.00	0.00	0.00	0.00	0.00	0.00	0.00	0.00	0.00	0.00
CO	0.00	0.00	0.00	0.00	0.00	0.00	0.00	0.00	0.00	0.00
O2	0.25	29.45	8.82	0.54	30.24	30.24	30.24	0.54	0.25	29.45
N2	0.95	110.78	33.19	2.03	113.76	113.76	113.76	2.03	0.95	110.78
Total Flow MOL/MIN	1.20	140.23	42.01	2.57	144.00	144.00	144.00	2.57	1.20	140.23
Total Flow KG/SEC	0.00	0.07	0.02	0.00	0.07	0.07	0.07	0.00	0.00	0.07
Total Flow L/MIN	0.00	0.00	1005.80	0.00	3447.57	3570.93	1789.62	31.94	14.92	1742.77
Temperature C	15.00	15.00	15.00	15.00	15.00	25.28	204.82	204.82	204.82	204.82
Pressure BAR	0.00	0.00	1.00	0.00	1.00	1.00	3.20	3.20	3.20	3.20
Vapor Frac	1.00	1.00	1.00	1.00	1.00	1.00	1.00	1.00	1.00	1.00
Liquid Frac	0.00	0.00	0.00	0.00	0.00	0.00	0.00	0.00	0.00	0.00
Density KG/CUM	0.00	0.00	1.21	0.00	1.21	1.16	2.32	2.32	2.32	2.32
Average MW	28.85	28.85	28.85	28.85	28.85	28.85	28.85	28.85	28.85	28.85

Data file created by ASPEN PLUS Rel. 9.3-1 on
 23:31:20 Wed May 27, 1998
 Run ID: BGNG_2

Stream	A6	A7	AC1	AC2	AC3
From	T2	C3		C4	E10
To	FC2	BG-COMB	C4	E10	
Phase	VAPOR	VAPOR	VAPOR	VAPOR	VAPOR
Mole Flow MOL/MIN					
CH4	0.00	0.00	0.00	0.00	0.00
C2	0.00	0.00	0.00	0.00	0.00
C3	0.00	0.00	0.00	0.00	0.00
C4	0.00	0.00	0.00	0.00	0.00
C5	0.00	0.00	0.00	0.00	0.00
H2O	21.67	0.00	0.00	0.00	0.00
H2	0.00	0.00	0.00	0.00	0.00
CO2	0.00	0.00	0.00	0.00	0.00
CO	0.00	0.00	0.00	0.00	0.00
O2	29.45	8.82	3800.00	3800.00	3800.00
N2	110.78	33.19	14295.00	14295.00	14295.00
Total Flow MOL/MIN	161.89	42.01	18095.00	18095.00	18095.00
Total Flow KG/SEC	0.07	0.02	8.70	8.70	8.70
Total Flow L/MIN	1603.34	832.77	448320.00	448050.00	464816.00
Temperature C	85.00	60.75	25.00	25.12	35.94
Pressure BAR	3.00	1.40	1.00	1.00	1.00
Vapor Frac	1.00	1.00	1.00	1.00	1.00
Liquid Frac	0.00	0.00	0.00	0.00	0.00
Density KG/CUM	2.77	1.46	1.16	1.17	1.12
Average MW	27.40	28.85	28.85	28.85	28.85

Data file created by ASPEN PLUS Rel. 9.3-1 on
 23:31:20 Wed May 27, 1998
 Run ID: BGNG_2

Stream	X1	X2	X3	X4	X5	X6	X7	X8	X9
From	FC2	E4	T3	FC1	BURNER	BURNER1	C2	T4	BG-COMB
To	E4	T3	BURNER	BURNER	BURNER1	C2	T4		
Phase	MIXED	MIXED	VAPOR	MIXED	VAPOR	VAPOR	VAPOR	VAPOR	VAPOR
Mole Flow MOL/MIN									
CH4	0.00	0.00	0.00	0.66	0.00	0.00	0.00	0.00	0.00
C2	0.00	0.00	0.00	0.00	0.00	0.00	0.00	0.00	0.00
C3	0.00	0.00	0.00	0.00	0.00	0.00	0.00	0.00	0.00
C4	0.00	0.00	0.00	0.00	0.00	0.00	0.00	0.00	0.00
C5	0.00	0.00	0.00	0.00	0.00	0.00	0.00	0.00	0.00
H2O	51.11	51.11	5.14	10.71	24.53	24.53	24.53	19.77	6.24
H2	0.00	0.00	0.00	7.36	0.00	0.00	0.00	0.00	0.00
CO2	0.00	0.00	0.00	9.63	10.29	10.29	10.29	10.29	3.22
CO	0.00	0.00	0.00	0.00	0.00	0.00	0.00	0.00	0.00
O2	14.72	14.72	14.72	0.25	9.98	9.98	9.98	9.98	2.49
N2	110.78	110.78	110.78	3.16	113.93	113.93	113.93	113.93	33.24
Total Flow MOL/MIN	176.62	176.62	130.65	31.77	158.73	158.73	158.73	153.97	45.19
Total Flow KG/SEC	0.07	0.07	0.06	0.01	0.07	0.07	0.07	0.07	0.02
Total Flow L/MIN	1513.58	1252.10	1296.59	260.33	3758.28	2908.91	6256.89	4176.56	1547.45
Temperature C	85.00	50.00	49.57	87.18	466.85	277.84	201.03	53.50	180.00
Pressure BAR	3.00	2.80	2.70	3.00	2.60	2.50	1.00	1.00	1.10
Vapor Frac	0.87	0.74	1.00	0.82	1.00	1.00	1.00	1.00	1.00
Liquid Frac	0.13	0.26	0.00	0.18	0.00	0.00	0.00	0.00	0.00
Density KG/CUM	2.97	3.59	2.83	2.84	1.17	1.51	0.70	1.03	0.82
Average MW	25.45	25.45	28.07	23.25	27.76	27.76	27.76	28.06	27.99

APPENDIX E: THOREB/SCANIA BUS AND BASIS FOR SIMULATIONS

Present Hybrid Bus Built by Scania and Thoreb

Power is delivered by batteries and an internal combustion engine. The bus power train has a series configuration, meaning that there is no direct mechanical connection between the ICE and the transmission. Instead, the ICE is connected to a generator, which converts the mechanical energy into electrical energy. The electrical energy generated by the ICE supplies the electrical motor. During deceleration the electrical motor serves as a generator supplying energy to the batteries, i.e. regenerative braking.

The ICE is a standard 2.3 litre Saab gasoline engine. To optimise its efficiency the ICE only operates in three modes, i.e.

- 0 rpm while driving on batteries,
- 2750 rpm (~37 kW) during stand-still or velocities < 7 km/h,
- 3500 rpm (~50 kW).

The difference between the total power demand and power generated by the ICE is supplied or stored by the batteries. The total power demand is a function of the bus drive cycle. The relation between the total power demand and the power supply is shown schematically in Figure E.1.

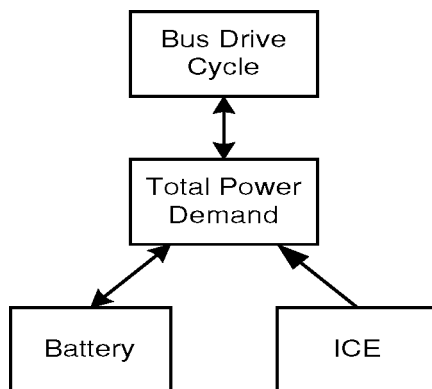


Figure E.2: Power flow in hybrid bus

The battery power in the ICE bus is supplied by 10 nickel-cadmium batteries connected in series. Each battery comprises 27 cells, with a discharge and charge potential of 1.2-1.5 V/cell. During operation, the batteries are monitored and controlled by a microprocessor chip. Parameters like battery temperature (change), time, voltage (change), and number of cycles are continuously measured and processed to regulate the charge and discharge voltages between 325 and 405 V. In practice voltages of 300 and 425 V have been measured. The rated battery capacity is 80 Ah (~25.9 kWh = 93,240 kJ).

Simulation Input Variables and Power Output Parameters and Simulation Logic

With the input variables in Chapter 6, Table 6.2, the output power of the FCS at time t is calculated by comparing the total power demand at time t and the power generated at time $t-1$. Figure E2 shows the simulation logic for calculating the FCS power output at time t . The FCS power output is simulated to follow the load. For instance, if at time t the total power demand is 25 kW, while the FCS power at $t-1$ was 12 kW, the FCS power at t will be adjusted to $12 + \text{acceleration}$. The power turn-up rate (A) and power turn-down rate (D) values determine the dynamic response time of the FCS to the power demand. If they are very low, the FCS is unlikely to follow load, and the demands on the battery power will be high. By varying the values of A and D , the required dynamic properties of the system can also be assessed for a power train without a battery.

The maximum power of the FCS (Max) can be optimised with respect to its dynamic performance, which in its turn will set the battery capacity. It may be useful to continuously operate the FCS during the drive cycle, keeping the system warm and avoiding many start-ups and shutdowns. The minimum FCS power (Min) can be for instance 10% of the maximum power, which during idling can be used to charge the batteries.

The batteries function as a load leveler in this application and have to endure many charge and discharge cycles. The battery lifetime is a function of the number of cycles and the depth of discharge ($\text{DOD} = \text{accumulative power discharge divided by the rated capacity}$). Typically, the number of cycles the battery can endure increases with

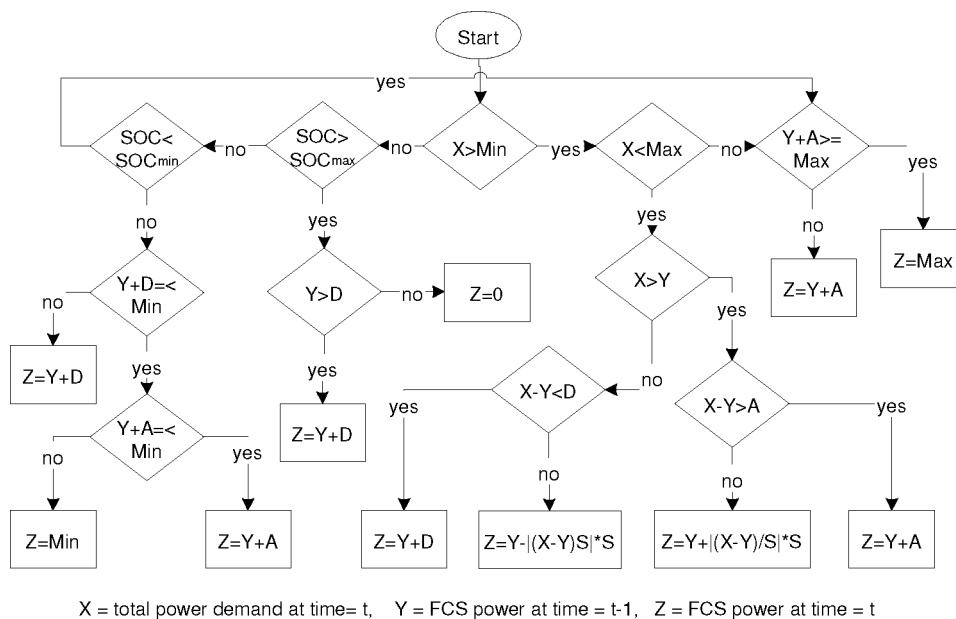


Figure E2: FCS power output simulation logic (t = time in seconds)

decreasing DOD. For example, the battery may survive a 1000 cycles at 80% DOD, but can probably deal with 10,000 cycle at 30% DOD. Hence, it is very important to maintain the batteries highly charged during the drive cycle. On the other hand, overcharging the battery also shortens its life and needs to be prevented at all times.

In the simulations here the minimum and maximum state-of-charge ($\text{SOC} = \text{available energy / rated capacity}$) are included in the calculations. If either of these values is

reached the FCS system stops its load following mode and will be dictated by the batteries' necessity to be charged or not overcharged. In other words, if the SOC at some point during the drive cycle reaches a lower value than desired, say 80% (= 20% DOD), the FCS will generate power until the SOC has reached the desired value. Alternatively, if the SOC reaches 100%, the FCS will be switched off completely.

The calculated average battery charge and discharge in the ICE power-train versus a FCS power train will show whether the battery capacity needs to be changed or not. If the average charge and discharge are much higher for the FCS bus, it is likely that more battery capacity is needed. Alternatively, if they are much lower, the battery capacity may be decreased.

If the maximum battery charge and discharge are calculated to be higher for the FCS system it will need to be assessed whether the current battery set-up can deal with these demands, depending on how often high charges and discharges occur during a drive cycle. As mentioned earlier, charging and discharging at a high rate may have a long-term detrimental effect on the batteries.

The power discharges are also expressed as %/s, i.e. the average of maximum power discharge rate divided by the rated capacity. These relative numbers become important when the number of batteries in the system is varied.

The fraction of the drive cycle in which the FCS actually generates the maximum power is a parameter which indicates whether the FCS is sized correctly for a given dynamic performance, e.g. if during 1% of the drive cycle the maximum output is reached the FCS is oversized. The drive cycle fraction the FCS is calculated to produce zero power is preferably small or none.

APPENDIX REFERENCES

Ackerman, F.J., Koskinas, G.J., Permeation of Hydrogen and Deuterium through Palladium-Silver Alloys, Journal of Chemical and Engineering Data, Vol 17, No 1, 1972, p51-55.

Agentun, B., Aspen Petroleum, Meeting held Nov 1997

Bechtold, R.L., Alternative Fuels Guidebook, Pub SAE, 1997

Cadwaller, S., Donovan, N., Fuelling Tomorrows Transport, FT Energy Publishing, 1995

Carpenter, I.W., Golunski, S.E., Alternative Feeds for Fuel-Processing by Partial Oxidation and Autothermal Reforming, ETSU F/02/00117/00/REP, 1998

Carslaw, D., Fricker, N., Natural Gas Vehicles – a realistic alternative?, British Gas NSCA Training Seinar, Feb 1995.

Chandler, K. et al, Alternative Fuel Transit Bus Evaluation Program Results, SAE 961082, 1996

Daimler Benz High Tech Report, 1995, p64-65

Danielson, H., Swebus, Meeting held Nov 1997

FT Automotive Analyst, Issue 29, June 1997, p5

IEA World Energy Outlook, 1995.

IEA/AIFS Automotive Fuels Survey, Volume 2, Distribution and Use, Dec 1996.

Owen, K., Coley, T., Automotive Fuels Reference Book, Edn 2, 1995.

Schmidt, P., Methanex, Personal Communication, Feb 1998.